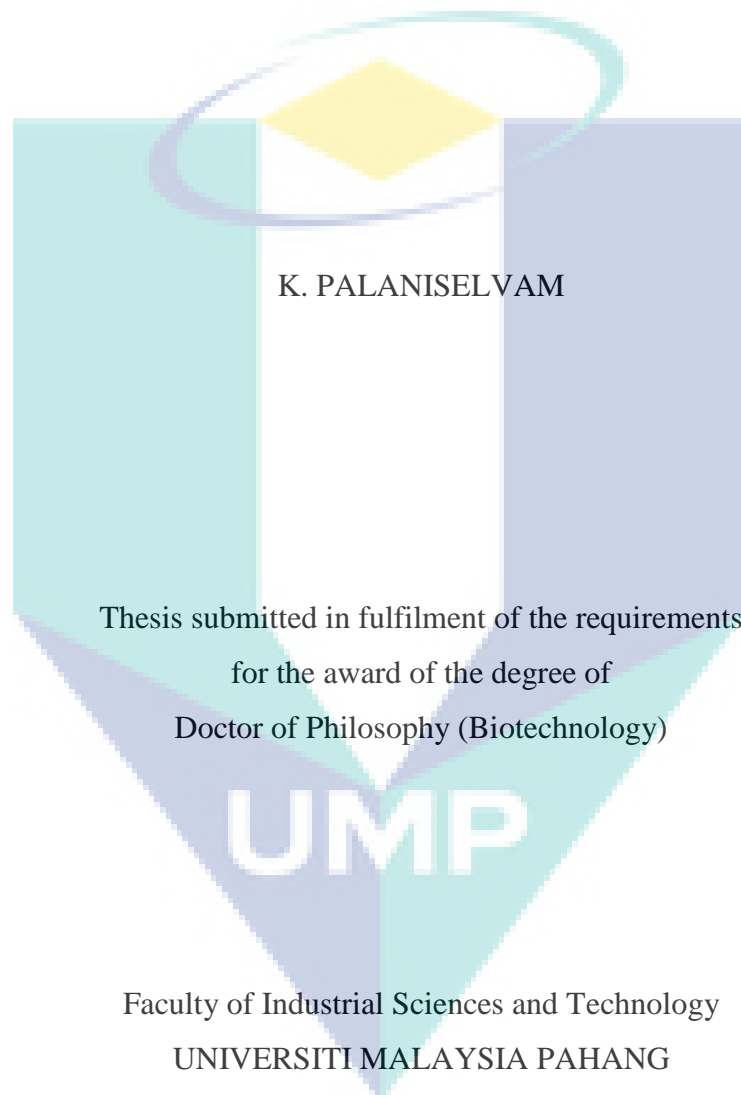


IN-VITRO BIOLOGICAL ACTIVITIES OF Au AND Ag NANOPARTICLES
BIOSYNTHESED USING *Commelina nudiflora* L. AQUEOUS EXTRACT



SEPTEMBER 2015

UNIVERSITI MALAYSIA PAHANG

DECLARATION OF THESIS AND COPY RIGHT

Name : K. PALANISELVAM
Date of birth : 10 MARCH 1986
Title : IN-VITRO BIOLOGICAL
ACTIVITIES OF Au AND Ag NANOPARTICLES
BIOSYNTHESIZED USING *Commelina nudiflora*
L. AQUEOUS EXTRACT
Academic Session : 2015/2016

I declared that this thesis is classified as:

- CONFIDENTIAL** (Contains confidential information under the Official Secret Act 1972)*
 RESTRICTED (Contains restriction information as specified by the organization where research was done)*
 OPEN ACCESS I agree that my thesis to be published as online open access (Full text)

I acknowledge that University Malaysia Pahang reserve the right as follows:

1. The Thesis is the Property of University Malaysia Pahang
2. The Library of University Malaysia Pahang has right to make copies for the purpose of research only.
3. The Library has the right to make copies of the thesis for academic exchange.

Certified By:

K. PALANISELVAM

Passport Number: H9856809

Date: 17 September 2015

DR. NATANAMURUGARAJ GOVINDAN

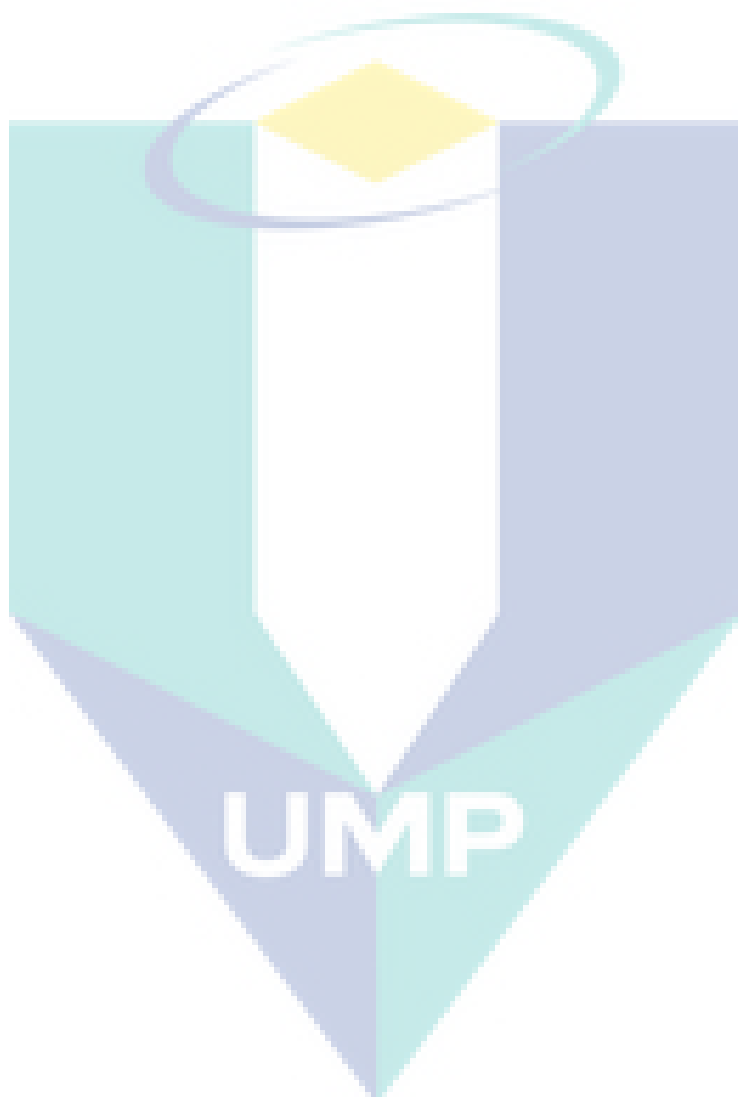
Passport Number: H2750927

Date: 17 September 2015

NOTES: *If the thesis is CONFIDENTIAL or RESTRICTED, please attach with the letter from the organization with period and reasons for confidentiality or restriction.

STATEMENT OF AWARD FOR DEGREE

Thesis submitted in fulfillment of the requirements for the award of the degree of
Doctor of Philosophy (Biotechnology)



SUPERVISOR'S DECLARATION

I hereby declare that I have checked this thesis and in my opinion, this thesis is adequate in terms of scope and quality for the award of the degree of Doctor of Philosophy in Biotechnology.



Signature :
Name of Supervisor : DR. NATANAMURUGARAJ GOVINDAN
Position : SENIOR LECTURER
Date : 17 SEPTEMBER 2015

Signature :
Name of Co-Supervisor : PROFESSOR DR. MASHITAH MOHD YUSOFF
Position : PROFESSOR
Date : 17 SEPTEMBER 2015

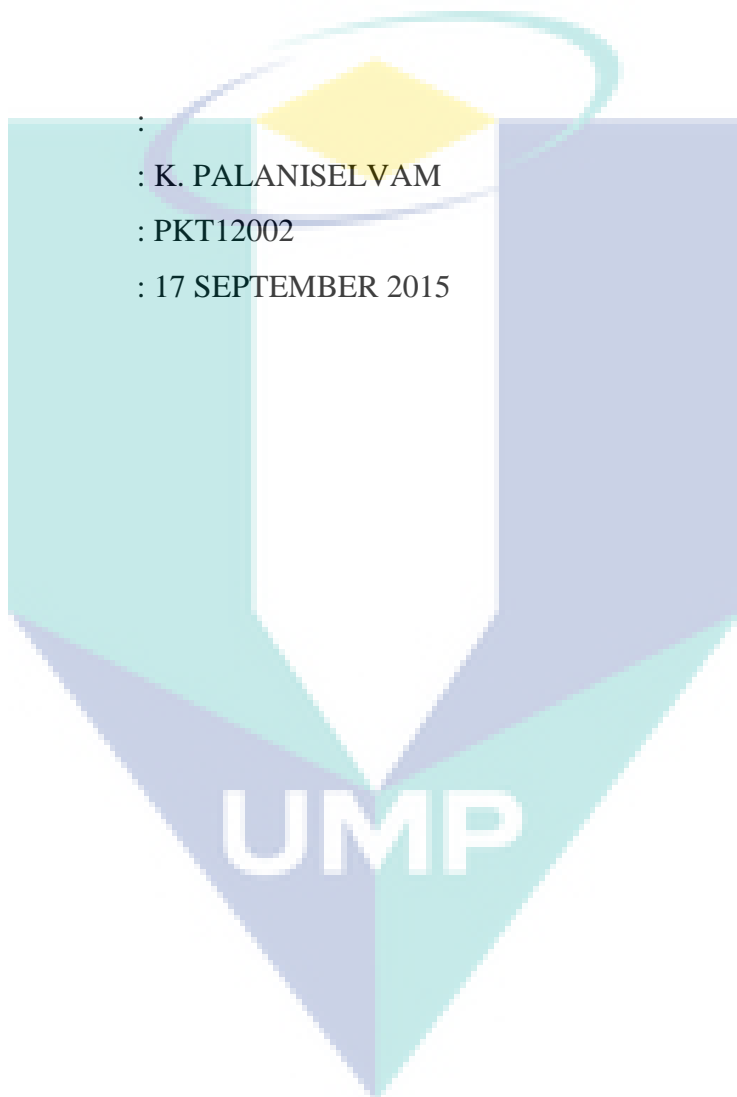
Signature :
Name of Co-Supervisor : DR. GAANTY PRAGAS A/L MANIAM
Position : SENIOR LECTURER
Date : 17 SEPTEMBER 2015

Signature :
Name of Field Supervisor : ASSOC. PROF. DR. SOLACHUDDIN J.A. ICHWAN
Position : ASSOCIATE PROFESSOR
Date : 17 SEPTEMBER 2015

STUDENT'S DECLARATION

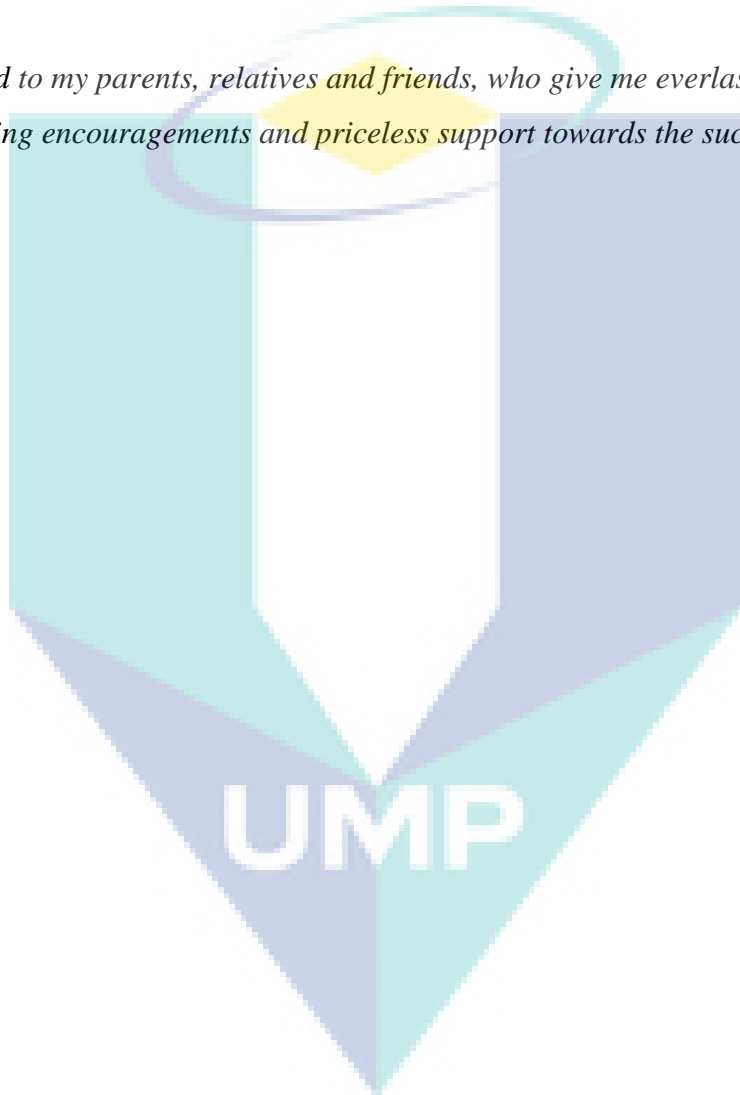
I hereby declare that the work in this thesis is my own except for the quotations and summaries which have been duly acknowledged. The thesis has not been accepted for any degree and is not concurrently submitted for award of other degree.

Signature :
Name : K. PALANISELVAM
ID Number : PKT12002
Date : 17 SEPTEMBER 2015



DEDICATION

*Dedicated to my parents, relatives and friends, who give me everlasting inspiration,
never-ending encouragements and priceless support towards the success of this study.*

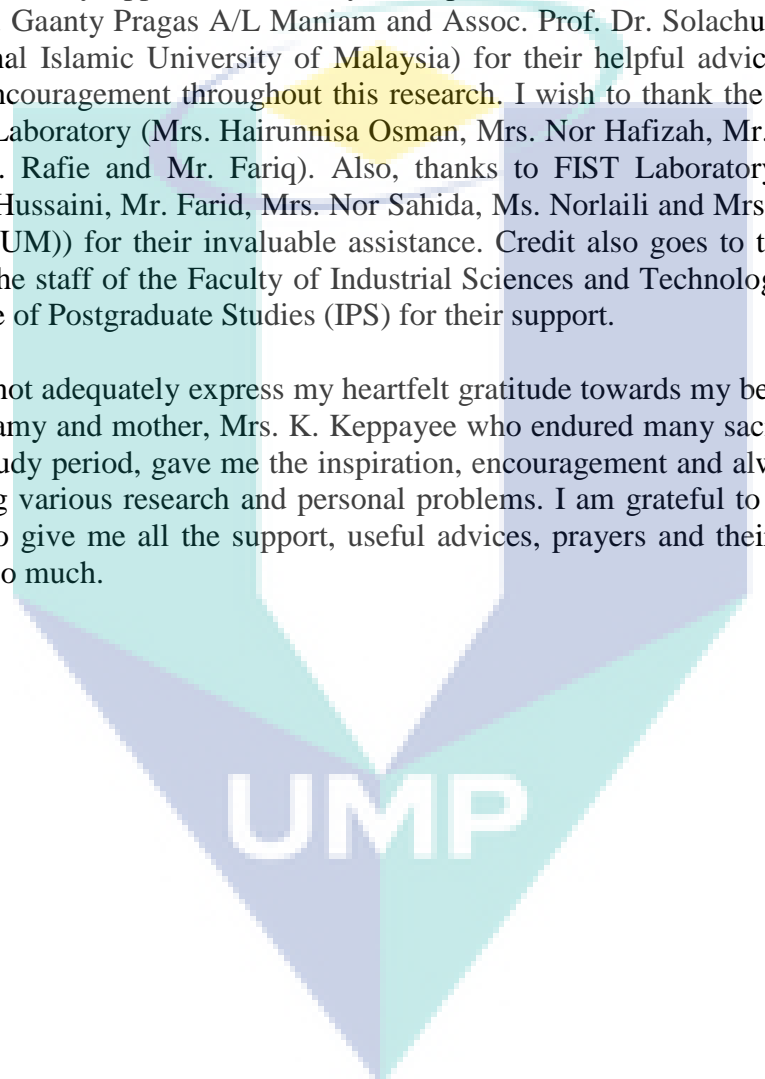


ACKNOWLEDGEMENTS

Thanks to GOD Almighty who gives me, HIS blessings for a good health and strength to complete my research work. Special thanks to my supervisor Dr. Natanamurugaraj Govindan, who has provided a significant contribution by giving all the guidance and support throughout my research work.

I also express my appreciation to my co-supervisors, Professor Dr. Mashitah Mohd Yusoff, Dr. Gaanty Pragas A/L Maniam and Assoc. Prof. Dr. Solachuddin J.A. Ichwan (International Islamic University of Malaysia) for their helpful advices, guidance and effective encouragement throughout this research. I wish to thank the Science Officers at Central Laboratory (Mrs. Hairunnisa Osman, Mrs. Nor Hafizah, Mr. Aimi Ilmar, Mr. Fahmi, Mr. Rafie and Mr. Fariq). Also, thanks to FIST Laboratory Assistants (Mr Muhamad Hussaini, Mr. Farid, Mrs. Nor Sahida, Ms. Norlaili and Mrs. Nordiana, Miss. Muzuea (IIUM)) for their invaluable assistance. Credit also goes to the Dean, Deputy Dean and the staff of the Faculty of Industrial Sciences and Technology (FIST), and to the Institute of Postgraduate Studies (IPS) for their support.

Words cannot adequately express my heartfelt gratitude towards my beloved father, Mr. C. Kuppusamy and mother, Mrs. K. Keppayee who endured many sacrifices during my graduate study period, gave me the inspiration, encouragement and always supports me in resolving various research and personal problems. I am grateful to my relatives and friends who give me all the support, useful advices, prayers and their patience to me, thank you so much.

The logo of Universiti Malaysia Perlis (UMPU) is a large, stylized letter 'U' composed of four overlapping triangles in shades of teal and light blue. The letters 'U', 'M', and 'P' are written in white, bold, sans-serif font across the center of the 'U' shape.

UMPU

ABSTRACT

In this study, *Commelina nudiflora* L. aqueous extract was used as a reducing and stabilizing agent for the synthesis of metallic gold and silver nanoparticles. The physico-chemical and biological properties of the biosynthesized gold and silver nanoparticles were studied in a nanoscale regime. The synthesized gold and silver nanoparticles physico-chemical properties were characterized by various analytical techniques such as UV-VIS, FESEM, XRD and FT-IR. The synthesized gold and silver nanoparticles were monodispersed, and the controlled shapes and tuneable surface properties were proven. Also, the reaction parameters such as pH, temperature, plant extract concentration and metal ion concentration have been optimized to synthesize the specific sizes and shapes of the nanoparticles. The synthesized gold and silver nanoparticles were spherical and triangular in shapes with the size range of between 25 to 45 nm and 50 to 150 nm respectively. The EDX spectra show strong peaks of both gold and silver nanoparticles which are more than 80% in the sample. The XRD data supports the claim that synthesized gold and silver nanoparticles are crystalline in nature. The plant extract contains various phytochemical constituents such as saponins, alkaloids, flavonoids and phenolic compounds. These secondary metabolites may be responsible for the Au and Ag ions reduction and also help in the formation of the metal nanoparticles. Furthermore, the *in-vitro* antioxidant ability of *C. nudiflora* extracts was studied by DPPH and ABTS radical scavenging assays. The aqueous plant extract showed significant activity in the free radical scavenging which were 63.4 mg/GAE and 49.10 mg/g in DPPH and ABTS respectively. Furthermore, the biosynthesized gold and silver nanoparticles have shown reduction in the cell viability and increased cytotoxicity on HCT-116 colon cancer cells with IC₅₀ concentration of 200 and 100 µg/ml. The flow cytometry experiments revealed that the gold and silver nanoparticles treated cells increased DNA fragmentation and significant changes were observed in sub G1 cell cycle phases compared with positive control. Finally, the mRNA gene expressions of HCT-116 cells were studied by RT-qPCR techniques. The pro-apoptotic genes were highly expressed in the gold nanoparticles treated HCT-116 colon cancer model. The apoptotic genes such as PUMA (++), caspase-3 (+) and caspase-8 (++) were moderately expressed in the treated samples compared with cisplatin. Overall, these findings prove that the *C. nudiflora* extract successfully synthesize metallic gold and silver nanoparticles with controlled size and shapes and also acts as a potent anti-colon cancer drug in the near future.

ABSTRAK

Penyelidikan ini adalah untuk menggunakan ekstrak akues tumbuhan *Commelina nudiflora* L. sebagai penstabil serta agen penurunan bagi penghasilan partikel nano logam emas dan perak menggunakan kaedah biosintesis. *C. nudiflora* tumbuhan rumpai yang boleh dimakan, ekstraknya digunakan untuk biosintesis nanopartikel emas dan perak dan pencirian fisio-kimianya dengan pelbagai teknik analisis seperti UV-VIS, FESEM, XRD dan FT-IR. Partikel nano emas dan perak yang dihasilkan secara biosintesis perlu diciri fizik-kimia dan biologinya pada skala nano. Partikel nano emas dan perak yang disintesis memiliki ciri pembauran mono seragam, bentuk terkawal dan sifat-sifat permukaan boleh ubah. Usaha untuk mengoptimumkan parameter tindakbalas seperti pH, suhu dan kepekatan ekstrak tumbuhan dan ion kepekatan logam untuk mensintesis saiz dan bentuk partikel nano tertentu juga dijalankan. Hasilnya menunjukkan bahawa pencirian fizik-kimia dari partikel nano emas dan perak masing-masing adalah bersifat kristal dengan pelbagai saiz antara 25-45 nm dan 50-150 nm. Juga, partikel nano emas dan perak yang terhasil secara biosintesis adalah berbentuk bulat dan segi tiga dilaporkan dalam kajian ini. Spektrum EDX menunjukkan puncak tenaga isyarat yang kuat daripada kedua-dua emas dan perak atom dalam julat di antara 2-3 keV. Sebaliknya, data XRD menyokong partikel nano emas dan perak disintesis adalah dalam keadaan kristal secara semula jadi. Juga, kami telah mengenal pasti beberapa jujuk fitokimia awal seperti saponin, alkaloid, flavonoid dan sebatian fenolik daripada ekstrak tumbuhan *C. nudiflora* menggunakan pelarut berbeza polariti. Metabolit sekunder mungkin turut terlibat dalam tindak balas penurunan dan juga membantu dalam pembentukan partikel nano logam. Keupayaan anti-oksidan *in vitro* ekstrak *C. nudiflora* dikaji dengan penentuan DPPH dan ABTS pencarian radikal. Ekstrak tumbuhan berair menunjukkan aktiviti yang penting dalam mengaut radikal bebas daripada 63.4 mg /GAE dan 49.10 mg /g dalam DPPH dan ABTS. Partikel nano logam emas dan logam perak terhasil dari ekstrak tumbuhan *C. nudiflora* ini dengan ketara mengawal pertumbuhan HCT-116 sel-sel kanser kolon secara *in-vitro*. Logam nano partikel emas dan perak yang terhasil telah berjaya mengurangkan sel hidup dan meningkatkan kadar sitotoksik pada sel kolon HCT-116 dengan kadar IC₅₀ 200 dan 100 µg / ml. Tambahan pula, eksperimen aliran sitometri menunjukkan kadar kepekatan IC₅₀ sel yang dirawat dengan partikel nano emas dan perak menunjukkan peningkatan fragmentasi DNA dan perubahan ketara diperhatikan pada sub G1, S, G2 fasa kitaran sel berbanding dengan kawalan. Ekspresi gen mRNA dalam HCT-116 telah dikaji dengan teknik QRT-PCR. Gen apoptotik amat terekspresi dengan tinggi dalam model HCT-116 kolon kanser yang dirawat, seperti PUMA (++) dan caspase-3 (+), caspase-8 (++) dengan ekspresi sederhana sampel dirawat berbanding dengan *cisplatin*. Secara keseluruhan, hasil dapatan ini telah menunjukkan bahawa ekstrak *C. nudiflora* sebagai sumber baru untuk sintesis logam partikel nano emas dan perak dengan saiz dan bentuk dikawal dan juga ia boleh diguna sebagai dadah anti-kanser kolon yang potensi dalam masa terdekat.

TABLE OF CONTENTS

	Page
SUPERVISOR'S DECLARATION	ivv
STUDENT'S DECLARATION	vi
ACKNOWLEDGEMENTS	viii
ABSTRACT	ix
ABSTRAK	xx
TABLE OF CONTENTS	xi
LIST OF TABLES	xvii
LIST OF FIGURES	xviii
LIST OF ABBREVIATIONS	xxii
CHAPTER 1 INTRODUCTION	
1.0 Chapter overview	1
1.1 Background of the study	1
1.2 Problem statement	4
1.3 Research objectives	5
1.4 Scope of the study	5
1.5 Statement of the contribution	6
CHAPTER 2 REVIEW OF LITERATURE	
2.0 Chapter overview	7
2.1 Nanomedicine	7
2.2 Biological resources for the synthesis of gold and silver nanoparticles	8
2.2.1 Plant extracts (broth) as a source	8
2.2.2 Microorganisms sources for synthesis of metallic nanoparticles	13
2.2.3 Enzymes reduced metal ions into NPs	20
2.2.4 Human cell lines as source for synthesis of metallic nanoparticles	21

2.3 Different physic-chemical factors inducing metal nanoparticles synthesis	22
2.4 Different methods used for synthesis of nanoparticles	22
2.4.1 Physical methods used for synthesis of nanoparticles	23
2.4.2 Chemical methods used for synthesis of nanoparticles	23
2.4.3 Biological approaches of nanoparticles synthesis	25
2.5 Pharmacological applications of metallic nanoparticles	25
2.5.1 Antibacterial and antifungal activities of NPs	25
2.5.2 Antifungal activity of Au, Ag nanoparticles	27
2.5.3 Antidiabetic management of metallic nanoparticles	27
2.5.4 Anticancer activities of metal NPs	28
2.6 Colon cancer in Worldwide & Malaysia	31
2.6.1 Development of colon cancer	33
2.6.2 Function of oncogene and tumor suppressor genes in colon cancer	33
2.6.3 Apoptosis	34
2.7 Molecular techniques used to evaluate colon cancer progression	35
2.7.1 Flow cytometry	35
2.7.2 Quantitative real time polymerase chain reaction (RT-qPCR)	36
2.8 Metal nanoparticles for catalysis	39
2.9 Commercial applications of biosynthesized metal nanoparticles	39
2.9.1 Waste water treatment	39
2.9.2 Cosmetics	40
2.9.3 Nanoparticles in food industry	40

CHAPTER 3 MATERIALS AND METHODS

3.0 Chapter overview	41
3.1. Plant collection and identification	41
3.1.1 Chemicals and glassware	42
3.1.2 Plant extracts preparation	43
3.2 Biosynthesis of metallic nanoparticles	43
3.2.1 Biosynthesis of gold nanoparticles	43
3.2.2 Biosynthesis of silver nanoparticles	43

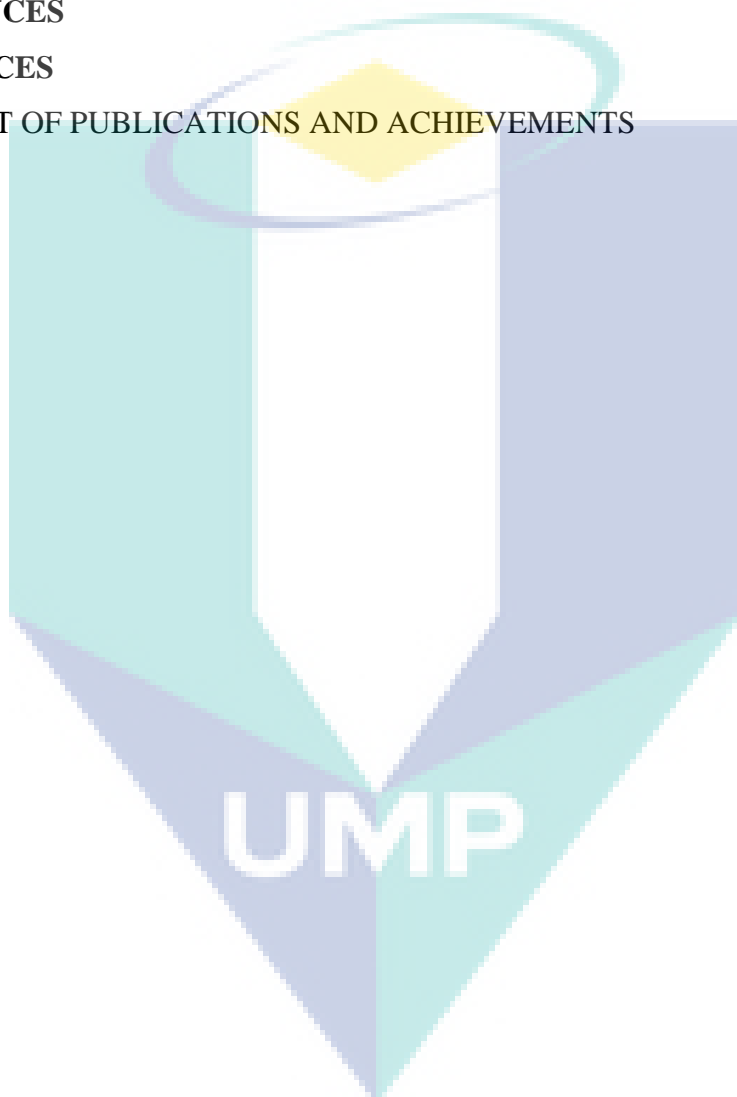
3.3 Characterization of synthesized nanoparticles	44
3.3.1 UV-Visible spectrophotometer analysis	45
3.3.2 FESEM analysis and EDX measurement	45
3.3.3 XRD characterization	45
3.3.4 FT-IR analysis	46
3.3.5 TGA and BET analysis	46
3.3.6 Particles size analyzer and Zeta potential study	46
3.3.7 Conventional methods for characterization of synthesized NPs	47
3.4 Bioactive compounds analysis	49
3.4.1 Hot extraction method by soxhlet apparatus	49
3.4.2 Preliminary phytochemical characterization of plant extracts	50
3.4.3 Determination of total phenolic content (TPC)	52
3.4.4 Determination of total flavonoid content (TFC)	52
3.4.5 GC-MS study	53
3.4.6 Bioactivity of plant extract	53
3.5 <i>In-vitro</i> antibacterial activity	54
3.5.1 Antibacterial activity of gold and silver nanoparticle	54
3.6 <i>In-vitro</i> antioxidant activity	54
3.6.1 DPPH assay of gold and silver nanoparticles	54
3.6.2 ABTS assay of gold and silver nanoparticles	55
3.7 <i>In-vitro</i> anticancer assays	55
3.7.1 Cell line and culture medium	55
3.7.2 Reagents, equipment's and kits used	55
3.7.3 Cells sub-culturing and maintenance	56
3.7.4 <i>In-vitro</i> MTT assay	56
3.7.5 Flow cytometry analysis	57
3.8 Molecular characterization of cellular studies	57
3.8.1 Quantitative RT-PCR studies	57
3.9 Statistical analysis	62

CHAPTER 4 RESULTS AND DISCUSSION

4.0	Chapter overview	63
4.1	Biosynthesis, characterization and biological properties of AuNPs	63
4.1.1	Biosynthesis of gold nanoparticles	63
4.1.2	Studies on UV- VIS spectra of gold nanoparticles	64
4.1.3	Structural and morphological study of gold nanoparticles	67
4.1.4	Confirmation of functional groups from gold nanoparticles sample	71
4.1.5	Analysis of particles size distribution and zeta potential studies	73
4.1.6	TGA and BET analysis of biosynthesized gold nanoparticles	75
4.1.7	Antibacterial activities of GNPs	76
4.1.8	Antioxidant activities of GNPs	78
4.2	Biosynthesis, characterization and biological application of AgNPs	79
4.2.1	Biosynthesis of silver nanoparticles	79
4.2.2	UV-Vis confirmation of biosynthesized AgNPs	80
4.2.3	Structural characterization of AgNPs using FESEM with EDX	82
4.2.4	Determination of crystalline nature of AgNPs using XRD	83
4.2.5	Particles size analyzer and zeta potential studies	85
4.2.6	Thermal gravimetric analysis and BET study of AgNPs	86
4.2.7	FT-IR analysis of AgNPs	88
4.2.8	Antibacterial study of AgNPs	89
4.2.9	Antioxidant activity of silver nanoparticles	91
4.3	Phytochemical characterization of <i>C.nudiflora</i> extracts	93
4.3.1	Identification of secondary metabolites from <i>C. nudiflora</i> extracts	93
4.3.2	GC-MS characterization of <i>C. nudiflora</i> crude extracts	95
4.3.3	Antibacterial activities of <i>C. nudiflora</i> extracts	97
4.3.4	Free radical scavenging activity on <i>C. nudiflora</i> extracts	99
4.4	<i>In-vitro</i> anticancer studies of biosynthesized gold and silver NPs	100
4.4.1	<i>In-vitro</i> MTT assay	100
4.4.2	Flow cytometry analysis	106
4.4.3	Morphological characterization	109
4.4.4	Quantitative real time polymerase chain reaction studies	110

CHAPTER 5 CONCLUSIONS AND RECOMMENDATIONS

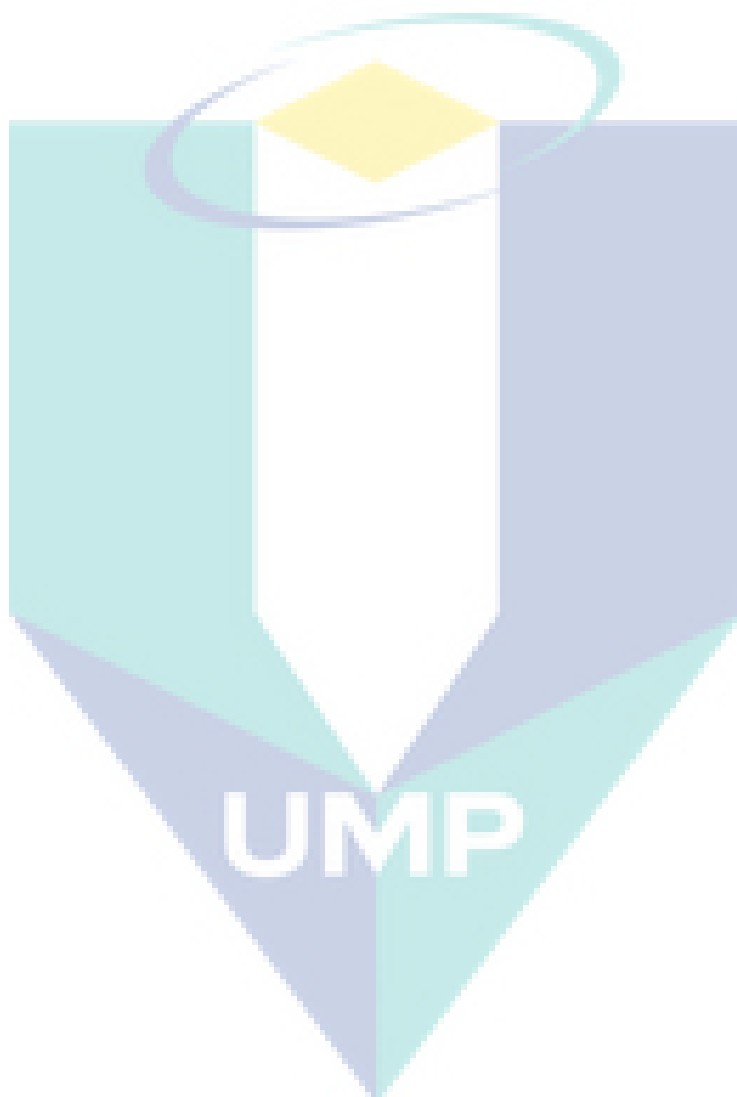
5.0 Chapter overview	117
5.1 Conclusions	117
5.2 Recommendations	119
REFERENCES	120
APPENDICES	153
A. LIST OF PUBLICATIONS AND ACHIEVEMENTS	153



LIST OF TABLES

Table No.	Title	Page
2.1	Summary of some plant derivatives involved in nanoparticles production and its biomedical applications	13
2.2	Summary of marine organisms biosynthesized metallic nanoparticles	19
2.3	Example of some molecular assays to characterize the colon cancer progression	38
3.1	Purity of RNA concentration from the experimental samples analyzed by nanodrop spectrophotometer	59
3.2	Required components for reverse transcription reaction (Master Mixture)	60
3.3	Prepared reagents mixture for pre-developed RT-qPCR reaction	61
3.4	Following Primers were used in the RT-qPCR reactions	61
3.5	Optimized qRT-PCR annealing reaction condition which is used to developed gene expression assays	62
4.1	Biosynthesis of metallic nanoparticles from biological substances and its reaction kinetics	66
4.2	Novel substrates using for biosynthesis of metallic nanoparticles	69
4.2	Antibacterial activity of biosynthesized silver nanoparticles against oral pathogenic bacteria	90
4.4	Preliminary identification of phytochemical constituents from <i>C. nudiflora</i> plant extracts	93
4.5	Quantitative analysis of phenolic and flavonoid contents from <i>C. nudiflora</i> crude extracts	94
4.6	Antioxidants activity of <i>C. nudiflora</i> plant extracts	94
4.7	Organic constituent's characterization by GC-MS	95

	from <i>C. nudiflora</i> extracts	
4.8	Summary of pros and cons of chemical and biological synthesis of nanoparticles	104
4.9	Calculated the RNA concentration from experimental samples	110



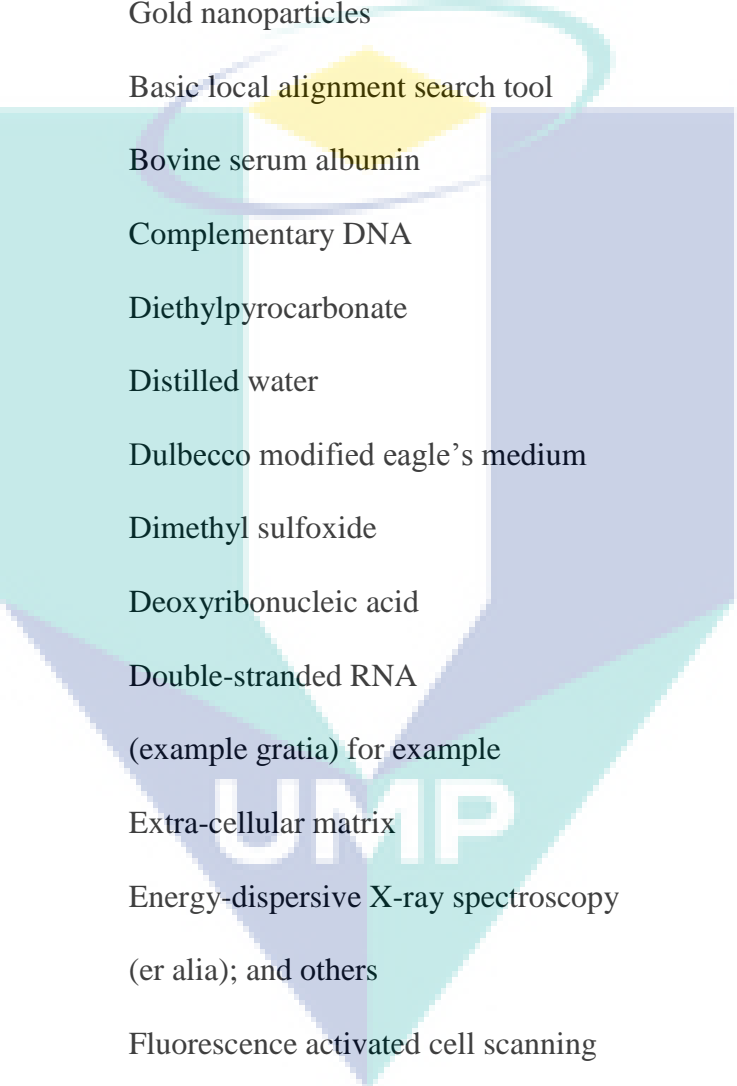
LIST OF FIGURES

Figure No.	Title	Page
2.1	Proposed mechanism of the phyllanthin stabilized gold and silver nanoparticles	9
2.2	Schematic representation of tannic acid reduction on silver ions into AgNPs	10
2.3	Possible mechanism for silver nanoparticles synthesis using <i>B. Licheniformis</i> . The biosynthesis of silver nanoparticle involving microbial NADH-dependent nitrate reductase enzyme that convert Ag^+ to Ag^0 through electron shuttle enzymatic metal reduction process	15
2.4	Proposed mechanism of Au biomineralization using <i>Rhizopus oryzae</i> fungi	18
2.5	Proposed mechanism of microbial enzymatic reduction gold ions into gold nanoparticles synthesis using <i>S. maltophilia</i>	21
2.6	AgNPs treated cells involved in the programmed cell death via apoptotic pathway	29
2.7	Different kind of cellular proteins that participate in programmed cell growth and differentiation function	30
2.8	Statistical report on age versus colon cancer patients in some Asian and Western countries	32
2.9	Colon cancer development from adenoma to carcinoma in different stages	33
2.10	Different gene expression in apoptotic intrinsic and extrinsic pathways	35
3.1	Photograph of <i>Commelina nudiflora</i> plant and dried in shadow condition	42
3.2	Reflux system set up used for biosynthesis of gold and silver nanoparticles by green chemistry methods	44
3.3	Flow chart of research methodology	47

3.4	Solvent extraction of <i>C.nudiflora</i> using soxhlet apparatus	50
4.1a	Colour indicates the reduction of H ₂ AuCl ₄ ions (a) plant extract (b) 10 ⁻³ H ₂ AuCl ₄ (c) mixture solution	64
4.1b	UV-VIS absorption spectrum of biosynthesized gold nanoparticles with time of intervals	64
4.2	Quantification of remaining Au ⁺ ions in the gold nanoparticles synthesized medium using ICP-MS	65
4.3	FESEM micrograph shows the different structure of gold nanoparticles by <i>Commelina nudiflora</i> extract	68
4.4	EDX graph expresses the presence of metallic gold from synthesized sample	69
4.5	Powder XRD of biosynthesized gold nanoparticles	70
4.6a	Functional groups are characterized by FT-IR spectra using <i>C.nudiflora</i> aqueous plant extract	72
4.6b	Functional groups are characterized by FT-IR spectra using <i>C.nudiflora</i> synthesized gold nanoparticles	73
4.7	Analysis of particle size distribution in plant synthesized gold nanoparticle sample	74
4.8	Zeta potential analyses of biosynthesized gold nanoparticles from <i>C. nudiflora</i> extract	74
4.9	TGA thermogram of <i>C. nudiflora</i> synthesized gold nanoparticles	75
4.10	BET plots of the synthesized gold nanoparticles	76
4.11	Antibacterial efficacy of AuNPs using <i>C. nudiflora</i> against different human pathogens a) <i>E.coli</i> b) <i>Bacillus subtilis</i> c) <i>Salmonella typhi</i> d) <i>Staphylococcus aureus</i>	77
4.12	A) DPPH free radical scavenging activity of different concentration of gold nanoparticles B) ABTS free radical scavenging activity of different concentration of gold nanoparticles	78
4.13a	a) <i>Commelina nudiflora</i> plant b) Colour formation after reduction of AgNO ₃ using <i>Commelina nudiflora</i>	80

	aqueous extract i) 5 min ii) 30min iii) 1 hrs iv) 2 hrs	
4.14	Quantification of remaining Ag ⁺ ions in the silver nanoparticles synthesized medium using ICP-MS	81
4.15	FESEM images of biosynthesized silver nanoparticles using <i>C. nudiflora</i> with different magnification powers	82
4.16	EDX spectrum of synthesized silver nanoparticles showing peaks between 2-4 keV	83
4.17	Powder XRD spectra of biosynthesized silver nanoparticles	84
4.18	Analysis of particle size distributions in synthesized silver nanoparticle sample	85
4.19	Zeta potential analyses of biosynthesized silver nanoparticles	86
4.20	TGA thermogram of <i>C. nudiflora</i> synthesized silver nanoparticles	87
4.21	BET plots of the synthesized silver nanoparticles	88
4.22	FT-IR spectra of AgNPs synthesized using <i>C. nudiflora</i> extract	89
4.23	The antibacterial efficacy of synthesized silver nanoparticles against oral pathogenic bacteria (a) <i>Staphylococcus aureus</i> (b) <i>E.coli</i> (c) <i>Porphyromonas gingivalis</i>	90
4.24	A) DPPH free radical scavenging activity of silver nanoparticles B) ABTS free radical scavenging activity of silver nanoparticles	92
4.25	GC-MS chromatogram of different solvent extracts from <i>Commelina nudiflora</i> a) Ethanol b) Aqueous	96
4.26	GC-MS chromatogram of different solvent extracts from <i>Commelina nudiflora</i> c) DCM d) Hexane e) Chloroform	97
4.27	Antibacterial activity of <i>C. nudiflora</i> extracts against human pathogenic bacteria a) Aqueous	98
4.28	Biosynthesized gold and silver nanoparticles on treated	101

	with HCT-116 colon cancer cells in 96 well plate	
4.29	Effect of cell viability in different concentration of biosynthesized gold and silver nanoparticles against HCT-116 cells by MTT assay (Bar diagram of gold nanoparticles)	102
4.30	Effect of cell viability in different concentration of biosynthesized gold and silver nanoparticles against HCT-116 cells by MTT assay (Bar diagram silver nanoparticles)	105
4.31	Flow cytometry histogram of HCT-116 cells treated with IC_{50} concentration of gold and silver nanoparticles for 24 h. a) Control b) gold nanoparticles (IC_{50}) c) AgNPs (IC_{50}) d) Negative control e) percentage of cell cycle	107
4.32	Typical confocal images (40 x magnifications) of HCT-colon cancer cells a) control, b) gold nanoparticles (IC_{50}), c) silver nanoparticles (IC_{50}) incubated for 48 hrs	109
4.33	The relative quantification of mRNA expression using RT-qPCR i) Melt curve of PUMA gene ii) mRNA expression of PUMA gene in HCT-116 cells treated with IC_{50} concentration AuNPs and AgNPs	111
4.34	i) Melt curve of Caspase-3 gene ii) mRNA expression of caspase-3 gene in HCT-116 cells treated with IC_{50} concentration AuNPs and AgNPs	112
4.35	i) Melt curve of Caspase -8 gene ii) mRNA expression of caspase-8 gene in HCT-116 cells treated with IC_{50} concentration AuNPs and AgNPs	113
4.36	i) Melt curve of Caspase -9 gene ii) mRNA expression of caspase-9 gene in HCT-116 colon cancer cells treated with IC_{50} concentration AuNPs and AgNPs	114

LIST OF ABBREVIATIONS

AgNPs	Silver nanoparticles
AgNO ₃	Silver nitrate
ANOVA	Analysis of variance
AuNP	Gold nanoparticles
BLAST	Basic local alignment search tool
BSA	Bovine serum albumin
cDNA	Complementary DNA
DEPC	Diethylpyrocarbonate
dH ₂ O	Distilled water
DMEM	Dulbecco modified eagle's medium
DMSO	Dimethyl sulfoxide
DNA	Deoxyribonucleic acid
dsRNA	Double-stranded RNA
e.g	(<i>example gratia</i>) for example
ECM	Extra-cellular matrix
EDS	Energy-dispersive X-ray spectroscopy
et al.,	(<i>er alia</i>); and others
FACS	Fluorescence activated cell scanning
FBS	Fetal bovine serum
FESEM	Field emission scanning electron microscope
Fig	Figure
g	gram
GNPs	Gold nanoparticles

HCT-116	Human colon cancer cell line
hrs	Hours
IC ₅₀	Inhibitory concentration at 50%
mg	Milligram
min	Minute
ml	Milliliter
MMP	Matrix metalloprotenase
mRNA	messenger ribonucleic acid
MTT	3-(4,5dimethylthiazol-2-yl)-2,5-diphenyl tetrazolium bromide
MW	Molecular weight
N	sample size
NaOH	Sodium hydroxide
NCI	National cancer institute
nm	nanometer
OD	optical density
p	the probability of obtaining the results
PBS	phosphate buffer saline
pH	phosphate ion concentration
RNA	Ribonucleic acid
RT	Room temperature
RT-PCR	Reverse transcription polymerase chain reaction
RT-qPCR	Real time quantitative polymerase chain reaction
TEM	Transmission electron microscopy
v/v	Volume/volume

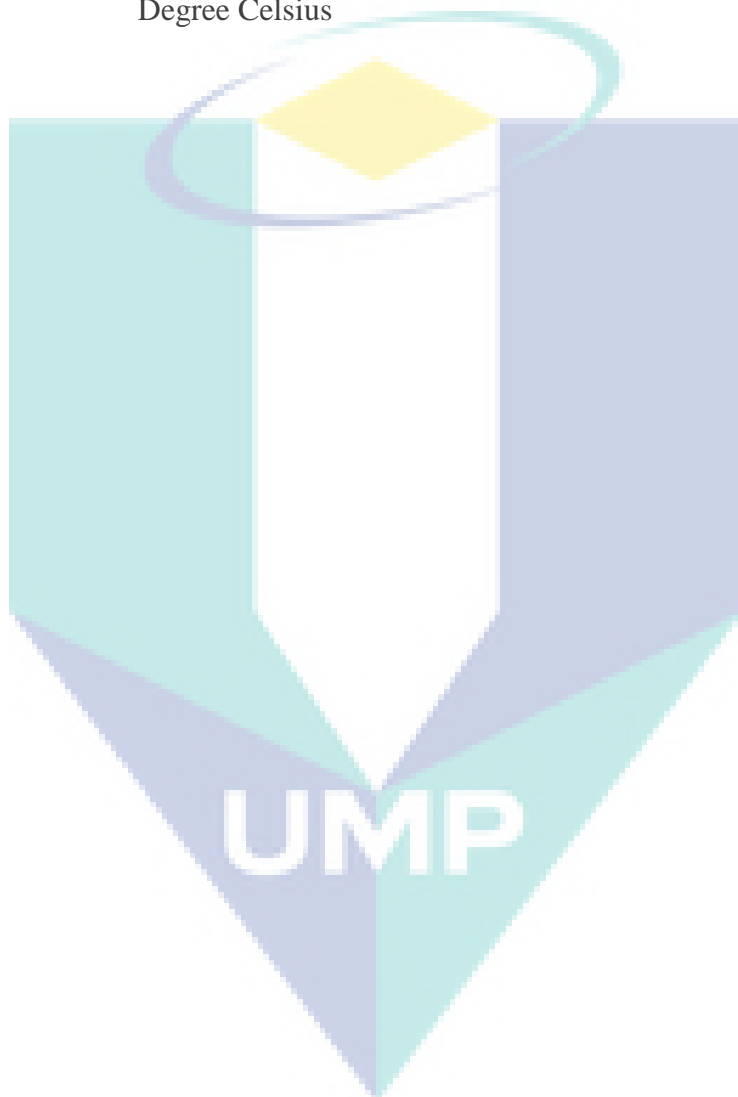
WHO World Health Organisation

LIST OF SYMBOLS

* Statistical significance denotation

μg Microgram

$^{\circ}\text{C}$ Degree Celsius



CHAPTER 1

INTRODUCTION

1.0 CHAPTER OVERVIEW

This chapter describes the rationale of this research. The literature review shows that metallic nanoparticles synthesized from plant resources offer antibacterial and anticancer properties. In addition, the scope of the study presents the synthesis of metallic nanoparticles using biological route and their biomedical applications. Finally, the research objectives are also provided.

1.1 BACKGROUND OF THE STUDY

Nanoparticles (NP) are the building blocks in nanotechnology and they have diverse applications in different fields such as biomedical, engineering, energy and environmental sciences. In general, nanoparticles are synthesized by physical and chemical procedures, as these methods produce the desired sizes of the particles in large scale (Akamatsu et al., 2003, and Seigneuric et al., 2010). However, the physical methods have some limits such as expensive, involve time consuming steps and complicated vacuum techniques are necessary. Usually, the chemical processes have two main problems. Firstly, high surface energy of nanoparticles may enhance the interaction with materials and they often undergo aggregation. This aggregation can be prevented by using polymers, surfactants and DNA on the nanoparticle surface. Secondly, concentrated chemicals are used as reducing and stabilizing agents (sodium borohydride, citric acid etc.) which may exhibit biological hazards to humans and the environment (Bigall and Eychmuller, 2010, and Antony et al., 2011). Hence, the chemical and physical syntheses of nanoparticles have limited applications in the

clinical fields. Therefore, the biological synthesis of nanoparticles is the alternative by using plants and microorganisms as substrates. Moreover, the biological mediated metallic nanoparticles are proven to be more biocompatible and have lower environmental toxicity. Thus, they can be useful for different biological applications including cancer treatments. The metallic NPs have been developed by using biological methods and evaluated in various preclinical or clinical studies, some of which have been approved for clinical cancer treatments (Chow, 2010; Reza Ghorbani et al., 2011). Moreover, the biosynthesized NPs also have the ability to reduce drug resistance and enhance therapeutic applications against chronic diseases. The biosynthesized metallic gold and silver nanoparticles are feasible drugs for treating cancer effectively due to the potent physico-chemical properties.

Cancer is the third leading cause of death worldwide after coronary diseases and diabetes. According to the World Cancer Report 2008 by WHO, the global cancer burden has doubled in the last four decades of the 19th century (Chithrani et al., 2006). In Malaysia, cancer is the second most dangerous class of disease. Among cancer, the colon cancer shows the highest rate recorded in Chinese and Indian followed by Malay citizens (Lim et al., 2006). Colon cancer is one of the most dangerous class of cancer and an early detection is difficult to be made. The cancer cells in the colon or rectum divide fast and uncontrollably, ultimately forming a malignant tumor. The colon and rectum are parts of the digestive system, which take up nutrients from food and water in the colon. Colon cancer is common in both men and women. The preliminary colon polyps can develop into malignant tumors (Jain et al., 2007). The traditional strategies for cancer treatment are surgery, radiation, and chemotherapy. But, these specialized therapies can be applied only at the preliminary stage of cancers. The physical method of cancer treatment is surgery. It is a good way to cure, particularly those which have yet to metastasize to distinct parts of the body (Douglas-Kinghorn, 2001). Once it is metastasized, the multiplications of cancer cells are difficult to be controlled. Therefore, these stages need new and more effective therapies.

The nanoscience has proposed many fabrication methodologies including biological synthesis method. The biological synthesis method has developed unique and

precise nanoparticles and it is possible to target cancer at different stages. On the other hand, the chemically synthesized nanomaterials also have specific sizes and shapes, but they are futile in clinical trials because of toxicity issues (Yoosaf et al., 2007). Therefore, the biosynthesis way is more effective, safe and may fulfill the following requirements: i) the drug concentration can be easily optimized which allows an effective dose at tumor cells without affecting normal cells, ii) could target tumor cells and prevent an uptake by normal cells, and iii) biological approach has a high biocompatibility.

Nanoparticle is defined as a sub-microscopic particle with the size that ranges between 1 to 100 nm. When the size of materials is reduced to the nano level, the properties change completely compared to bulk materials (Canizal, 2001, and Chaloupka et al., 2010). Gold nanoparticle (GNP) is a novel metal, has been utilized in many areas especially cancer diagnostics, coatings, thermal therapy, electronics and biotechnology (Gardea-Torresdey et al., 2003, and Kumar et al., 2007). GNPs can easily pass through the vasculature, be localized in targeted areas, and control the DNA transcription in cancer cells. The biological syntheses of gold nanoparticles are cheap, reliable and eco-friendly because of the naturally available plants acting as reducing and stabilizing agents and do not require any downstream process for purification of products. The plant extract contains various bioactive compounds which is able to reduce metal ions into metallic nanoparticles at room temperature (Sau et al., 2010).

On the other hand, silver nanoparticles also have unusual properties such as high antimicrobial activity, particle stability and surface chemistry (Krug et al., 1999, and Labouta and Schneider, 2010). Silver nanoparticles have specific surface plasmon resonance (SPR) peak wavelengths of between 450 nm (violet light) to 530 nm (green light). Different wavelengths express different particle sizes, shapes and surface properties (Jain et al., 2007). The AgNPs have been widely used as antimicrobial agents in healthcare, food industry, textile coatings and electronic devices (Reza-Ghorbani et al., 2011). Also, the AgNPs have been incorporated in many commercial products and approved by a range of accredited bodies, including the FDA (USA), SIAA (Japan) and KTR and FITI (Korea) (El-Nour et al., 2010).

1.2 PROBLEM STATEMENT

In this generation, the nanosized materials are very popular and they have numerous applications in different fields. The synthesis of nanoparticles by chemical and physical methods have been well established and successfully reported in literature. But, these methods use chemical precursors as a stabilizing and capping agents to promote the synthesis reaction. Therefore, these syntheses are not suitable for clinical use and harmful for living organisms and higher animals. However, plant extracts could act as a natural reducing and capping agent in reducing the reaction. The wide availability of bioactive compounds (metabolites) guarantees the metal ions reduction into metallic nanoparticles. In this study, potential edible weed plant *C. nudiflora* aqueous extract was used for the nanoparticles synthesis by environmental approaches.

On a different note, the increasing mortality of colon cancer cases in Asian countries is a big problem that needs to be controlled and treated. Also, the available cancer drugs are expensive and ineffective at different stages of cancer. According to the report of National Cancer Registry (Malaysia) the most frequent cancer cases is breast cancer and followed by colon cancer. The synthetic anticancer drugs (cisplatin, doxorubicin etc.) are costly and involve multiple purification processes in developing the product. The biosynthesis of metallic nanoparticles using plants is becoming a more fashionable and promising in drug development. However, other biological resources such as bacteria, fungi and algae need a huge investment for a large scale culturing and maintenance. Due to that, plant resources could be a better alternative resource for nanoparticles synthesis. The biosynthesis of nanoparticles uses plant extracts with no addition of any chemical stabilizing and capping agents, therefore, it could be 99% useful for all clinical studies. The plant mediated nanoparticles are highly effective, cost less and could be a counter point for future cancer therapy. In this study, *C. nudiflora* plant extract was used to synthesize gold and silver nanoparticles and evaluate the potent anticancer properties in HCT-116 colon cancer cells. Nevertheless, the mechanism of nanoparticle formation and function of colon cancer activity need to be explored in future. Although, the different molecular assays support the potential of

synthesized gold and silver have potent for *in-vitro* anticancer activities, the animal model studies are needed for further confirmation of metallic nanoparticle functions and their behavior.

1.3 RESEARCH OBJECTIVES

In this PhD work three objectives are focused. The specific goals were as follows:

- To biosynthesize Au and Ag nanoparticles using *Commelina nudiflora* aqueous extract and to characterize them by different analytical techniques such as UV-Vis, FESEM, EDX, XRD, FTIR, particle size analyser and zeta potential.
- To isolate and conduct a preliminary identification of the potential bioactive compounds from *C. nudiflora* extract using GC-MS.
- To evaluate *in-vitro* anticancer efficacy of synthesized Au, Ag nanoparticles against HCT-116 colon cancer cells and to conduct molecular characterization of HCT-116 colon cancer cells using flow cytometry and RT-qPCR techniques.

1.4 SCOPE OF THE STUDY

The goal of this study is to develop metallic Au and Ag nanoparticles using *C.nudiflora* aqueous extract and to study their potential biomedical applications such as *in-vitro* antibacterial and anticancer activities. The following research objectives require different experiments. For the first objective, the following experiments were used:

- Identify the weed plant, *C.nudiflora* for the biosynthesis of Au and Ag nanoparticles
- Optimize the ratio of plant extract (10 ml, 25 ml, 50 ml and 100 ml) and metal ion (10^{-2} M, 10^{-3} M, 10^{-4} M, 10^{-5} M) solution

- Optimize the temperature (35 °C, 50 °C, 60 °C, 70 °C) and pH (6, 7, 8) of the mixture of plant extract and metal precursor solution
- Identify the morphology, crystalline nature and metal composition using FESEM, XRD and EDX ,then, the functional groups and study the thermal stability by using FT-IR, TGA
- Identify the antibacterial and antioxidant properties of synthesized Au and Ag nanoparticles

For the second objective, the following procedures were used,

- Isolate bioactive metabolites from *C.nudiflora* using soxhlet apparatus
- Identify the phytochemical constituents using standard phytochemical screening procedure and GC-MS techniques
- Identify the antibacterial and antioxidant activity of *C.nudiflora* plant extract

For the third objective, the following experiments were carried out,

- Measure the cytotoxicity of Au and AgNPs against HCT-116 colon cancer cells
- Study the cell cycle phases in control and Au, Ag nanoparticles treated HCT-116 cells
- Determine the apoptotic genes expression in colon cancer cells treated with Au and Ag nanoparticles and cisplatin

1.5 STATEMENT OF THE CONTRIBUTION

This study produces biosynthesized Au and Ag nanoparticles using *Commelina nudiflora* aqueous extract for the first time. Thus, the *C.nudiflora* synthesized metal nanoparticles have the potential for *in-vitro* and the antibacterial antioxidant properties are proven. It is also reported that the *C.nudiflora* aqueous extract contains a cluster of bioactive metabolites which act as a natural reducing and stabilizing agent. Finally it is reported for the first time that the biosynthesized Au and Ag nanoparticles have effectively treated the HCT-116 colon cancer in *in-vitro*.

CHAPTER 2

REVIEW OF LITERATURE

2.0 CHAPTER OVERVIEW

This chapter describes the literature related to this research, various methods of synthesis of metallic nanoparticles using bio-substrates and their biomedical applications. Besides, different methods used to synthesize metallic nanoparticles and their bioactivities such as antimicrobial, antidiabetic and anticancer properties are also shown. In addition, the pros and cons of nanoparticles synthesis using other synthesis methods such as physical and chemical methods are also discussed. The detailed studies on plants used for the synthesis of metallic nanoparticles and its redox mechanisms are included. Furthermore, a few cancer molecular techniques and their principles are discussed too.

2.1 NANOMEDICINE

Nanoparticles promise a revolutionary in modern medicine for diagnosing and treating various chronic diseases particularly cancer and microbial infections (Dreaden et al., 2011). The studies in metallic nanoparticles have evolved as a major research direction in modern medicine to miniaturize drug size at nanoscale from macro scale level (Dykman and Khlebtsov, 2011). It is a well admitted science research that has the importance in several areas including medicine, pharmaceutical, opto-electronics, sensing and catalysis (Dong et al., 2007). The syntheses of monometallic and bimetallic nanoparticles such as Au, Ag and Au-Ag have shown a good impact in biomedical applications (Klabunde and Mulukutla, 2001). The biosynthesis of nanosized elements has used different resources such as plants, bacteria, fungi, micro and macroalgae (Seeman, 1982, and Liu, 2006).

2.2 BIOLOGICAL RESOURCES FOR THE SYNTHESIS OF GOLD AND SILVER NANOPARTICLES

2.2.1 Plant extract (broth) as a source

Biosynthesis of metal nanoparticles using plant extracts is an eco-friendly method and is a one-step synthesis procedure. Plants are the largest photosynthetic autotrophs (organisms capable of synthesizing their own food from inorganic substances, using light or chemical energy (e.g) green plants, algae, and certain bacteria) and have a high biomass production in terrestrial environment (Asharani et al., 2009). Plants utilize more than 70% of light energy from sun and convert it into chemical energy in the form of glucose. The plant products are being used as sustainable and renewable resources for the synthesis of nanoparticles (Narayanan and Sakthivel, 2011). However, an exact mechanism of the synthesis of nanoparticles using plants has not yet been elucidated. But, several hypothetical mechanisms have been proposed for nanoparticles formation using plant extracts (Jha et al., 2009, and Sujitha and Kannan, 2013). The biological synthesis procedure is a single step process and could eliminate the elaborate process of maintaining cell cultures and downstream processes (Sheeba and Thambidurai, 2009, and Nagati et al., 2012). Plant extracts contain various secondary metabolites such as alkaloids, flavonoids, saponins, phenolics, polysaccharides, proteins with electron-shuttling compounds which are usually involved in the synthesis of metal nanoparticles.

Shankar and et al. (2004) proposed that an *A. indica* aqueous plant extract reduces sugars (aldoses) and ketone which take place in the reduction of ionic chloroaurate into gold nanoparticles. Similarly, Richardson et al. (2006) asserted that plant leaf extracts contain carbohydrates and proteins which act as reducing agents for silver ions reduction. In addition, Chandran et al. (2006) reported that the formation of gold nanoparticles from an *Aloe vera* extract shows a relatively increased UV-vis absorbance peak with respect to time which is due the gradual growth of nanoparticles in the synthesis medium. Kasthuri et al. (2009) also studied the biosynthesis of gold nanoparticles using apiin isolated from *Lawsonia inermis*. The isolation of apiin was

done with methanol, which acts as the reducing and stabilizing agent in the formation of gold nanoparticles. The FTIR results confirmed that the strong interaction of carbonyl group of apiin with metal ions prevents the aggregation and facilitates the formation of nanoparticles. Philip (2011) produced different sizes and shapes of gold nanoparticles by varying the ratio of metal salt and leaf extract of *H. rosasinensis*. The synthesized gold nanoparticles were mainly spherical, triangular, hexagonal and dodecahedral with the size of ~14 nm calculated by TEM analysis.

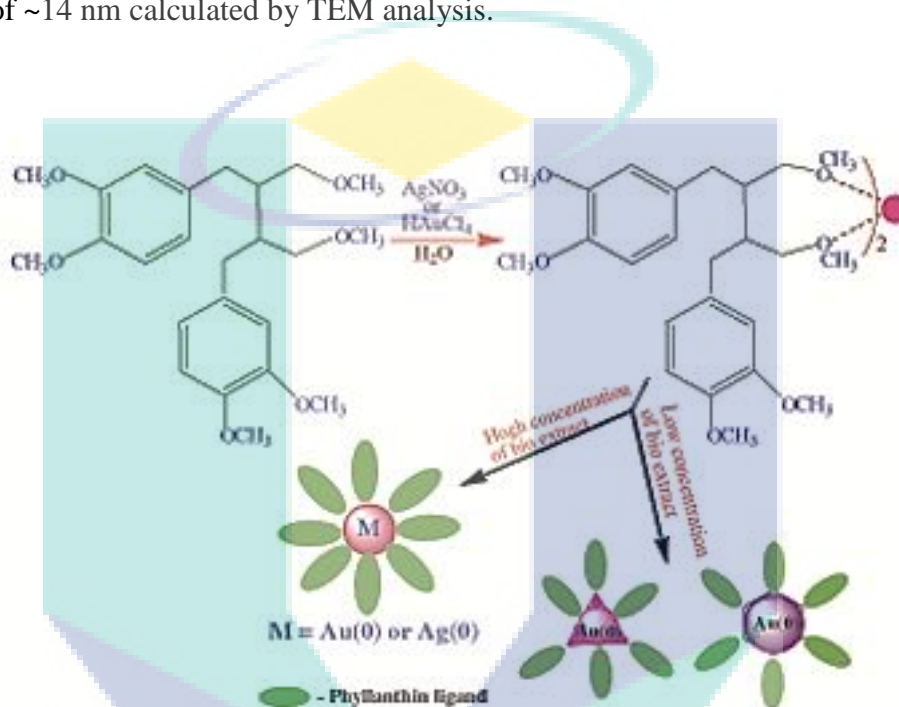


Figure 2.1: The proposed mechanism of phyllanthin stabilized gold and silver nanoparticles

(Source: Kasthuri et al., 2009)

FTIR spectra confirmed that the synthesized gold nanoparticles were stabilized through amino (NH₂) groups. The phyllanthin extract contains a wide range of secondary metabolites which promote the reduction of HAuCl₄ ions into Au metallic nanoparticles (Figure 2.1). On the other hand, a low concentration of plant extract facilitates the formation of triangular or hexagonal-shaped AuNPs. A high concentration of phyllanthin extract produces higher spherical NPs and this is confirmed by TEM analysis. Also, the electron donating nature of -OCH₃ (phenolics) group plays a vital role in the reduction reaction and synthesizing NPs.

In the last few decades, plant extracts or decoctions were used as an effective antimicrobial agent in controlling harmful pathogens. For instance, silver metal can fight against infectious agents, prevent spoilage of foods and cure wounds. At present, many researches have explored nano Ag as one of the better anti-bacterial agent. Figure 2.2 shows that the tyrosine amino acid residues are involved in the Ag^+ reduction under alkaline conditions. The alterations of the reaction conditions by increasing pH could causes the silver ion reduction in the presence of phenolic group in tyrosine (Selvakannan et al., 2004).

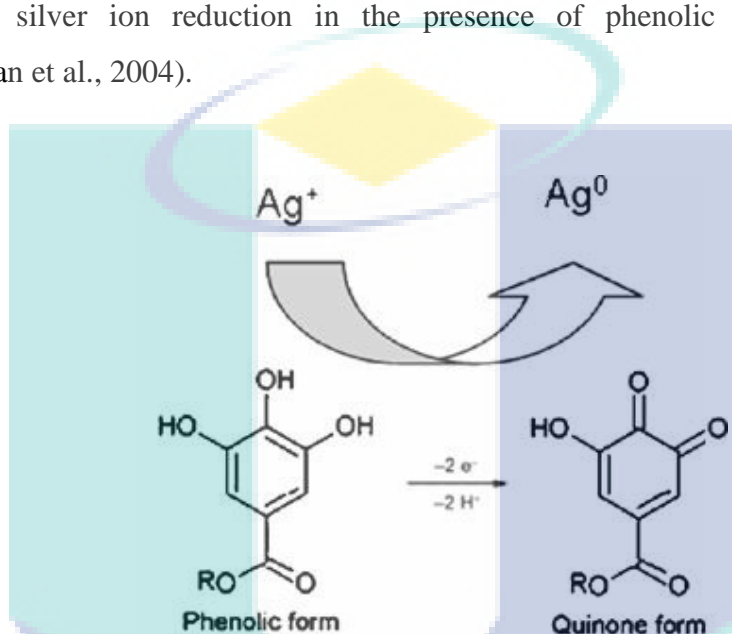


Figure 2.2: Schematic representation of tannic acid involved in the reduction of silver ions into nano-Ag

(Source: Sivaraman et al., 2009)

Tea and oak wood extracts contain different groups of polyphenolic compounds that act as reducing agents for silver nanoparticles synthesis. The silver nanoparticle shapes and sizes can be controlled by different molar ratio of silver nitrate solution and tannic acid. Also, phenolic compounds act rapidly as reducing agents where colour reaction is completed in 6 seconds which is faster than the chemical synthesis way. Dipankar et al. (2012) produced silver nanoparticles from aqueous leaf extracts of *I. herbstii*. The silver nanoparticles properties were proven by spectrophotometry studies which demonstrated UV-Vis characteristic peak of IhAgNPs at 460 nm. This confirmed the formation of the silver nanoparticles in the synthesis medium which is similar to

SPR peaks for silver nanoparticles prepared by chemical reductions. Table 2.1 shows the plant metabolites mediated metallic nanoparticles in biological approaches.

The *Aloe vera* extract synthesized silver nanoparticles using silver nitrate solution as the chemical precursor. The reaction was carried out with the presence of ammonia, which facilitated the formation of a soluble silver complex (diamine silver (I) chloride). The reaction mixture turned pale yellow after 24 hours of reaction and exhibited an absorbance peak at 410 nm (Chandran et al., 2006). Similarly, *C. zeylanicum* also synthesized the Ag nanoparticles. The aqueous plant extract contains complex polyols that are believed to have played a major role in the bioreduction of Ag ions. *C. zeylanicum* bark is also rich in terpenoids, including linalool, eugenol and methyl chavicol which contribute to the distinct aroma of the plant and the synthesis of nanomaterials. The *M. edule* aqueous leaves extract has the potential as a source for production of silver nanoparticles with environmentally friendly protocol. Water soluble compounds such as saponins and flavanoids are present in the *M. edule* extract. These compounds might be responsible for the reduction of silver and gold ions to metallic silver and gold nanoparticles. Also, the plant extract and AgNO₃ mixture solution color change indicates the formation of silver nanoparticles in the solution (Elavazhagan and Arunachalam, 2011). So, the different secondary metabolites from plant resources could be an excellent bioreductant for green synthesis of metal nanoparticles.

***Commelina nudiflora* L.**

Kingdom: Plantae; Sub-kingdom: Tracheobionta; Super Division: Spermatophyta; Division: Magnoliophyta; Class: Liliopsida; Sub Class: Commelinidae; Order: Commelinales; Family: Commelinaceae; Genus: *Commelina*; Species: *Commelina nudiflora* L.

Commelina nudiflora is a slender, nearly smooth creeping annual herb. It has simple branches of 15 to 30 cm long, reclining on the ground with roots at the nodes. The roots are fibrous and soft. The leaves are rather thick, linear, narrowed into base sheath, measuring from 3 to 10 cm long and 4 to 10 mm wide. The whole plant is edible and traditionally used to cure various acute and chronic diseases. In China, the plant

decoction is used to treat diarrhea and digestive problems. Also, the Egyptians use it for stomach obstruction. Indians use it to treat burns, itches and boils on skin. In Malaysia, the plant leaves are applied on scurf. In many countries, the plant is used for eye, ear, nose and throat related diseases, urinary tract diseases and gynecological treatment (Salata, 2004). The weed plant *C.nudiflora* possesses diuretic properties and control various urinary diseases. Also, it is used to treat other infectious diseases such as trauma, mumps and influenza.

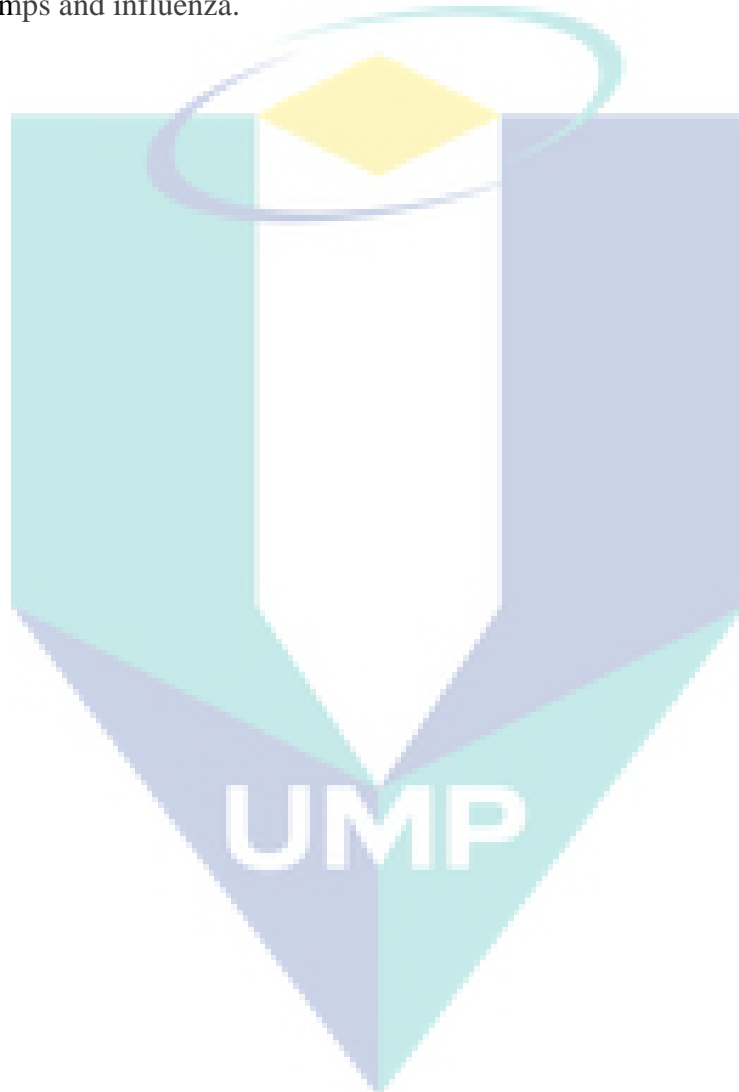


Table 2.1: Summary of plant derivatives synthesized metal nanoparticles in biosynthesis method and its biomedical applications

Plant used	Nanoparticles	Parts of plant	Plant metabolites involved in bioreduction	Pharmacological applications	Cited
<i>Alternanthera sessilis</i>	Ag	Whole	amine, carboxyl group	antioxidant, antimicrobial	Niraimathi et al., 2012
<i>Andrographis paniculata</i>	Ag	Leaves	alkaloids, flavonoids	hepatocurative activity	Suriyakalaa et al., 2013
<i>Artemisia nilagirica</i>	Ag	Leaves	secondary metabolites	antimicrobial	Song and Kim, 2009
<i>Cassia auriculata</i>	Au	Leaves	polysaccharides, flavonoids	antidiabetic	Santhosh kumar et al., 2011
<i>Cinnamon zeylanicum</i>	Ag	Leaves	water soluble organics	antibacterial	Sathishkumar et al., 2009
<i>Citrullus colocynthis</i>	Ag	Calli	polyphenols	antioxidant, anticancer	Satyavani et al., 2011
<i>Citrus sinensis</i>	Ag	Peel	water soluble compounds	antibacterial	Kaviya et al., 2011
<i>Dillenia indica</i>	Ag	Fruit	biomolecules	antibacterial	Singh et al., 2013
<i>Dioscorea bulbifera</i>	Ag	Tuber	diosgenin, ascorbic acid	antimicrobial	Ghosh et al., 2012
<i>Euphorbia prostrata</i>	Ag	Leaves	protein, polyphenols	antiplasmicidal	Zahir and Rahuman, 2012
<i>Gelcemium sempervirens</i>	Ag	Whole	protein, amide, amine group	cytotoxicity	Das et al., 2011
<i>Mirabilis jalapa</i>	Au	Flowers	polysaccharides	antimicrobial	Vankar and Bajpai, 2010
<i>H. canadensis</i>	Ag	Whole	phenolics, protein	cytotoxicity	Das et al., 2011
<i>T. graecum</i>	Au	Seed	flavonoids	catalytic	Aromal et al., 2012

2.2.2 Microorganisms source for synthesis of metallic nanoparticles

Microbes have many advantages in bioprocess industries including resistance towards heavy metal stress, oxidation-reduction reactions, and transport biomolecules across cell membrane and entrapment in extracellular capsules (Malik, 2004). Microbial bioreduction mechanisms might involve various kinds of secretory proteins,

carbohydrates and biomembranes. The microbial α -NADPH-dependent nitrate reductase (44 kDa) is involved as a bio-reductant in *in vitro* syntheses of silver nanoparticles. It acts as capping agents from microbial resources (Kumar et al., 2007). Duran et al. (2005) explained microbial metabolites such as quinine derivatives of naphthoquinones and anthraquinones which also act as redox substances in the reduction of ionic silver.

Bacteria as a precursor for biosynthesis of metallic NPs

Synthesis of inorganic nanomaterials use both unicellular and multicellular microorganism such as bacteria, algae and seaweed. Gurunathan et al. (2008) studied the supernatant of *E. coli* culture synthesized AgNPs, an environment-friendly method. Since then, the controlling of particle size and high yield of Ag nanoparticles present a big challenge in large scalable applications. Hence, a group of scientists provided the optimum reaction conditions and parameters for the maximum synthesis of metallic nanoparticles with control in particles size. The nitrate nutrient medium of bacteria culture contributing to the maximum synthesis of nanoparticles was reported. The supernatant culture of *E. coli* has faster conversion rate of more than 95%, compared with chemical synthesis method.

The microbial synthesized AgNPs have many positive attributes due to their smaller size, high stability, good conductivity and catalytic properties which make them suitable for many clinical applications. Moreover, the extra-cellular synthesis of nanoparticles could be a great advantage in pilot scale operations and easy downstream processings.

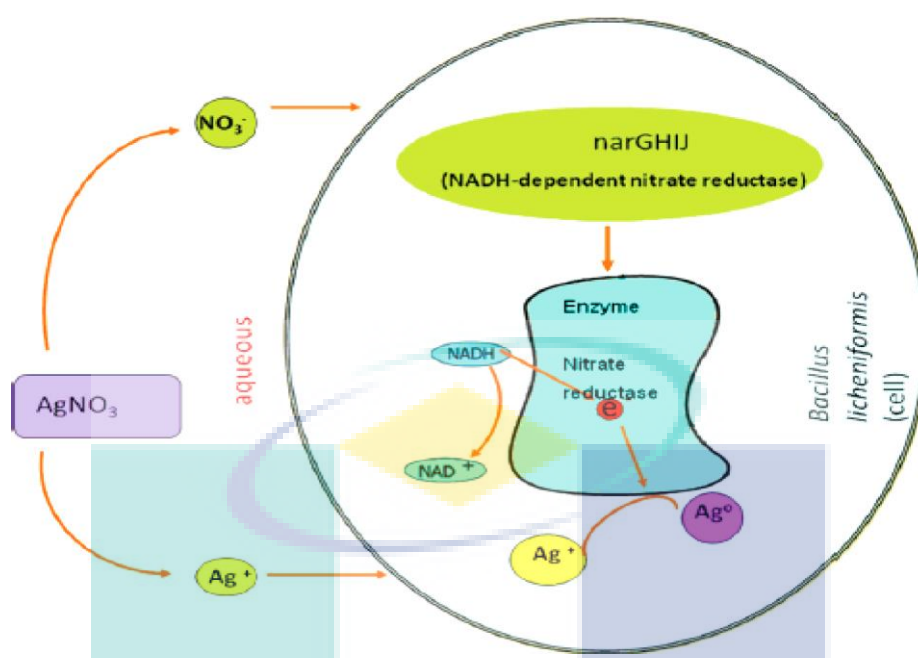


Figure 2.3: Possible mechanism of silver nanoparticles synthesis using *B. licheniformis*. The biosynthesis of silver nanoparticle involving microbial NADH-dependent nitrate reductase enzyme that may convert Ag^+ to Ag^0 through electron shuttle enzymatic metal reduction process

(Source: Kaliswaralal et al., 2010)

Plectonema boryanum UTEX 485, a filamentous cyanobacterium has been used to synthesize controlled size gold nanoparticles in a green chemistry method. The exponential growth culture was used and it reacted with aqueous $\text{Au}(\text{S}_2\text{O}_3)$ and AuCl_4 solutions at 25 to 100 °C for up to 30 days. After the reaction, the product was precipitated and observed in an electron microscope which showed the result of cubic gold nanoparticles and octahedral gold platelets (Lengke et al., 2006).

Fungi as a source for nanoparticles synthesis

Fungi is a spore producing microorganisms and it has many advantageous compared to other microbes. Generally, fungal mycelial mesh can withstand flow pressure, agitation and other conditions in downstream processing (Mukherjee et al., 2002, and Senapati et al., 2004). Fungal cultures are used to synthesize metallic

nanoparticles mediated by secretory proteins and precipitate outside the cells and devoid of unnecessary cellular components in the nanoparticles products. So, it can be directly used for biomedical applications (Nath and Banerjee, 2013). Figure 2.4 illustrates the fungal culture synthesis of gold nanoparticles in green chemistry approaches.

The extracellular syntheses of metallic nanoparticles have many advantages such as unnecessary adjoining cellular components in the synthesis medium and down stream processing. Fungus can synthesize nanoparticles from outside the cell wall. Fungus produces enormous secretory components including proteins and enzymes which could act as reducing and capping agents in the synthesis of nanoparticles. Shankar et al. (2003) reported rapid reduction of gold ions to zero-valent gold nanoparticles using endophytic fungus *Colletotrichum* sp. The fungus species is isolated from the leaves of a geranium plant (*Pelargonium graveolens*). It produces gold particles that are spherical in shape with the size that ranges from 8 to 40 nm. Also, fungus produces glutathione metabolites that bind either through free amine group or cysteine amino acid residues to synthesize gold nanoparticles. Similarly, *Trichothecium* sp. fungus was used at stationary phase condition where it has successfully reduced Au^{3+} to GNPs. TEM images explored the well-defined morphology such as triangle and hexagonal gold nanoparticles synthesized by the fungal culture. The average size of gold nanoparticles was found to be in the range of 5 to 200 nm and the Scherrer's ring pattern was the characteristic of face centred cubic (fcc) gold (Ahmad et al., 2005).

Bhainsa and D'Souza, (2006) studied the biosynthesis of silver nanoparticles using spore producing fungus *A. fumigatus* as a natural substrate. After the addition of silver nitrate with fungal cultures, the product was formed in 10 minutes. TEM micrograph showed the nanoparticles with variable shapes, predominantly in spherical and triangular shapes. Also, Mukherjee et al. (2001) proposed biological synthesis of gold nanoparticles using *Verticillium* sp in a one pot synthesis step. The gold nanoparticles were synthesized on the surface of the cytoplasmic membrane of fungal mycelium. The fungal extracellular extract successfully synthesized well-defined spherical, few triangles and hexagonal nanoparticles with good dispersity. On TEM analysis, ultrathin sections of fungal mycelia shown on the cell wall contain quasi-

hexagonal morphology of nanoparticles. Vigneshwaran et al. (2007) showed that the *Aspergillus flavus* mediated syntheses of silver nanoparticles were accumulated on the surface of cell wall when incubated with silver nitrate solution for 72 hours.

Similarly, Gade et al. (2008) reported that the *A. niger* isolated from soil produced spherical in shape silver nanoparticles with the size of 20 nm in diameter. The reduction of Ag^+ ions occurred by the presence of nitrate-reductase enzyme in the medium as proven by UV-Vis spectra. The fungal mass of *Phoma glomerata* is an efficient candidate for biosynthesis of silver nanoparticles with the size range of 60 to 80 nm and spherical in shape. These biological derived silver nanoparticles exhibited antibacterial activity against various pathogenic bacteria such as *E. coli*, *P. aeruginosa* and *S. aureus* (Birla et al. 2009).

Kathiresan et al. (2009) studied rhizospheric fungus, *Penicillium fellutanum*, which is isolated from mangrove root-soil of *Rhizophora annamalayana* Kathir. *Penicillium fellutanum* synthesis controls the size and shapes of the silver nanoparticles within 24 hours. Furthermore, the TEM micrograph revealed that the synthesized nanoparticles were spherical in shape with the sizes that range from 5 nm to 25 nm. The purified 70 kDa fungal protein was partially confirmed as a capping agent for the nanoparticles formation. Mukherjee et al. (2002) examined the synthesized gold nanoparticles using fungus and successfully synthesized gold nanoparticles in spherical and triangular shapes with the size range of 20 to 40 nm. The electrophoresis study revealed that the protein of molecular mass between 66 kDa and 10 kDa was involved in the nanoparticles stabilization. Similarly, Senapati et al. (2004) proposed extracellular synthesis of silver nanoparticles and bimetallic gold-silver (Au–Ag) alloy nanoparticles using *F. oxysporum*.

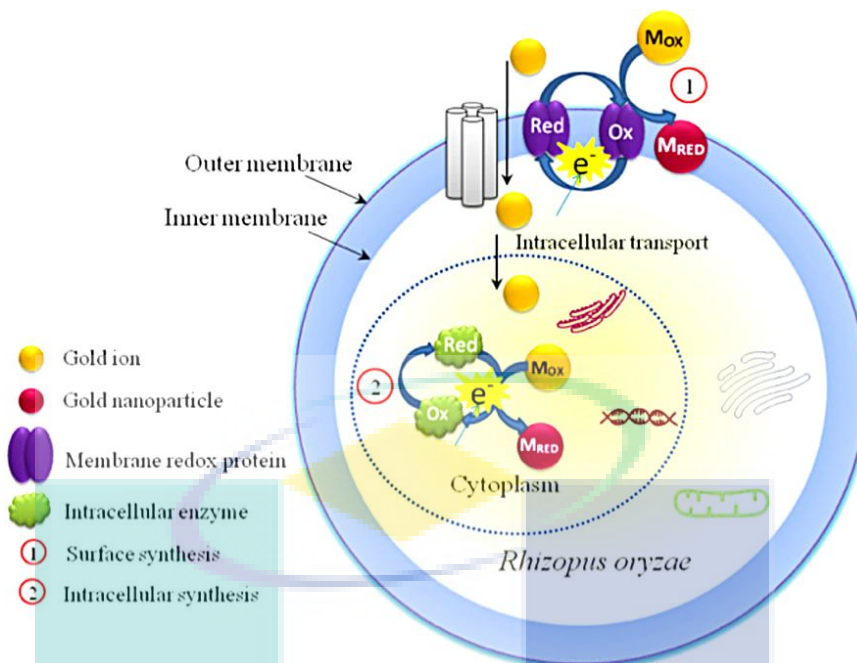


Figure 2.4: Proposed mechanism of Au biomineralization in *Rhizopus oryzae* fungi

(Source: Das et al., 2012b)

Marine organisms as source for NPs synthesis

Marine organisms produce remarkable nanofabricated structures from their cell wall, shells, pearls and bones. The marine microorganisms such as bacteria, cyanobacteria, yeasts, fungi, and micro-macro algae are reported to successfully synthesize inorganic nanoparticles either in intracellular or extracellular extracts. The mangroves, salt marshes sand dune and marine animals such as finfish and sponges are also reported as potential sources for synthesizing metallic nanoparticles (Asmathunisha and Kathiresan, 2013). The exopolysaccharide is a potent therapeutic substance and originates from different marine and terrestrial microorganisms. The biofloculant substances are secreted from marine organisms and they are promising alternate substances for the synthesis of metallic nanoparticles. Sathiyarayanan et al. (2013) studied a biofloculant (MSBF17) producing marine sponge-associated *Bacillus subtilis* MSBN17 under submerged fermentation.

Microalgae diatom has silica material in its cell wall. Diatom contains high amount of unsaturated fatty acids and lipids which synthesize gold and silica

composites in biological methods. The silicate nanoparticle has the potential in applications in commercial industries such as a barrier to gas, and packaging. Other marine organisms such as dinoflagellates, sponges, seaweeds also synthesize metallic nanoparticles in green chemistry methods as shown in Table 2.2. The marine sponge *Acanthella elongata* produces gold nanoparticles at room temperature and with the optimum pH condition at 6.5. The sponge extract contains water-soluble organics which act as a potential stabilizing agent in the reduction of metal ions (Asmathunisha et al., 2013). Also, silver nanoparticles are synthesized using cod liver which acts as a natural reducing agent as well as a surfactant. The fish oil contains different functional metabolites such as carboxylate, amide and amine groups which trigger *in situ* generation of organically capped silver nanoparticles.

Table 2.2: Summary of marine organisms used for biosynthesis of nanoparticles
(Asmathunisha and Kathiresan, 2013)

Organisms	Name of Species	Types of nanoparticles	Size (nm)	Biological activity	Authors and year
Marine microbes	<i>Spirulina platensis</i>	Silver Gold Bimetallic	7-16 6-10 17-25	-	Govindaraju et al., 2008
Marine algae	<i>Sargassum wightii</i>	Gold	8–12	–	Singaravulu et al., 2007
Marine spermatophytes	<i>Xylocarpus mekongensis</i>	Silver	5–20	Antimicrobial	Asmathunisha et al., 2010
	<i>Citrullus colosynthis</i>	Silver	85–100	Anticancer	Satyavani et al., 2011

Marine bacteria *P. aeruginosa* M6 when isolated from mangrove ecosystem is a potential source for the synthesis of silver nanoparticles. The cell-free extract (CFE) of *P. aeruginosa* M6 demonstrates the synthesis of silver nanoparticles using two physical methods, such as boiling conventional thermal treatment (CTT) and microwave treatment (MWT) at an alkaline condition of pH 9. The Atomic Force Microscopy (AFM) results confirmed that the large-sized, aggregated nanoparticles were

synthesized via MWT (M-NPs). Fourier Transform Infrared (FT-IR) graph showed both C-NPs and M-NPs were capped with proteins and extra cellular metabolites (Boopathi et al., 2012).

2.2.3 Enzymes reduced metal ions

Enzymes are widely used as biocatalysts in food, chemical, pharmaceutical, and fermentation industries. Biocatalysts have selective substrate specificity and catalytic activity in most of the chemical reactions. Nangia et al. (2009) proposed NADPH-dependent reductase enzyme which is present in the *Stenotrophomonas maltophilia* that could convert Au^{3+} to Au^0 through electron shuttle enzymatic metal reduction process (Figure 2.5). The NADPH enzyme has enabled the production of stable metallic GNPs via biosynthesis method. The gold chloride and enzyme redox-reaction takes place in two steps. Firstly, AuCl_4^- ions and bacterial enzymes react in optimum conditions and rapidly reduced to Au^+ ions. Secondly, the latter product is reduced by metallic gold nanoparticles in the presence of NADPH, and then encapsulation of GNPs by charged NADP^+ species. The following redox reaction occurs in the presence of NADPH:



The HR-TEM and UV-Vis spectroscopic studies proved that there were two major distributions in particles size with the size range of 20 to 100 nm. The smaller particles are mostly stabilized by the cyclic octapeptide, i.e. curcacycline A and cyclic nonapeptide namely, curcacycline B. Alternatively, the larger or irregular shape particles are mainly stabilized by curcain. Curcain is an enzyme, present in the latex of plant extract (Bar et al., 2009).

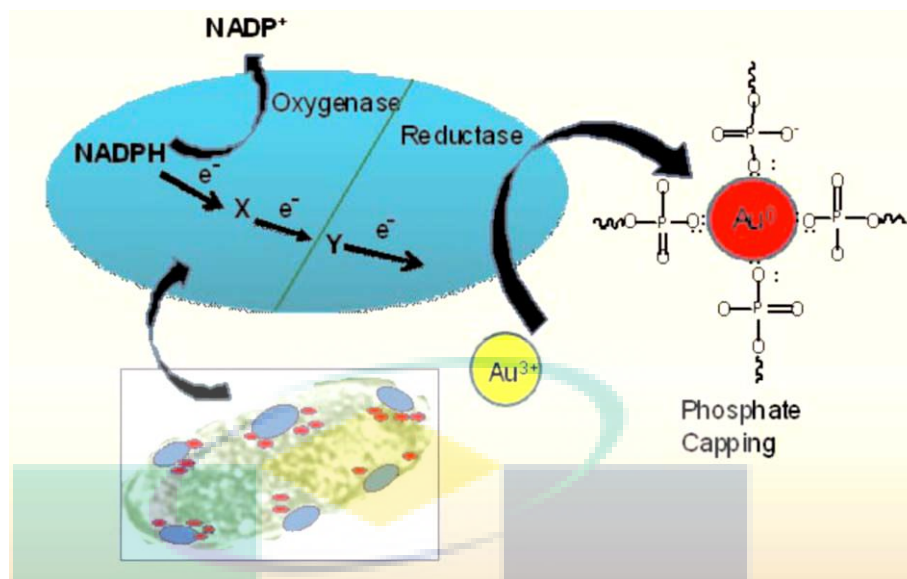


Figure 2.5: Proposed mechanism of microbial enzymatic reduction of gold ions into gold nanoparticles using *S. maltophilia* extract

(Source: Nangia et al., 2009)

The environmentally benign and renewable latex of *J. curcas* could be used as an effective capping and reducing agent for silver nanoparticles synthesis. The biosynthesized silver nanoparticles are quite stable and no colour changes were observed, even after a month or so, if the nanoparticle solutions are kept in a light proof condition.

2.2.4 Human cell lines as source for synthesis of metallic nanoparticles

Human cells are heterotrophic which means that they depend on energy and nutrients from autotrophs. The cells could produce some metal nanoparticles in *in vitro* conditions that mimic their natural cell environment. For instance, incubation of 1 mM of tetrachloroaurate solution with human cancer cells like SiHa (malignant cervical epithelial cells), SKNSH (human neuroblastoma) and HeLa (malignant cervical epithelial cells), and non-cancer cells like HEK-293 (non-malignant human embryonic kidney cells) synthesize gold nanoparticles with the size range of between 20 to 100 nm. The nanoparticles are identified in the cytoplasm regions and in the nucleus of the cells (Anshup et al., 2005).

2.3 DIFFERENT PHYSICO-CHEMICAL FACTORS INDUCING METAL NANOPARTICLES SYNTHESIS

The hydrogen ion concentration (pH) of the synthesis medium responds for the different sizes and shapes of nanoparticles formation. Shankar et al. (2003) reported that the *Aloe vera* extract produces Au-Ag core nanoparticles in various sizes and shapes by the fluctuating of the pH of the synthesis medium. Similarly, biosynthesis of nanoparticles using *alfalfa* plant extract produces different sizes by increasing the pH of the medium. On the other hand, temperature is also one of the stimulating factors in the nanoparticles synthesis procedure. Raju et al. (2011) revealed that a high temperature could increase the formation of higher spherical NPs and nano triangles, whereas the lower reaction temperatures mostly increase the nano triangle formation. The difference in the morphology of nanoparticles is mainly percentage or the amount of the salt precursor in the reaction mixture. The concentration of salt could alter the reduction ability and sizes of the nanomaterials. The metallic crystal structure has been controlled using the plant biomass as substrates. In addition, the reaction time is one of the major factors to evaluate the reduction of metal ions into bulk metal. The UV-Vis absorbance peak value indicates the reduction rate of NPs in the medium (Rai et al., 2006). So, the pH, temperature, metal ion concentration, plant extract concentration and secondary metabolites play a major role for the biosynthesis of metallic nanoparticles and their biological activity.

2.4 DIFFERENT METHODS USED FOR SYNTHESIS OF NANOPARTICLES

Generally, metal nanoparticles are prepared by different methods such as chemical and physical approaches. These methods have successfully produced pure metallic silver nanoparticles with specific sizes and shapes. But, these methods require external stabilizers and capping agents to initiate the reduction reaction and protect the nanoparticles against agglomeration.

2.4.1 Physical methods used for synthesis of nanoparticles

There are different kinds of physical methods used to synthesize metallic nanoparticles. These methods do not involve toxic chemicals but usually long radiation exposure and high temperature are necessary. The physical methods include physical vapor condensation (pvc), microwave irradiation, arc-discharge, sonochemical (Sapsford et al., 2013), photo-catalytic reduction, photo-chemical or radiation–chemical reduction, ultra-violet irradiation, metallic wire explosion, photo-reduction, reverse micelle based methods, laser ablation and thermolytic process (Rajasekharreddy et al., 2010, and Howes et al., 2014).

2.4.2 Chemical methods used for synthesis of nanoparticles

Chemical methods are established techniques to synthesize metallic nanoparticles in an efficient and faster way. However, these methods need external stabilizing agents to promote the reactions which perhaps produce adverse effects to human and living organisms. The different chemical methods to synthesize NPs are sono-chemical, polyols, matrix chemistry, sol gel method, chemical reduction, photochemical method (irradiation), electrolysis and pyrolysis etc, (Chimentao et al., 2004, and Sau and Rogach, 2010). The different polymers and ligands act as stabilizers for the preparation of metal nanoparticles in chemical methods. Some popular stabilizing agents are poly (N-isopropylacrylamide) (Chen and Akashi, 1997), nitrocellulose (NC) or cellulose acetate (CA), octanethiol (Dassenoy et al., 1998) and so on. The polymer (or ligand) serves not only as a stabilizer, but also as a shape and size directing agent.

Ion exchange method

The different ion exchange resins are used for the production of metallic NPs with varying sizes. In this method, metal ions are initially adsorbed into a polyamide surface and then, reduced to metal NPs via hydrogen reduction (Akamatsu et al., 2003).

Sol gel process

In this mechanism, the reagents (metal ion solutions) are rapidly added into a reaction vessel which contains a hot coordinating solvent such as alkyl phosphate, pyridine and alkylamine furan (Qu and Dai, 2005). This quick addition of reagents increases the chemical precursor concentration, with the solution becoming supersaturated due to the high chemical reaction temperatures. As a result, a short nucleation burst occurs. This method produces a nanocluster growth of metal species, and maybe uniform and mono-dispersed.

Precipitation

In the precipitation process, organic molecules are utilized to control the reagents and metal ions in solution and the product formed in the precipitated form (Senapati et al., 2005). The physical and chemical factors such as reactant concentration, pH and temperature are optimized for the syntheses of metal and non-metal nanoparticles by precipitation.

Pyrolysis

Pyrolysis is one of the established methods in chemical synthesis procedure. It has been used to prepare different types of nanoparticles including metals, metal oxides, semiconductors and composite materials. Generally, the pyrolytic synthesis of materials in powder form is used to get uniform nanosized material, and revisions of the procedure need to be done such as slowing of the reaction or decomposition in an inert solution (Senapati et al., 2005).

Micelles

A variety of nanoparticles such as Pd, Pt, Rh and Ir have been synthesized using reversed micelles method with reducing agents such as NaBH_4 , N_2H_4 and H_2 being

used (Ingelsten et al., 2001). The method has some drawbacks such as water content of the micelles seems to greatly affect the shape of nanoparticles (Qi and Wang, 2005).

2.4.3 Biological approaches of nanoparticles synthesis

Physical and chemical methods of nanoparticle fabrication usually involve toxic chemicals and long radiation, temperature exposure which is harmful to the environment (Tomczak et al., 2007). Nowadays, scientists have turned to biological synthesis method because the control over size distribution of nanoparticles. In recent times, the living organisms such as plants, bacteria, fungi and algae are used as potential reducers for metal ions. Besides, the plants have recently been explored as potential biofactories for the synthesis of metallic nanoparticles such as gold, silver, zinc, CdS, Ti, copper and Ni (Stepp and Moreman, 2001, and Sanchez-Mendieta and Vilchis-Nestor, 2012).

2.5 PHARMACOLOGICAL APPLICATIONS OF METALLIC NANOPARTICLES

2.5.1 Antibacterial and antifungal activities of NPs

In the recent days, the increasing microbial resistance towards the available antimicrobial agents has been a major problem in pharmaceutical and medical industries. Due to that, a development of a novel antimicrobial agent is needed to inhibit the growth of multidrug resistance pathogenic microorganisms (Yeo et al., 2003, and Mukherjee et al., 2014).

Gold and silver have been known as potential antimicrobial agents with unique properties such as high conductivity, stability, larger surface area to volume ratio and high binding capacity with pathogenic organisms. Therefore, NPs effectively act against resistant microbes and become a broad spectrum of antimicrobial agents. AgNPs are also known to possess bactericidal effects against clinical pathogens (Antony et al., 2011). The biosynthesized silver nanoparticles using fruit extract of *T. terrestris* have an

excellent antimicrobial activity against clinically isolated multidrug resistant human pathogens. The synthesized silver nanoparticles have effectively control the *S. pyogenes*, *S. aureus*, *B. subtilis*, *P. aeruginosa* and *E. coli* with the highest zone of inhibition rate measured (Gopinath et al., 2012).

Similarly, the biologically derived silver nanoparticles using leaves of *A. indica* have excellent antimicrobial activity. The antimicrobial mechanism was demonstrated where silver nanoparticles have increased the membrane permeability and respiration activities of bacterial cells. Also, these plant mediated silver nanoparticles could be useful in the industrial effluent treatment process for reducing the microbial load (Krishnaraj et al., 2010). Kumar and Yadav, (2008) reported that the silver with oxygen association, reacts with sulfhydryl ($-S-H$) groups on the cell wall of bacteria and forms $R-S-S-R$ bonds, thereby blocks the respiration of the bacterial cells and causes the death of the cells.

In addition, the silver nanoparticles have a considerable antimicrobial activity against gram positive bacteria compared with gram negative bacteria species. The gram negative bacteria outer membrane contains high lipopolysaccharide and a thick peptidoglycan layer. The negatively charged AgNPs can bind with the positively charged bacterial cell wall better. Due to that, AgNPs have a stronger bind with the rigid peptidoglycan layer of gram negative bacteria (Sanvicens and Marco, 2009). Fayaz et al. (2010) study supported that gram negative bacteria were killed more rapidly than gram positive bacteria. Similarly, Sarkar et al. (2007) reported silver nanoparticles have greater bactericidal effect compared to penicillin antibiotics. The silver NPs have greater affinity to react with sulfur- or phosphorus-containing biomolecules in the cell wall of microorganisms. Therefore, the sulfur-containing proteins in the membrane or inside the cells or phosphorus-containing elements like DNA are preferential binding sites for silver nanoparticles.

2.5.2 Antifungal activity of Au, Ag nanoparticles

The fungicidal mechanism of biosynthesized metallic nanoparticles has proven to be more effective than commercial antibiotics like fluconazole and amphotericin. The plant derived Ag, Au nanoparticles are damaged cell membranes of *Candida* sp. and finally fungal inter cellular components were disturbed and cell function was destroyed (Logeswari et al., 2011). Most of the commercial antifungal agents have limited applications clinically. Also, there are more adverse effects and less recovery from microbial diseases. Subsequently, the commercial drugs induce side effects such as renal failure, increased body temperature, nausea, liver damage, and diarrhea. Accordingly, nanoparticles were developed for novel and effective drug against fungal microbes. The fungal cell wall is made up of high polymer of fatty acid and protein. The multifunctional AgNPs have promising activity against spore producing fungus and effectively destroy the protein layer. The fungal cell membrane structure significant changes were observed by treating with metallic nanoparticles (Gardea-Torresdey et al., 2002).

The biosynthesized gold nanoparticles inhibited the growth of *Candida* isolates by involving different kinds of mechanisms. The H⁺-ATPase-mediated proton pumping activity, and the glucose induced the acidification of the cultured extracellular medium. The interaction of metal compound with the plasma membrane is sufficient to affect the function of the enzyme. Thus, gold nanoparticles may directly interact with the protein, which serves as the primary reason for fungal death. Secondly, the gold being a soft acid and might interact strongly with the soft bases like SO₃-containing proteins in the membrane or phosphorus containing bases in the DNA, thus controlling their normal functions like synthesis, repair and replication mechanisms eventually leading to the cell death (Wani and Ahmad, 2013)

2.5.3 Antidiabetic management of metallic nanoparticles

Diabetes Mellitus (DM) is a group of metabolic dysfunction with uncontrolled sugar level in blood. The insulin pills, certain foods and a balanced diet can prevent it at

certain levels. However, the biosynthesized nanomaterials could be an alternative drug to control the diabetes mellitus effectively. Daisy et al. (2012) showed that the gold nanoparticles have good therapeutic effects against diabetic induced animal models. The synthesized gold nanoparticles significantly reduced the level of liver enzymes such as alanine transaminase, alkaline phosphatase, serum creatinine, and uric acid in treated diabetes mice. Also, the gold nanoparticles treated diabetic model showed a decrease of HbA_{1c} (glycosylated hemoglobin) level and maintained the normal HbA_{1c} range. Swarnalatha et al. (2012) explored the *Sphaeranthus amaranthoides* mediated silver nanoparticles where they inhibited α -amylase and acarbose sugar in diabetes induced animal models. Also, the α -amylase inhibitory bioactive components were present in the ethanolic extract of *S. amaranthoides* (Manikanth et al., 2010). Likewise, Pickup et al. (2008) reported that the nanoparticles are potent therapeutic agents to control diabetes with less side effects. Clinical studies revealed that the silver nanoparticles which treated mice successfully controlled the sugar level of 140 mg/dl compared with the diabetes induced group.

2.5.4 Anticancer activities of metal NPs

Cancer is the second leading disease that causes death worldwide. Currently, five in two deaths in Asian countries are due to cancer. Cancers can attack people at any ages, and about 70% of all cancers are diagnosed in late disease condition (Tong, 2010, and Mohanpuria et al., 2008). There are different types of cancers such as breast, oral, cervical, lymphocyte and colon cancer. The various commercial drugs are available in market which are able to control them in the preliminary stages, but in a metastasis stage, they are less active. Also, conventional anticancer therapies have lack of generality and effectiveness in advanced stages of the disease. Apart from that, they have numerous adverse effects such as using long radiation or toxic chemicals in the treatment process. On the other hand, the introduction of biological nanomaterials has developed newer therapeutic approaches against cancer, and it could control cancers at the cellular and genomic levels (Sun, 2007).

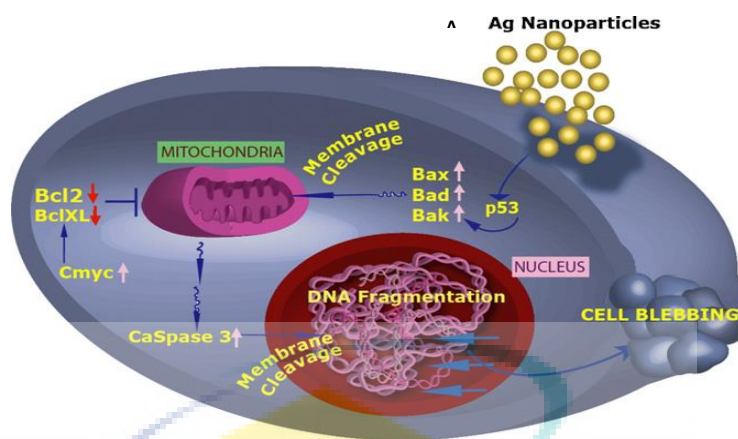


Figure 2.6: AgNPs treated cancer cells are involved in the programmed cell death via apoptotic pathway

The metallic SNPs have specific affinity molecules on their surface to attach to the outer membrane of the pathogens and damage the structure of cell walls and the activation of p53 protein in cancers. The p53 is known as an activator of pro-apoptotic genes where it activates bax, bad and bak genomic proteins. These proteins mainly cause mitochondrial membrane leakage and release Cyt C. The Cyt C is involved in the cascade reaction for activating caspase genes mediated cell death. Caspase-3 gene is induced by metallic silver nanoparticles which led to the cleaving of nuclear membrane and the stimulation of DNA fragmentation. The up-regulation of C-myc oncogene in the cancer model could induce the programmed cell death in cancer. Also, the AgNPs stimulate the apoptotic signals and down-regulation of anti-apoptotic genes, bcl-2 and bcl-XL and consequent cell death occurs (Gopinath et al., 2010).

The biosynthesized nanomaterials have less toxicity due to the bio-substrates used as a precursor. The fundamental aspect of apoptosis is induced by metallic nanoparticles and thus, their subsequent uses would depend on physico-chemical properties of nanoparticles (Smith et al., 2012). The metal nanoparticles act as a potential drug to induce the apoptotic mechanism including nuclear condensation, membrane blebbing and DNA fragmentation (Sudhakar, 2009). Figure 2.6 shows the therapeutic strategies of Au and Ag nanoparticles to control the molecular behaviours of cancer. The AgNPs induce apoptosis in cancer cells by stimulating the tumor suppressor genes, the genes which are responsible for the programmed cell death. The AgNPs have

higher affinity with mammalian cells and eventually stimulate the p53 dependent or mitochondria mediated DNA fragmentation which leads to programmed cell death (Sonavane et al., 2008).

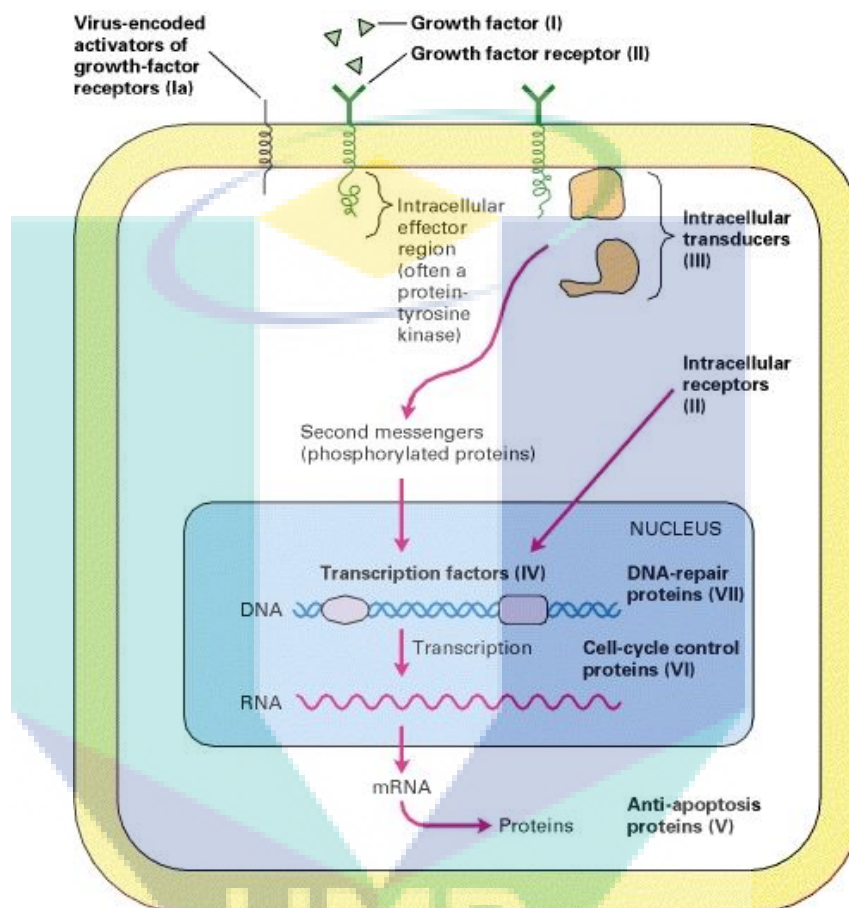


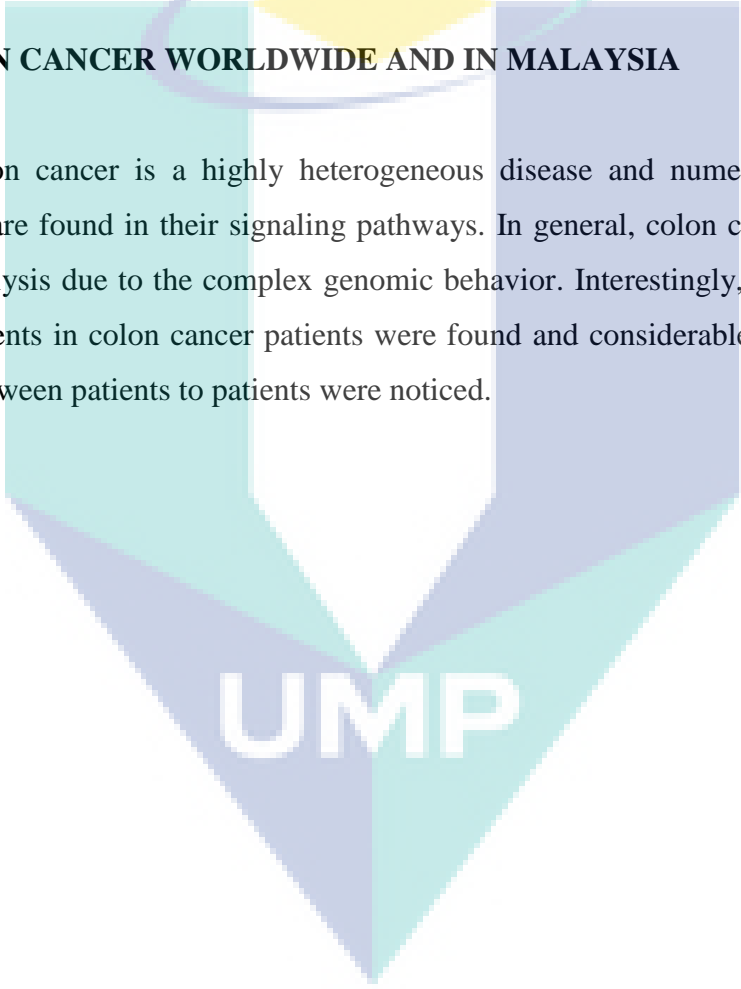
Figure 2.7: Different kinds of cellular proteins participating in the programmed cell death and its differentiation function

Interestingly, seven important proteins are involved in the cell development and their functions such as, growth factors (I), growth factor receptors (II), signal transduction proteins (III), transcription factors (IV), pro- or anti-apoptotic proteins (V), cell cycle control proteins (VI), and DNA repair proteins (VII). Unfortunately, the mutations/ chemical agents may change the structure or expression of proteins from either classes I – IV, and eventually over expressing the active oncogenes. The different cellular proteins are involved in the apoptosis signaling pathways which induce the apoptosis in cells as shown in Figure 2.7.

The bio-mediated nanoparticles induce oxidative stress (reactive oxygen species, ROS), in the cells. These free radicals may cause DNA damage and disturbing the intrinsic apoptosis pathway (Roco, 2003). Caspase is a group of genes, which plays a vital role in both the initiation and execution of apoptosis. The AgNPs treated cells up-regulate the caspase-3 gene expression. The up-regulated gene expression was observed in the AgNP which treated both the BHK21 and HT29 cells, and then induced the programmed cell death (i.e. apoptosis) in cancer cells.

2.6 COLON CANCER WORLDWIDE AND IN MALAYSIA

Colon cancer is a highly heterogeneous disease and numerous exo-genomic alterations are found in their signaling pathways. In general, colon cancer is limited in genetic analysis due to the complex genomic behavior. Interestingly, some of genomic rearrangements in colon cancer patients were found and considerable changes in DNA samples between patients to patients were noticed.

The logo for UIMP (Universiti Malaysia Perlis) is a shield-shaped emblem. It features a central white shield with a yellow diamond at the top. The shield is flanked by two vertical bars, one light blue on the left and one light purple on the right. The bottom of the shield is a downward-pointing triangle, split into light blue on the left and light purple on the right. The letters 'UIMP' are written in white, bold, sans-serif font across the bottom of the shield.

UIMP

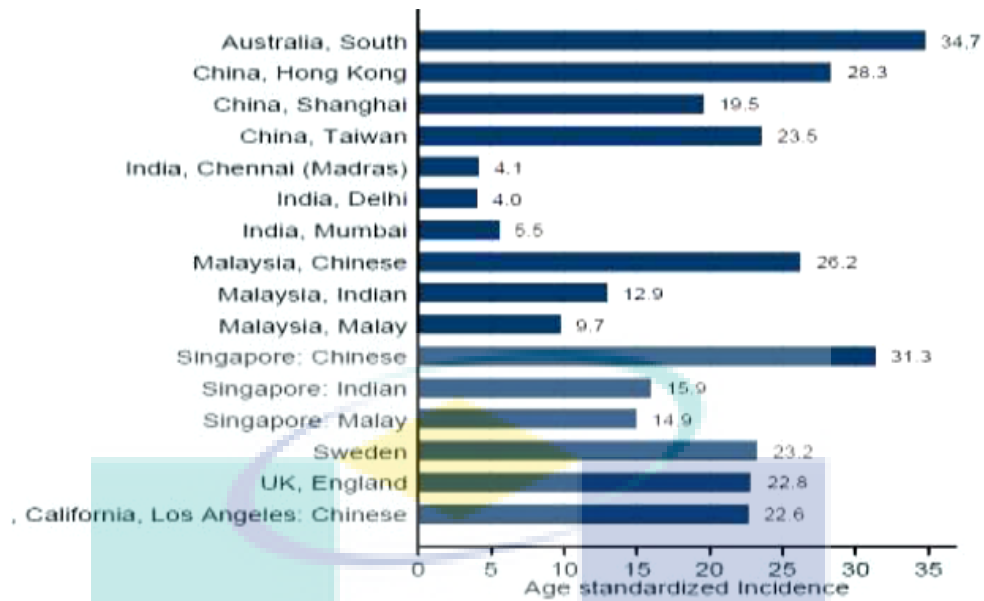


Figure 2.8: Statistical report on colon cancer patients in some Asian and Western countries

(Source: Lim et al., 2008)

According to the National Cancer Registry (Malaysia), the most frequent cancer found is breast cancer (18%) and followed by colon cancer (12%) among Malaysians (Lim et al., 2008). Colon polyps or lesion lead to the formation of 75% to 80% of all colorectal cancer, although 20% to 25% affected are younger individuals who have a family history of colon cancer (Rodriguez-Moranta et al., 2005). Colon cancer still contributes to a high mortality rate due to the average survival time after its detection. It is due to the lack of clinical treatments and less understanding of the causes of the disease (Prakash et al., 2008). Figure 2.9 shows colon cancer development in many stages where in each stage the loss in normal functional and molecular behavior of normal cell functions are observed.

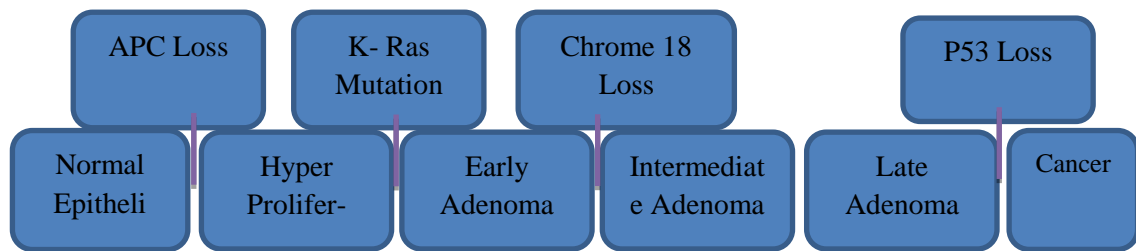


Figure 2.9: Development of colon cancer from adenoma to carcinoma in different stages

2.6.1 Development of colon cancer

The human gastro-intestinal tract is a complex system and it is composed of intraluminal breakdown like gastric acid, pancreatic enzymes and bile acids. These components are involved in the prevention of adhesion like intestinal motility and mucus layer. The intestinal motility, when disturbed, may promote bacterial overgrowth and form solid tumor. In addition, colon cancer has also been developed by different environmental factors such as poor diet and family background (Neutra and Forstner, 1987; Lichtenberger, 1995). Colon cancer develops in different stages that are stage i, stage ii, stage iii and stage iv.

2.6.2 Function of oncogene and tumor suppressor genes in colon cancer

Oncogenesis or tumorigenesis is a multistage step that has been characterized by both the activation of cellular oncogenes and by the loss of function of tumor suppressor genes. Colorectal cancer has been associated with the down regulation of oncogene and tumor suppressor genes (Lekeufack and Brioude, 2006). The progression of colorectal cancer involves many genes and it regulates normal growth of cells in *in vitro* and *in vivo*.

2.6.3 Apoptosis

Normally, programmed cell death mechanism may occur in two different modes which are apoptosis and necrosis. Necrosis is the ordinary cell death which is associated with inflammation and physical or chemical changes of cells. For instance, cells loss or depletion of energy and nutrition leads to cell death. Apoptosis is one of the fundamental and complex cellular signaling processes whereby a living organism maintains homeostasis. Figure 2.10 shows different genes involved in the apoptotic pathways. The apoptosis process is considered by different stages such as nuclear condensation, membrane blebbing and DNA fragmentation. In cancer condition, the rate of apoptosis is pathologically decreased or damaged. Generally, apoptosis activates pro-apoptotic proteins such as PUMA, Bax, Bcl and Bak. They are released from the mitochondria to activate caspase proteases and eventually regulate apoptosis mechanisms. When these pro-apoptotic signals are not released, the cell cannot die (Lekeufack and Brioude, 2006).

The intrinsic apoptotic pathway is closely related with pro- and anti-apoptotic signals of genes. Preclinical studies indicate that the members of p53 and Bcl-2 proteins regulate the permeability of the mitochondrial membrane and determine the pro or anti-apoptotic signal released inside the cell. The current molecular cancer research has been widely used to block the tumorigenesis mechanisms. The anti-apoptotic proteins such as Bcl-X_L, Bax and Bak is bind with BH3 (interacting-domain death agonist) domains. The BH3 gene is a Bcl-2 protein family. The BH3 is relieved by pro-apoptotic proteins (eg, BIM, BID, BAD, NOXA, PUMA) which alternately bind with anti-apoptotic proteins like Bcl-X_L. The normal cells are involved in cellular stress, as a result upregulation of these BH3- proteins, and eventually initiate apoptosis via intrinsic apoptotic pathway.

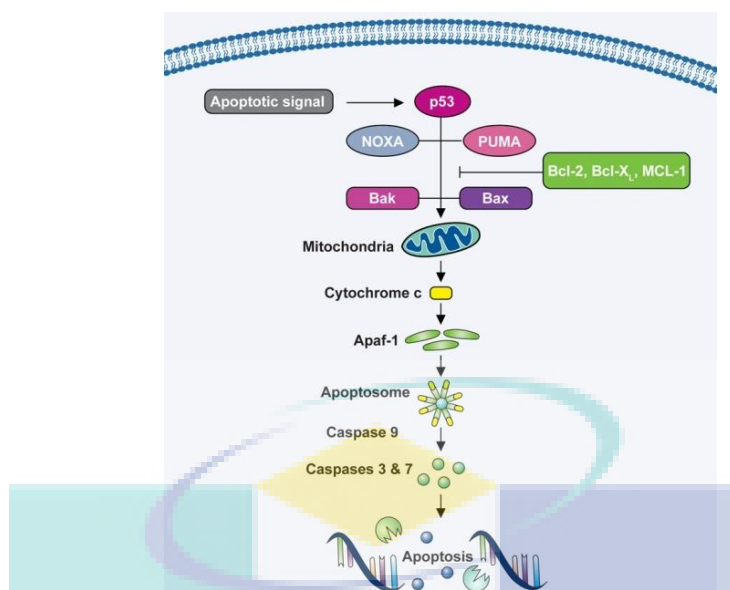


Figure 2.10: The different gene expressions in intrinsic and extrinsic apoptotic pathways

Caspases is an enzyme and family of cysteine proteases. It is contributing a major role in apoptosis. The initiator caspases (including caspase-2, -8, -9, -10, -11, and -12) are related to pro-apoptotic signals. Once activated, these initiator caspases, eventually stimulate the effector caspases such as caspase-3, -6, and -7 which initiate cleavage in downstream. Also, it regulates apoptosis by cleaving cellular proteins through specific Asp residues. The extrinsic pathway begins outside the cells, and activation of different pro-apoptotic receptors on the cell surface. These are activated by pro-apoptotic molecules which are known as pro-apoptotic ligands. The extrinsic pathway has been seen as the same effector caspase machinery as the intrinsic pathway.

2.7 MOLECULAR TECHNIQUES TO EVALUATE CANCER PROGRESSION

2.7.1 Flow cytometry

Flow cytometry is a molecular technique that can provide detailed characteristics of cells. Flow cytometry instrumentation is considerably smaller, and is a user friendly operation mode. The technique is used to analyze various types of clinical samples such as biological specimens, blood, bone marrow, cerebrospinal fluid, urine, and tissues. Also, it can measure the total number of cell size, fragmented DNA or RNA content,

and evaluate the wide range of membrane-bound and intracellular protein. Flow cytometry can measure fluorescence characteristics of single cells (including nuclei, microorganisms and latex beads). Fluorescent dyes are propidium iodide and annexin V bind with different cellular components such as DNA or RNA and emit the lights. The cells with fluorescent dyes can pass a light source through the flow cytometry. The fluorescent molecules are excited to a higher energy state and confirm the cell changes and development. These fluorescent dyes are mainly intercalated into the DNA helical structure. The fluorescent signal is directly proportional to the amount of DNA in the nucleus and can identify gross gains or losses of DNA from samples. In particular, the flow cytometry study can give clear strategies of different phases of the cell cycle including cellular DNA content (Brown and Wittwer, 2000). It could be possible to determine the alteration of cell cycle and the effect of drugs against adherent cells or cancer models.

2.7.2 Quantitative real time polymerase chain reaction (RT-qPCR)

Real time quantitative polymerase chain reaction (RT-qPCR) is one of the common molecular techniques to detect DNA, RNA and protein expression in biological samples. This technique is conducted to qualitatively detect the gene expression through the creation of cDNA transcripts from RNA, and to measure the amplification of DNA using SYBR green dyes or fluorescent probes (Taylor et al., 2010).

Ribonucleic acid (RNA)

The isolation of RNA from samples was followed by TRizol method. The collected RNA samples were stored in an appropriate condition (at 80 °C freezer and/or in RNA storage solution) until further analysis. RNA is highly sensitive and can be easily degradable from the environmental RNase and DNase. Therefore, RNA extraction procedure should be carried out free of RNase and DNase environment and using RNase free water to remove any nucleic acid contamination in the work place. Moreover, the reducing number of samples handling of ~15 to 20 samples in a single

batch may minimize the handling time during the RNA extraction procedure (Gingrich et al., 2006).

RNA quality control

The high integrity RNA (not degraded) is essential for the experiments. This is one of the most critical points in the RT-qPCR experiments. RNA impurities may lead to the inhibition of the RT-PCR reactions and can lead to varying or incorrect quantification results. The RNA purity can be measured by spectrophotometrically at $OD_{260/280}$. An $OD_{260/280}$ of 1.8 to 2.0 indicates the RNA is in good quality. Once, the quality of RNA has successfully met the standards, immediately it can be proceeded for an RT-qPCR assay. The quality of RNA samples should not contain protein or other nucleic acid contaminants.

Reverse transcription steps

Total RNA samples are reverse transcribed into cDNA immediately by avoiding the risk of RNA degradation from multiple freeze/thaws where the protocol is as described by Taylor et al., (2010). Further, reverse transcribed RNA can be stored frozen at -20°C or -80°C until use.

SYBR green and probes

SYBR green is the easiest and the least expensive real-time PCR detection method. SYBR is a dye bind with double standard minor groove of DNA.

Primer and amplicon design

Primer-Blast (www.ncbi.nlm.nih.gov/tools/primerblast/index.cgi?LINK_LOC=BlastHome Ad) is a program developed by NCBI that is used for primer designing. Primer sequences are ensured to be unique and specific for the gene of interest. The both forward and reverse primers are designed carefully by following the steps such as,

1) target sequence should be specific and an efficient amplification of the products 2) target sequence should be unique, 75 to 150 bp long with GC content between 50 to 60%, and a melting temperature of 55 to 65 °C and 3) it should not contain any secondary structures and hairpin motifs.

Validation of RT-qPCR reaction

The optimization of RT-qPCR condition is one of the most important steps which include getting the optimal range of reaction efficiency, primer annealing temperatures and specificity. These steps can ensure that the reaction conditions, buffers and primers have been optimized and cDNA samples are not contaminated with other enzymes.

Selection of reference genes

In RT-qPCR experiments, reference genes are called housekeeping genes and used as controls to normalize the raw data. A reference gene is one that does not exhibit any expression at various experimental conditions or time points. Therefore, the reference genes must be carefully selected based on the experimental data.

Table 2.3: Example of some molecular assays characterization of colon cancer progression

S. No.	Assay	Parameters
1.	Molecular analysis	1.DNA damage 2. Gene expression 3. Cell cycle analysis 4. Protein expression

Table 2.3 demonstrates the important molecular assays used to analyze the cancer behavior. Additionally, other molecular techniques such as western blotting, gel electrophoresis, MALDI-TOF are also useful to characterize the protein expression and

protein–protein interaction in cancer models. It could be useful for the development of drugs against cancer.

2.8 METAL NANOPARTICLES FOR CATALYSIS

Metal nanoparticles are special type of nanomaterials, which exhibit different catalytic performances in chemical reaction and energy conversion process. Nanoparticles have been shown to enhance catalytic reactions in enzyme kinetics, bioprocess and food industries (Tao et al., 2014). Professor El Sayed et al. investigated the effect of metal nanoparticles in different catalytic reactions, and proved metal nanoparticles as good stabilizers and drastically promote the chemical reactions. Also, Astruc et al. (2005) studied that the bimetallic Pt-RuNPs catalyze the methanol electro-oxidation with enhanced activities compared to commercial catalysts. Gold nanoparticle is an interesting material in the field of catalysis. Cuenya, (2010) reviewed that bulk gold is practically inert, besides nanometer-sized gold particles have been proven to be highly active in several reactions, including low-temperature oxidation of CO, partial oxidation of hydrocarbons, the water–gas shift reaction and reduction of nitrogen oxides.

2.9 COMMERCIAL APPLICATIONS OF BIOSYNTHESED METAL NANOPARTICLES

2.9.1 Waste water treatment

Recently, nano sized products have immense applications in every day life. There are also various eco-friendly nano products available in commercial market with high efficiency such as water purifier, bone and teeth cement, facial cream and homemade products (Kouvaris et al., 2012). For instance, silver, silica and platinum nanoparticles have various applications in personal care and cosmetics and they are used as ingredients in various products such as sunscreens, anti-aging creams, toothpastes, mouthwash, hair care products and perfumes. The silica nanomaterials are used as ingredients in various commercial products. Also, the modified silica nanomaterials are

used as excellent pesticide control and they are used in a variety of non-agricultural applications.

2.9.2 Cosmetics

The metal nanoparticles are used as a preservative agent in food and cosmetic industries. Also, the metallic nanoparticles are used for various commercial applications mainly cosmetics, pharma coating materials and food preservatives (Songland and Kim, 2009, and Kokura et al., 2010). The nanosized metal nanoparticles such as gold, silver and platinum nanoparticles are also broadly applied for various commercial products such as shampoo, soap, detergent, shoes and so on. The chemical ingredients are mostly synthetic, and they cause side effects to human being. As a result, the green metallic nanoparticles serve as an alternative for preservative agents in healthcare and food industries.

2.9.3 Nanoparticles in food industry

Silver metal is a highly heat conducting material and due to that, it is widely used in mechanical devices. Also, it is used in heat liable instrumentation such as PCR lid and UV-spectrophotometer. Nanosilver is used as a coating material in instruments. It is highly stable at high temperatures and without interference of the samples (Weiss et al., 2006). In food industries, the food products get high microbial contaminations due to the various open scale processes such as in manufacturing, processing and shipping of raw materials. Therefore, there is a need to develop a cost effective biosensor to evaluate the quality of the products. The metallic nanoparticles have been developed as biosensors and effective in detecting pathogens in different stages of contaminants. Finally, the biosynthesis of nanoparticles using plant extracts with metal salt is a novel green chemistry method and effectively controls the various pathological conditions.

CHAPTER 3

MATERIALS AND METHODS

3.0 CHAPTER OVERVIEW

This chapter provides the information about the materials and methods which were used in this study. The plant extract was used to synthesize the nanoparticles and the characterizations of their physico-chemical properties were studied using different analytical techniques such as UV-Vis spectrophotometer, FESEM, EDX, XRD, FT-IR, particles size analyzer and zeta potential. Also, the biological properties of the synthesized nanoparticles such as antibacterial and antioxidant activities were carried out in this study. Besides, the *in-vitro* anticancer activity against HCT-116 colon cancer cells was evaluated. The *in-vitro* anticancer study was evaluated by mRNA gene expression using the qRT-PCR technique. Furthermore, the morphological characterization and flow cytometry study were also carried out.

3.1 PLANT COLLECTION AND IDENTIFICATION

Commelina nudiflora is an edible weed plant and it has a variety of medicinal importances for human. It is available in many countries mainly Malaysia, Indonesia, India and other tropical regions such as Burma, Vietnam and eastern parts of China. The whole healthy plant *C. nudiflora* (*rumpit tahi itek*) was procured from Maran, Pahang state, Malaysia in March 2012. Figure 3.1 shows processed *C. nudiflora* plant materials in dry and powder form. The plant was selected for this study on the basis of its availability, medicinal property and cost-effectiveness. The plant was taxonomically authenticated by Associate Professor. Dr. Norazian Mohammad Hassan, Kulliyah of

Pharmacy, International Islamic University, Malaysia. The voucher specimen was deposited at Kulliyyah of Pharmacy.

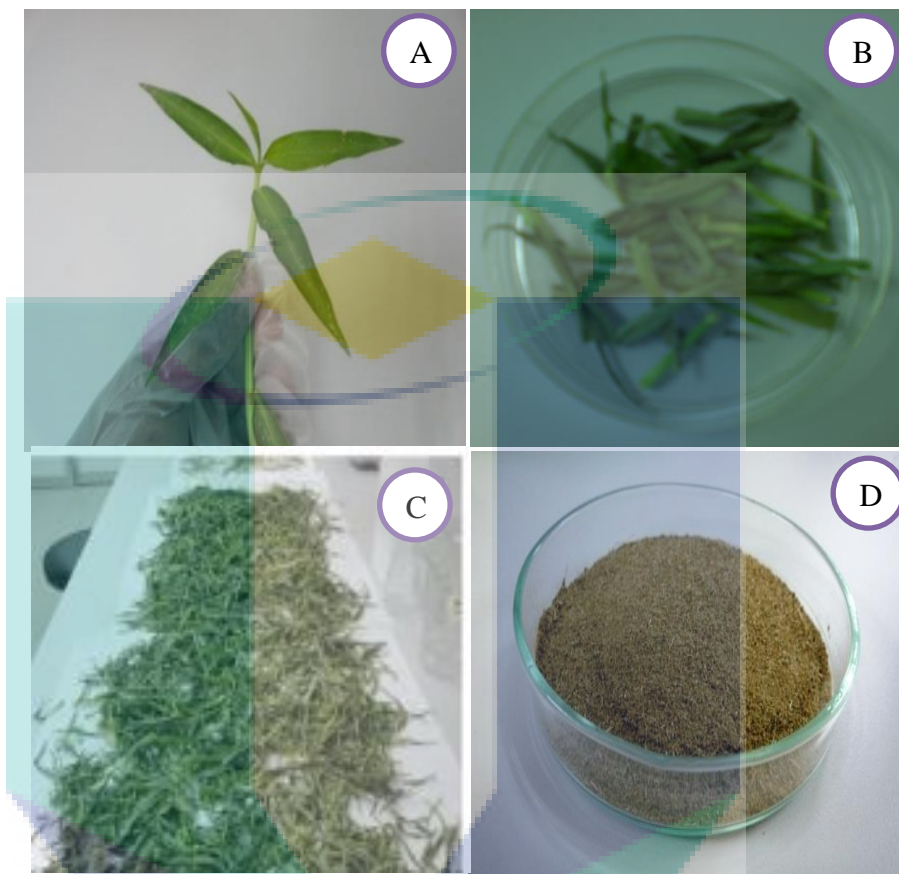


Figure 3.1: Photographs of *Commelina nudiflora* plant a) whole *C. nudiflora* plant b) cleaned with tap water c) dried in shadow condition d) Powder form of *C.nudiflora*

3.1.1 Chemicals and glasswares

Chloroauric acid (HAuCl_4), silver nitrate (AgNO_3), sodium chloride (NaCl), ascorbic acid, autylated hydroxyanisole (BHA), 2,2-diphenyl-1-picrylhydrazyl (DPPH) and 3-ethylbenzothiazoline-6-sulphonic acid (ABTS) were purchased from Sigma-Aldrich Chemicals, (USA). Other solvents and chemicals were of analytical grade and used throughout the experiments without further purification. All experiments reagents were prepared using Milli-Q (MQ) water unless stated otherwise. All glasswares were rinsed twice with de-ionized water.

3.1.2 Plant extract preparation

Fresh and healthy whole plants were rinsed thoroughly with running tap water followed by distilled water to remove all the dust and unwanted debris, then cut into small pieces and used for extract (broth) preparation.

Then, 10 g of finely incised plants were weighed separately and added with 100 ml distilled water in a 250 ml flat bottom flask. The mixture was boiled for about 25 minutes at 65 °C. The extracts were filtered through Whatman No. 1 filter paper, and the procured clear solutions were stored in a refrigerator at 4°C, until further use. All reactions were conducted in sterile conditions to maintain the effectiveness and accuracy of the reaction.

3.2 BIOSYNTHESIS OF METALLIC NANOPARTICLES

3.2.1 Biosynthesis of gold nanoparticles

An amount of 20 ml of *C. nudiflora* aqueous extract was added with freshly prepared aqueous solution of 80 ml of $\text{HAuCl}_4 \cdot 3\text{H}_2\text{O}$ (10^{-4} M) and briskly stirred for 10 minutes in a reflux system at 37 °C (Figure 3.2). The color formation indicates that the gold ions were reduced into nano-gold in 30 minutes at room temperature. The formation of pale yellow into pink colour shows the nanoparticles formed in the solution. The experiment was optimized with molar solution of gold precursor and the plant extracts to achieve the different morphologies of nanoparticles (Narayanan and Sakthivel, 2008, and Philip, 2009).

3.2.2 Biosynthesis of silver nanoparticles

The aqueous plant extract of 30 ml was added with 170 ml aqueous solution of AgNO_3 (10^{-4} M) and stirred for 30 minutes. Reduction took place gradually and it was completed in 30 minutes as shown by the pale yellow colour that changed into stable light brown colour of the solution, which shows Ag^+ ions were completely converted

into metallic silver nanoparticles. The mixture solutions have been optimized by different concentrations of plant extract and metal ion solution. The nano-Ag was synthesized at room temperature with the optimum pH of 6.5 (adjusted using NaOH). All the synthesized solutions were found to be stable for more than 90 days and showed a slight precipitation and no colour changes were observed (Philip and Unni, 2011).

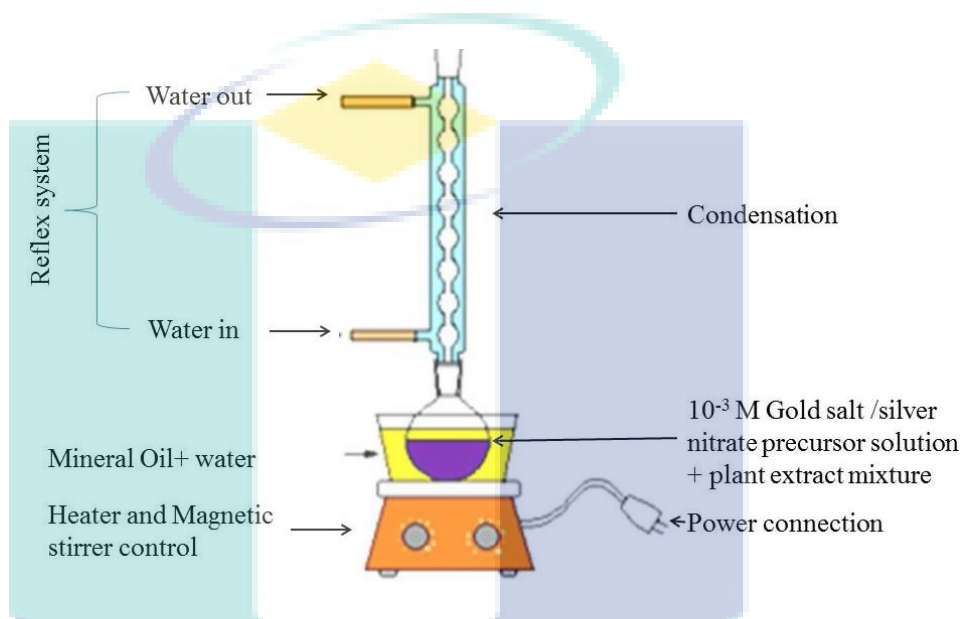


Figure 3.2: Reflux system set up used for the biosynthesis of gold and silver nanoparticles in green chemistry methods

3.3 CHARACTERIZATION OF SYNTHESIZED NANOPARTICLES

After the complete reduction of gold and silver ions, the synthesized nanoparticles were separated using centrifugation at 12000 rpm for 15 minutes. The NPs (solid mass) that were obtained were washed twice with distilled water and dried in an oven at 65 °C for 4 hours. After that, the dried nanoparticles powder was subjected to different analytical techniques to characterize their physico-chemical and biological properties.

3.3.1 UV-vis spectrophotometer analysis

The prepared *C. nudiflora* aqueous extract was added with HAuCl_4 (0.01M) and AgNO_3 (0.01M) and the growth of nanoparticles was confirmed by the change of colour in the synthesized solution. Then, the mixture solutions were subjected to UV-vis spectrophotometer (T80 series of UV-Vis spectrophotometer, PG instruments Ltd, China) at the wavelength of 300 to 800 nm, at regular time intervals where the absorption spectra was measured.

3.3.2 FESEM analysis and EDX measurement

The synthesized gold and silver nanoparticles morphology was characterized using FESEM, (JEOL JSM 7800F) with the optimum voltage at 10 kV. The nanoparticles sample was tipped in microtip, transferred to a sample plate and analyzed by several imaging modes. EDX analysis was conducted with the same FESEM instrument which confirmed the elemental composition from the synthesized gold and silver nanoparticle samples.

3.3.3 XRD characterization

The crystalline nature of the biosynthesized gold and silver nanoparticles was analyzed by a powder X-ray diffraction instrument (Rigaku mini flux II). The fine powder was drop-coated on a glass plate in the instrument with Cu- $K\alpha$ radiation source in powder diffractometer $\lambda = 1.541 \text{ \AA}$, operating voltage at 30 kV and current of 15 mA. The X-ray patterns were obtained in the 2θ range of 10 to 85° , using a 0.05° step size. The particle size was calculated using Scherer's equation (1918).

$$D = \frac{K\lambda}{\beta_{\text{cor}} \cos\theta}, \text{ with } \beta_{\text{cor}} = (FWHM_{\text{sample}}^2 - FWHM_{\text{ref}}^2)^{\frac{1}{2}} \quad \text{----- (1)}$$

where D is the average crystallite domain size perpendicular to the reflecting planes, $K=0.94$, λ is the X ray wavelength ($\lambda=1.5406 \text{ \AA}$) and θ represents the diffraction angle,

β is the full width at half maximum (FWHM). To eliminate the additional instrumental broadening, the FWHM was corrected using the FWHM from a large-grained reference sample. This modified formulae is valid for the calculation of crystalline size of nanoparticles > 100 nm (Enzo et al., 1988).

3.3.4 FT-IR analysis

The FTIR spectrum of purified gold and silver nanoparticles was obtained on FT-IR PERKIN Elmer spectrum 100, FTIR spectrometer, USA. The fine crystalline AuNPs, AgNPs powder and plant extract were added separately with KBr pellets and mixed well using mortar and pestle to prepare pellet and this was done using a pelletizer at 5 lbs pressure. The finely prepared thin pellet was placed in a sample holder of FTIR machine. The instrument was operated on transmission mode at the resolution of 1, and the spectra range between 4000 to 400 cm^{-1} .

3.3.5 TGA and BET analyses

The thermal stability of the gold and silver nanoparticles was confirmed by the thermogravimetric analysis (TGA) instruments. The thermo gravimetric analysis (TGA) of gold and silver nanoparticles was monitored on a Mettler Toledo (Gas controller GC 20 Star system, USA) thermal analyzer at a scanning rate of 10 jC/min . BET is essential for the determination of the surface area of the nanomaterials. The BET instrumentation (Micromeritics ASAP-2020, surface area and porosity analyzer, GA USA) is used to characterize the surface area of the synthesized nanoparticles.

3.3.6 Particle size analyzer and Zeta potential study

The range of the particle size distribution of the nanoparticles and polydispersity were determined by a particle size analyzer (90 Plus Particle Size Analyzer, Brookhaven Instruments Corporation). Particle size was determined by measuring the time dependent fluctuation of scattering laser light, when the nanoparticles underwent the Brownian motion. Furthermore, the potential surface charges of the AuNPs and Ag

NPs were evaluated by dynamic light scattering (DLS) in back scattering mode, using a laser particle zetasizer (Malvern 110, Zetasizer) at 28 °C, pH-4.

Figure 3.3 shows the flow of methods that was used in this research work. Firstly, the biological route synthesis of nanoparticles and characterization of their physico-chemical properties such as size, shape and crystalline nature was conducted. Secondly, the plant extract which is used for the synthesis of nanoparticles to characterize their phytochemical constituents by a standard phytochemical test and GC-MS analysis. Finally, the synthesized nanoparticles were evaluated for their biological properties such as *in-vitro* antibacterial and anticancer properties.

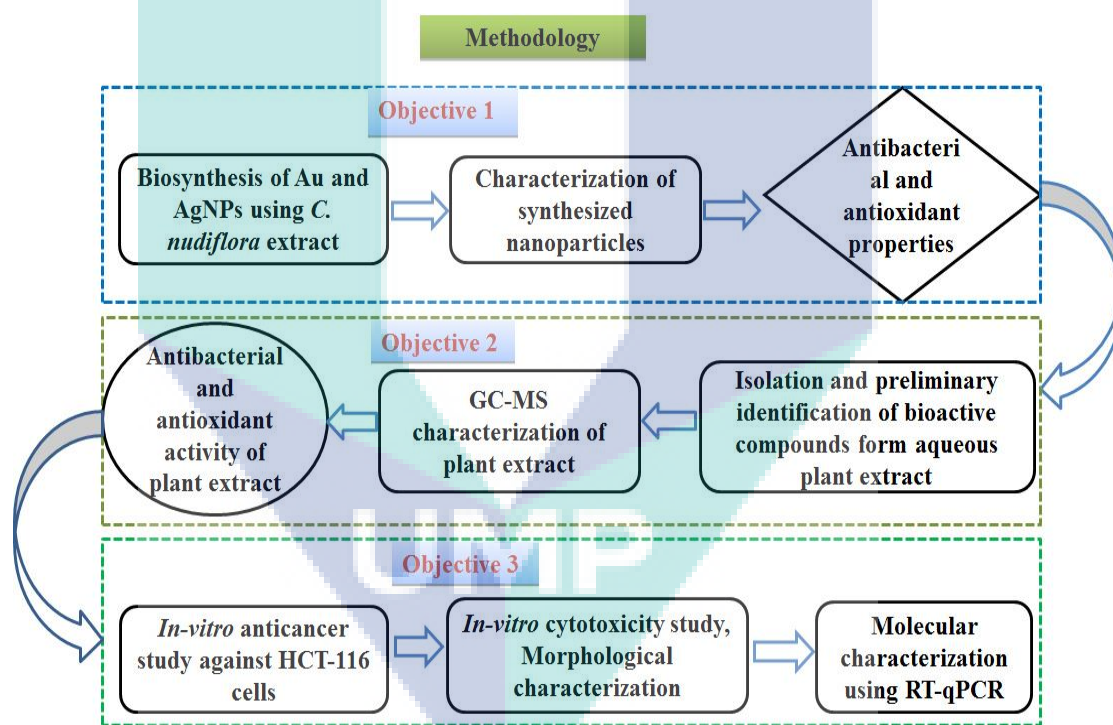


Figure 3.3: Flow chart of research methodology used in this study

3.3.7 Conventional methods for characterization of synthesized nanoparticles

The characterization of physico-chemical properties of metallic nanoparticles can be covered by a wide spectrum of techniques such as UV- Vis spectrometry, FESEM,

EDX, TEM, BET, TGA, particle size analyzer and zeta potential (Toshima and Yonezawa, 1998). Also, some newer methods have also been used to characterize and confirm the nanocrystals structures and their physico-chemical parameters.

- The ultraviolet-visible spectrophotometer is an indirect method to characterize the reduction of metal ions to metallic nanoparticles. The UV-Vis spectra of bimetallic nanoparticles are often found to be different from those of monometallic, and also with those of physical mixtures. These results do not directly suggest the detailed structure, but can be used to suggest the formation of bimetallic nanoparticles or monometallic nanoparticles (Hutter and Fendler, 2004, and Murphy, 2010).
- TEM study is used to determine the average diameter and the range of distribution of nanoparticles. The TEM images of the metal nanoparticles are a source of important information of morphology and the state of aggregation. The electron beam can be focused onto a single particle by TEM to obtain information from individual particles (Choi et al., 2007).
- FT-IR spectroscopy specifically investigates the adsorbed small molecules on the surface structure of the nanomaterials (Tabrizi et al., 2009).
- XRD (X-Ray Diffraction) particularly examines the crystal structure of metal nanoparticles. The diffraction patterns of the monometallic nanoparticles, physical mixtures and their purity of sample can be studied. The structure of nanoparticles can be verified by XRD spectra with computer-simulated ones (Zhu et al., 1998, and Hanauer et al., 2007).
- XPS (X-ray Photo Spectroscopy) is a method to find the concentration of a particular metal. This technique is often used to determine which atoms are preferentially located on the surface region, and which are preferentially located in the particle core (Sun et al., 2000, and Liu and Hurt, 2010).

- EDX (Energy Disperse X-ray spectroscopy) is an effective *in-situ* technique which is attached with an electron microscope (SEM and FESEM) for the determination of the metal nanoparticle composition (Harada et al., 1992). The electron beam can be spotted on different parts of the particle to investigate the variations in regional compositions, which often reveal non-uniformity in the composition (Rethy et al., 2007).
- NMR spectroscopy can also be used to infer the local environment in metallic particles from NMR shifts (known as knight shifts) (Ford, 1986).
- ICP-MS is used to evaluate the conversion percentage of metal salts into metallic nanoparticles and find the percentage of reduction rate of salts (Mott et al., 2010, and Rai and Duran, 2011).

3.4 BIOACTIVE COMPOUNDS ANALYSIS

3.4.1 Hot extraction by soxhlet apparatus

An amount of 10 g of *C.nudiflora* fine powder was extracted in 250 ml solvents (different polar solvents) by soxhlet extraction apparatus (Miller, 1972). The obtained extracts were subjected to a vacuum evaporator to evaporate excess solvents. After that, the dried crude extracts yield was weighed and used for further experimental studies. Figure 3.3 shows the soxhlet apparatus used for the extraction of plant metabolites.



Figure 3.3: Performing an extraction of *C. nudiflora* using soxhlet apparatus

3.4.2 Preliminary phytochemicals identification of plant extracts

The crude plant extract samples were dissolved in the solvents and the qualitative confirmation of major phytochemical constituents such as alkaloids, flavonoids, phenolics, saponins, steroids, tannins, carbohydrates and volatile oils was carried out by the standard identification procedure (Trease and Evans, 1989, and Harbone 1998).

Test of alkaloids

In a test tube containing 1 ml of plant extract, a few drops of dragendorff's reagent was added and the color developed was noticed. The appearance of orange color indicates the presence of alkaloids.

Flavonoids test

5 ml of 1% hydrochloric acid (0.1 M) with 2 ml of extract were shaken with sodium hydroxide (1%). The appearance of yellow colour indicated the presence of flavonoids.

Test of phenolics

In 1 ml of extract, 2 ml of distilled water and a few drops of 10% ferric chloride were added and the appearance of blue or green color indicated the presence of phenols.

Saponins test

1 ml of the plant extract was added with 10 ml water and mixed well. The mixture was vigorously shaken for 1 to 2 minutes. The persistent froth (1 cm height) observed it indicated the presence of saponins in the sample.

Steroids test

The plant extract was dissolved in 2 ml of chloroform in a dry test tube. Then, 10 drops of acetic anhydride and two drops of concentrated sulphuric acid (0.1M) were added. The solution became red, then blue and finally became bluish, which indicated the presence of steroids.

Test of tannins

One drop of ferric chloride (1%) was added to 2 ml of the extract, and the appearance of bluish or greenish black coloration indicated the presence of tannins.

Carbohydrates test

In a test tube, 5 ml of the plant extract was treated with 5 ml of Fehling's solutions (A & B) and was heated; the appearance of a red precipitate indicates the presence of reducing sugars.

Volatile oils

2 ml of plant extract and 0.1 ml of diluted sodium hydroxide (0.01M) were added with a few drops of diluted hydrochloric acid. The formation of white precipitate indicates the presence of volatile oils in the extract.

3.4.3 Determination of total phenolic content (TPC)

The total phenolic content of *C. nudiflora* extracts was determined using folin-ciocalteu phenol reagent method as described by Manian et al. (2008). A stock solution of plant extracts was prepared in different aliquots (0.1, 0.2, 0.3, 0.4, 0.5 mg/ml). One ml of plant extracts was put in test tubes and 0.5 ml of folin-ciocalteu phenol reagent (FC) was added (FC reagent was dissolved in distilled water with 1:1 ratio). Then, 2.5 ml of 20% sodium carbonate was added in each tube and finally the mixture was mixed uniformly using vortex and then the test tubes were kept in a dark condition for 40 minutes. The UV-vis absorbance spectra were recorded at 725 nm using glass cuvettes. To minimize the standard error, the reaction was performed in triplicate. The obtained result was expressed in milligram of gallic acid equivalent (mg GAE).

3.4.4 Determination of total flavonoid content (TFC)

The total flavonoid content of plant extracts was determined using colorimetric method as described by Manian et al. (2008). Concisely, 100 µl of each plant extract (1mg/ml) was made up to 1 ml by using distilled water and followed by the addition of 75 µl of 10% sodium nitrate solution. After 6 minutes, 150 µl of 5% aluminium chloride solution was added, then 0.5 ml of 1M NaOH was also added to the test tubes. The

mixture samples were made up to 2.5 ml by using distilled water and mixed thoroughly. The UV-V absorbance values were read immediately at 510 nm. The results were expressed as mg/g butylated hydroxytoluene (BHT) equivalents.

3.4.5 GC-MS study

The basic organic and inorganic chemical profile of plant extract was studied using gas chromatography and mass spectrometry. It is one of the established diagnostic tools to characterize the volatile and semi volatile compounds from samples. GC-MS analysis of the plant extract was performed by Agilent GC-MS built with bonded-phase fused silica capillary column (30mm×0.25mm ID; d=0.25) (J&W Scientific, Folsom, CA). The GC-MS operating key procedure for volatile and semi volatile organic compounds are as follows. Column flow used highly reactive helium as a carrier gas at 1.5 ml/min. The splitless injection was maintained at 260 °C. The splitless injection mode was used with the split ratio of 40:1. The transfer line temperature was set at 260 °C. The mass analyzer (m/z) was set at 60 eV, electron impact source temperature was 200°C, electron-multiplier voltage of 1588 mV and solvents delay of 2 minutes. All scanned data were obtained by the full-scan mass spectra within the scan range of 50 to 400 amu. The oven temperature program was as follows: initially from 190 to 250 °C at ramp rate of 220 °C/min, and from 200 to 260 °C at ramp rate of 1 °C/min. Finally, the acquired spectrum of plant extracts were compared with the standard known database in the NIST library and scrupulous compounds were confirmed to be present (Lisec et al., 2006).

3.4.6 Bioactivity of plant extracts

The crude extracts were tested for each pathogenic microorganism. The treated Mueller Hinton agar plates were incubated at 37 °C for 24 hours. The antimicrobial activity was determined by measuring the zones of inhibition (mm) formed after incubation.

3.5 IN-VITRO ANTIBACTERIAL ACTIVITY

3.5.1 Antibacterial activity of gold and silver nanoparticles

Antibacterial activity of AgNPs was performed by disc diffusion assay (NCCLS, 1997). The four indigenous cultures were used for the antibacterial assay which were *Staphylococcus aureus* (ATCC 25923), *E.coli* (ATCC 10536), *Bacillus subtilis*, *Porphyromonas gingivalis* (ATCC 35664). The MH agar plates were prepared and bacterial cultures of 20µl was added in each agar plate and spread evenly using sterile 'L' rod. Further, the different concentrations of AuNPs and AgNPs disc (50, 75, and 100 µg/ml) prepared with control (streptomycin) were placed in the plate. After that, the petri plates were covered with parafilm and incubated at 37 °C for 24 hours. After completing the incubation, the zone of inhibition was measured by mm scale. Minimal inhibitory concentrations of biosynthesis of gold and silver nanoparticles were determined by micro dilution method using 96-well micro titer plates (BD Falcon, 96-well microplate, UK). The MIC values were interpreted as per the standard guidelines.

3.6 IN-VITRO ANTIOXIDANT ACTIVITY

3.6.1 DPPH assay of gold and silver nanoparticles

The free radical scavenging activity of the biosynthesized gold and silver nanoparticles was determined by DPPH assay. The different concentration of gold and silver nanoparticles (20, 50, 75, 100 and 120 µg/ml) were used to evaluate the antioxidant properties. The gold nanoparticles were taken into aliquots 0.5 to 2.5 ml and added 1ml of 3 mM methanolic DPPH solution and making a final volume of 4 ml using distilled water. The solution was mixed properly and allowed to stand for 30 minutes at 30 °C. The absorbance of the tested solution was read at 517 nm using a UV-Vis spectrophotometer (Sidduraja and Becker, 2003). Ascorbic acid was used as a reference control for DPPH antioxidant assay. The following formula was used to calculate the percentage of,

$$\text{DPPH radical scavenging activity} = \left(\frac{\text{Control OD} - \text{biosynthesized gold solution OD}}{\text{Control OD}} \right) \times 100$$

3.6.2 ABTS assay of gold and silver nanoparticles

ABTS is used to calculate the potential free radical scavenging activity of GNPs and SNPs assay. ABTS salt (7.0 μM) and potassium persulphate (2.45 μM) were mixed equally and kept in a dark condition for 16 hours, after that, it was used for the production of ABTS cation (ABTS^+). The fine powder of AuNPs and AgNPs were prepared using different concentrations at (20, 50, 75, 100 and 120 $\mu\text{g/ml}$) and the aliquots at 0.5 to 2.0 ml of gold and silver samples were transferred into 2 ml of 80% ethanolic dissolved in ABTS^+ solution. After that, the absorbance of the gold and silver nanoparticles was measured at 734 nm in UV-Vis spectrophotometer. Thus, the control was used without nanoparticles (Sidduraja and Becker, 2003).

$$\text{ABTS radical scavenging activity} = \left(\frac{\text{Control OD} - \text{biosynthesized gold solution OD}}{\text{Control OD}} \right) \times 100$$

3.7 *IN-VITRO* ANTICANCER ASSAYS

3.7.1 Cell line and culture medium

Human colon cancer (HCT-116) cells were purchased from National Center for Cell Sciences, Japan. The cells were *in-vitro* cultured in DMEM medium, supplemented with 20% FBS (Fetal Bovine Serum), 1% of peni-strep antibiotics (it is called as DMEM complete medium) and the humidified incubator was set at 37 °C with 5% CO_2 .

3.7.2 Reagents, equipment and kits used

Trizol reagent (sigma, USA), PCR grade water, cDNA synthesis kit, PCR, master mix, SYBR green and RT-PCR reagents were procured from (Qiagen, Germany). All other reagents, pipette tips were used with high quality PCR grade level.

3.7.3 Cell subculturing and maintenance

The cells growth was carefully monitored and the medium was changed every second or third day as per the conditions and the mycoplasma test was performed normally in a month using fluorescent Hoechst 33258 staining which denoted no contamination in the experimental culture. Once the cells confluent of 70 to 80% was reached, the cells were sub cultured in 10 mm dishes. The attached monolayer cells were washed twice with PBS and then detached by treating with trypsin (1% trypsin containing 0.01% PBS) for 2 minutes and cells are used for further experimental studies.

3.7.4 *In-vitro* MTT assay

MTT- (3-(4,5- dimethylthiazol-2-yl)-2,5-diphenyl-tetrazolium bromide) assay with little modifications was used to determine the cell viability of the biosynthesized gold and silver nanoparticles (Jayaraj et al., 2013). Briefly, HCT-116 colon cancer cells were seeded into 96-well plates of approximately 5×10^4 cells at 37 °C in 5% CO₂ atmosphere for 24 hours. The cells confluence were checked (should be > 70%) and then treated with different concentrations of biosynthesized gold and silver nanoparticles (12.5 µg/ml, 25 µg/ml, 50µg/ml, 100 µg/ml, 200 µg/ml and 400 µg/ml) and negative control (water), plant extract (1mg/ml) for 24 hours of incubation. The positive control contains only MTT reagents without cells. After incubation, the medium was carefully removed from each well and added 30µl of MTT (5 mg/ml) and incubated for 4 hours at 37 °C. The purple color formazone crystals were formed and dissolved in 100 µl of DMSO and read in a microtiter plate reader (Beckman Coulter LD 400 °C Luminescence detector) at 570 nm. The absorbance (OD) value was converted to percentage of viability using the following formulae:

$$\% \text{ of cell viability} = \frac{\text{OD value of treated samples}}{\text{OD value of control}} \times 100$$

3.7.5 Flow cytometry analysis

Cell cycle analysis (percentage of apoptotic cells) was performed by flow cytometry using propidium iodide staining. The HCT-116 colon cancer cells were grown in an exponential phase where cells density of 1×10^6 cells/ 10 mm dish and allowed to adhere overnight. After that, the cells were treated with IC_{50} (200 and 100 $\mu\text{g/ml}$) concentration of gold and silver nanoparticles for 24 hours. After prescribed treatment time, the cells were harvested by trypsinization. Then, cells were washed with cold PBS solution and fixed with ice cold 70% ethanol at 4°C overnight. The cells were then resuspended in PBS containing 0.5% Triton X-100 and then, 0.1mg/ml RNase was added. The mixture was incubated at 37°C for 1 hour. After 1 hour, 50 μl of propidium iodide was added (Sigma-Aldrich P4170) and kept in a dark room for 45 minutes. After 45 minutes of incubation with propidium iodide at room temperature, the cells were analyzed on a flow cytometer (FACS Calibur, Becton Dickinson), equipped with an air-cooled argon laser providing 15 mW at 480 nm (Blue laser) with standard filter setup. The percentages of each cell cycle phases were analysed using Cellquest Pro software (Gajendran et al., 2014)

3.8 MOLECULAR CHARACTERIZATION OF CANCER CELLS

In this study, the mRNA gene expression of PUMA, caspase-3, caspase-8 and caspase-9 was studied. The HCT-116 colon cancer cells were treated with AuNPs and AgNPs samples for 24hours before the completion of treatment period (~ 18 hrs) where the cells were collected and evaluated for gene expression study.

3.8.1 Quantitative RT-PCR studies

Homogenizing samples and RNA extraction

Briefly, the total RNA was isolated from treated HCT-116 cells using Trizol reagent according to the manufacturer's protocol (Invitrogen, USA). Firstly, the plates were completely removed off of the medium and rinsed twice with PBS. As per the total

volume of cells, one ml of Trizol® (Sigma Aldrich, Malaysia) reagent was added into each plate. After the dissociation of the surface cells, they were carefully scraped by a cell scraper and transferred to 2ml sterile eppendorf tubes. Then, the collected cells were incubated for 5 minutes at room temperature (Homogenized samples can be stored at -80 °C for a maximum of 30 days)

Phase separation

Then, 200 µl of chloroform was added into the samples and mixed well by vortex intermittently for 15 seconds. The mixture was kept for 2 to 3 minutes for incubation at room temperature. After incubation, the samples were centrifuged at 12000 g for 15 minutes at 4 °C. The mixtures were separated into three different phases such as lower red phenol chloroform phase, upper colourless aqueous phase and interphase. The upper aqueous phase was carefully collected without interruption of other layers and transferred into a new 1.5 ml sterile tube.

RNA precipitation

For the precipitation of RNA, 500 µl of 100% isopropanol was added into the aqueous phase collected tube and mixed well by using vortex for 15 seconds. The mixture was incubated for 10 minutes at ambient temperature and then, centrifuged at $9000 \times g$ for 10 minutes at 4 °C. The RNA sample was a precipitated gel like pellet on the side of the tube.

RNA wash and resuspension

The supernatant was completely removed from the tube and the RNA pellet was kept for drying and further washing process. After that, the RNA pellet was washed with 1ml of 75% ethanol, vortexed well and centrifuged at $8000 \times g$ for 15 minutes at 4 °C. The excess amount of ethanol supernatant was removed carefully and allowed 5 minutes for air dry. The RNA pellet was partially dissolved with 20µl of RNase free

water and vortexed well. After that, the samples were incubated in a heat block set at 55 °C for 15 minutes.

Spectrometric analysis

The integrity of the total RNA was evaluated by nano UV-Vis spectrophotometer (thermos syntific nanodrop (TM) 1000, USA) with the optical density ratio at 260nm to 280nm (accepted calculated value is between 1.6 and 2.1) (Table 3.1).

Table 3.1: Purity of RNA concentration of experimental samples analyzed by nanodrop spectrophotometer

Sample Name	Nucleic acid (ng/ml)	Spectra × 10 ng /ml	RNA concentration (µg/ml)	After dilution (a) (/ 10)	Conversion to 5 µg/µl
PC	534	5340	5.34	0.534	9.36
NC	1193	11930	11.93	1.193	4.19
S1	620	6200	6.2	0.62	8.06
S2	922	9220	9.22	0.922	5.42

(PC: positive control; NC: Negative control; S1: gold nanoparticles; S2: silver nanoparticles)

Reverse transcription reaction and cDNA synthesis

Reverse transcription reaction (master mixture preparation) was carried out by commercial Ominiscript reverse transcription kit (Qiagen) according to the manufacturer's instruction. The preparation of cDNA used 5 µg of RNA per reaction (approximately 2µl volume) along with 2 µl of reverse transcriptase enzyme.

Table 3.2: Required components for reverse transcription reaction (Master Mixture)

Required components	Volume (μl)
4 μ g RNA in Rnase free water	(adjusted)
10X Buffer RT	4
dNTPs mixture	4
Oligo-dT primer	0.4
Omniscript Reverse Transcriptase	2
Final volume	40

The master mixture reaction components such as RT buffer, dNTP and oligodT primer and non specific primers were added to the tube and incubated for 1 hour at 37 °C (Table 3.2). Finally, the single strand complementary DNA (cDNA) was synthesized.

Validation of RT-qPCR and its reaction steps

Quantitative Real-time PCR (RT-qPCR) was performed using a cDNA (equivalent of 10 ng of total RNA) from each sample with the specific primers for PUMA, caspase-3, caspase-8 and caspase-9. A housekeeping gene, β -actin was used as an internal control. (Table 3.3) The reaction was carried out with 10 μ l of SYBR GREEN mix (Qiagen) as per the manufacturer's guidelines. The designed non-specific primers were adopted from primer BLAST software (NCBI). The qRT-PCR reaction mixture contained 2x Quantitect SYBR Green PCR master mix, reaction mixture (cDNA), primer mix and DEPC water as shown in Table 3.4. RT-qPCR reaction was monitored using a Corbett Real-Time PCR thermocycler system (Germany). The samples were performed in triplicate.

Table 3.3: Prepared reagents mixture for pre-developed RT-qPCR reaction

Components	Amount (μ l)
2X master mix	7
Primer mix	1
cDNA	2
H ₂ O	4
Total volume	14

Table 3.4: Following Primers were used in the RT-qPCR reactions

<i>In-vitro</i> cancer cell	Gene of interest	Primers
HCT-116 colon cancer cells	β -actin	Forward 5'- AATCCCATCACCATCTTCCA -3' Reverse 5'- CCTGCTTCACCACCTTCTTG -3'
	PUMA	Forward 5'- GACCTCAACGACAGTACGA -3' Reverse 5'- GAGATTGTACAGGACCCTCCA -3'
	Caspase-3	Forward 5'- TGGCATACTCCACAGCACCTGGTT-3' Reverse 5'- ATGGCACACAAAGCGACTGGATG -3'
	Caspase-8	Forward 5'- CATCCAGTCACTTTGCCAGA -3' Reverse 5'- GCATCTGTTTCCCCATGTTT -3'
	Caspase-9	Forward 5'- TTCCCAGGTTTTGTTTCCTG -3' Reverse 5'- CCTTTCACCGAAACAGCATT -3'

Table 3.5 illustrates the RT-qPCR reaction steps and their set up with the following conditions according to the reference with minor modifications.

Table 3.5: Optimized qRT-PCR annealing reaction condition used to develop gene expression assays

Choice of gene	Optimized PCR amplification reaction				
	Prenaturation	Denaturation	Annealing	Extension	No. of cycles
PUMA	95 °C, 15 min	95 °C, 10 sec	55 °C, 30 sec	72 °C, 30 sec	50
Caspase-3	95 °C, 15 min	95 °C, 10 sec	55 °C, 30 sec	72 °C, 30 sec	40
Caspase-8	95 °C, 15 min	95 °C, 10 sec	55 °C, 30 sec	72 °C, 30 sec	50
Caspase-9	95 °C, 15 min	95 °C, 10 sec	55 °C, 30 sec	72 °C, 30 sec	50
β- actin	95 °C, 15 min	95 °C, 10 sec	55 °C, 30 sec	72 °C, 30 sec	50

In this experiment, the relative quantification of target mRNA gene expression from PUMA, caspase-3, caspase-8 and caspase-9 genes were analysed in control and experimental samples. The obtained mRNA expression results have been normalized by a reference gene expression (e.g. housekeeping genes). The following equation is used to calculate the average of the mRNA expression in treated and control samples.

$$\text{Normalization} = (\text{Mean value of treated} / \text{Mean value of control})$$

3.9 Statistical analysis

The obtained results were expressed as mean \pm standard deviation (SD) and the data were analyzed with the student's *t*-test, one-way analysis of variance (ANOVA). The difference was considered as statistically significant at $p < 0.05$. All experiments (n=3) were carried out in triplicate.

CHAPTER 4

RESULTS AND DISCUSSIONS

4.0 CHAPTER OVERVIEW

In this chapter, the results of the synthesized gold and silver nanoparticles and its *in-vitro* antibacterial, anticancer activities are presented. The synthesized metal nanoparticles sizes, shapes, crystalline nature and their functional groups are reported. In addition, the phytochemical analysis, GC-MS characterization, antibacterial and antioxidant activities of the aqueous plant extracts are provided. Furthermore, the metallic nanoparticles were characterized by their potential *in-vitro* anticancer ability against HCT-116 colon cancer cells. Also, the cell cycle pattern and gene expression profile of gold and silver nanoparticles treated with HCT-116 cells are discussed.

4.1 BIOSYNTHESIS, CHARACTERIZATION AND BIOLOGICAL PROPERTIES OF AuNPs

4.1.1 Biosynthesis of gold nanoparticles using *C.nudiflora*

Figure 4.1a shows the colour reaction of gold nanoparticles using *C. nudiflora* extract. After the mixing of the plant extract and 10^{-3} tetrachloro aureate solution, the colour of the medium gradually changed from yellow to violet. This indicates that the redox reaction occurred and confirmed the gold nanoparticles formation in the mixture solution. After the reduction completed, the reaction was continued until 24 hours to check the stability of the synthesized nanoparticles. Nevertheless, the colour change did not occur in the solution and the colour intensity retained for 3 months.

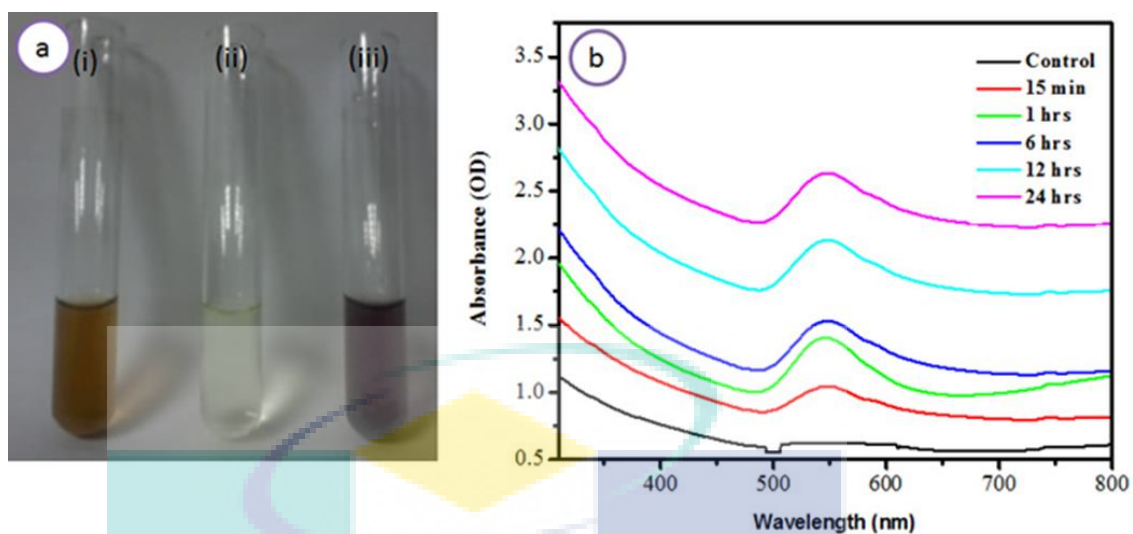


Figure 4.1a: Colour indicates the reduction of HAuCl_4 ions (a) plant extract (b) 10^{-3} HAuCl_4 (c) mixture solution. **Figure 4.1b** UV-VIS absorption spectrum of biosynthesized gold nanoparticles with different time intervals

4.1.2 Studies on UV- VIS spectra of gold nanoparticles

Figure 4.1b illustrates the UV-Vis spectra of gold solution with function of time. The UV-Vis results show that the surface plasmon resonance (SPR) peak becomes broad and sharper. The peaks position between 540 to 550 nm regions which indicates the gold nanoparticles formed in the mixture. The free electrons of metallic nanoparticles may induce the surface plasmon resonance (SPR) and absorption frequencies (Jain et al., 2006).

Dubey et al. (2010) studied the increasing concentration of metal ion (10^{-4} to 10^{-2} M) could increase the particles formation and did not find any significant changes at the peak of visible or IR region. Also, the highest contact time of aurete salt and plant extract showed that the UV-Vis spectra became sharper with higher absorbance value. The formation of nanoparticles started in 15minutes and gradually reached 100% growth rate within 2 hours. However, the UV-Vis absorbance range was not much different when observed between the synthesis times. Likewise, Singh et al. (2010) observed there was a maximum absorbance peak at 516, 534 and 564 nm on the different ratio of HAuCl_4 and clove extract mixture. The peak of gold spectra is also

based on the presence of counter ions such as Na^+ and K^+ in the solution. These counter ions come from the plant extract and it may enhance the redox reaction and also initiate the colour formation in the mixture. In this study, the gold ions were completely converted into gold nanoparticles in 2 hours, after that, no colour changes were seen in the synthesis medium. The different plant extracts produced metallic nanoparticles in various time intervals as described in Table 4.1. The role of pH in the biosynthesized nanoparticles could be a key factor to produce the desired size. The synthesized gold nanoparticles are highly stable, uniform and spherical in shape, but the lower pH might increase the particle aggregation in the sample. In biological synthesis, when the temperature was increased to $100\text{ }^\circ\text{C}$, the activation energy was faster but reducing the power of the biological moieties may change (Sneha et al., 2001). So, the biomolecules were affected by increasing the reaction temperature in the biosynthesis route.

The reduction of Au^+ ions using *C. nudiflora* extract was initiated to be 1500 ppm at the optimum pH 7. The conversion rate of metal ion was calculated using ICP-MS where it shows more than 95% was reduced within 24 hours (Figure 4.2). Similarly, Pandey et al. (2013) proved that the 90 percentage of metallic salt conversion into metallic nanoparticles was within 18 hours.

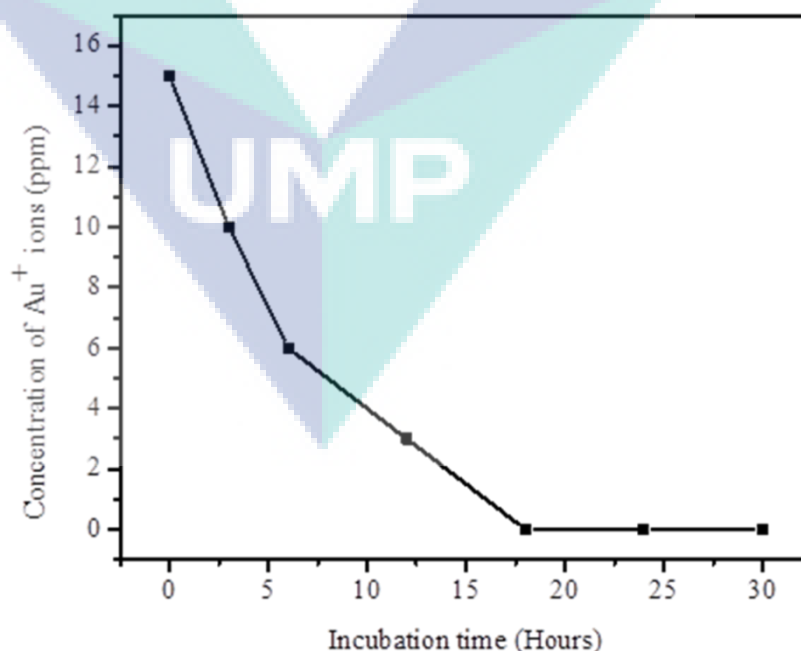


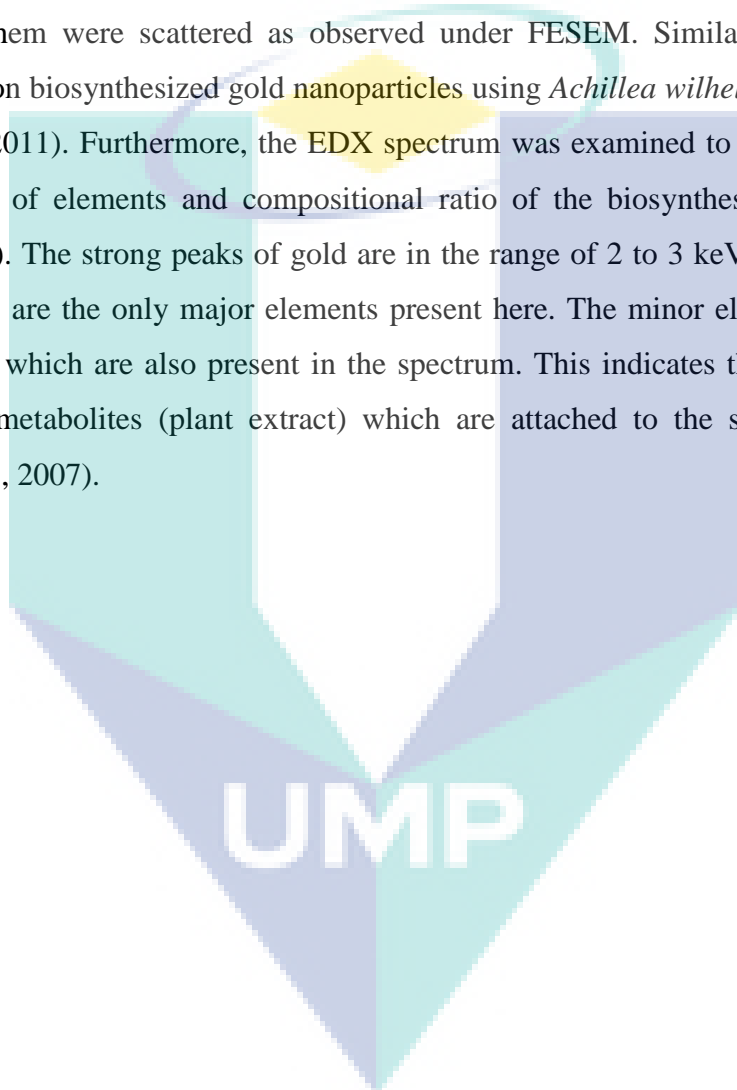
Figure 4.2: Quantification of Au^+ ions reduction in the synthesized medium using ICP-MS

Table 4.1: Biosynthesis of metallic nanoparticles using plants and microorganisms and their reaction kinetics

Biological precursors	Type of nanoparticles	Reduction time	References
Plant			
<i>Punica granatum</i>	gold	60 sec	Ganesh Kumar, et al., 2013
<i>Anacardium occidentale</i>	gold	5 min	Sheny et al., 2011
<i>Prunus armeniaca</i>	gold, silver	8min	Dauthal and Mukhopadhyay, 2013
<i>cypress leaves</i>	Gold	10min	Noruzi et l., 2011
<i>Black Tea</i>	gold, silver	30min	Begum et al., 2009
<i>Coleus amboinicus</i>	Gold	1 hr	Narayanan and Sakthivel, 2010
<i>Cassia auriculata</i>	Gold	10min	Ramamurthy et al., 2013
<i>Crocus sativus</i>	Gold	2 hr	Vijayakumar et al., 2011
<i>Commelina nudiflora</i>	Gold	2 hr	[current study]
<i>Volvariella volvacea</i>	gold, silver	2.5 hr	Philip et al., 2009
<i>Szygium aromaticum</i>	gold, silver	24 hr	Singh et al., 2010
Fungus			
<i>Aspergillus niger</i>	Gold	24 hr	Sugunan et al., 2007
<i>Candida sp.</i>	Gold	5 hr	Wani et al., 2011
Algae			
<i>Navicula atomus (diatom)</i>	gold-silver	2hr	Schrofel et al., 2011
<i>Nostoc ellipsosporum (green algae)</i>	gold	48hr	Parilal et al., 2012
Bacteria			
<i>Pseudomonas fluorescens</i>	Gold	48 hr	Rajasree and Suman, 2011
<i>Geobacillus stearothermophilus</i>	Gold	24 hr	Fayaz et al., 2011

4.1.3 Structural and morphological study of gold nanoparticles

Figure 4.3 shows the typical FESEM images of synthesized gold nanoparticles. The synthesized gold nanoparticles are higher in density of polydispersed spherical AuNPS of various sizes from 50 to 150 nm with a very small percentage of rectangle and rod shaped structures observed. Most of the nanoparticles were aggregated and only a few of them were scattered under FESEM. Similar morphology was elucidated on biosynthesized gold nanoparticles using *Achillea wilhelmsii* flower extract (Andeani, 2011). Furthermore, the EDX spectrum was examined to observe the spatial distribution of elements and compositional ratio of the biosynthesized nanoparticles (Figure 4.4). The strong peaks of gold are in the range of 2 to 3 keV, which confirmed that AuNPs are the only major elements present here. The minor elements are oxygen and carbon which are also present in the spectrum. This indicates the existence of the secondary metabolites (plant extract) which are attached to the synthesized sample (Dong et al., 2007).



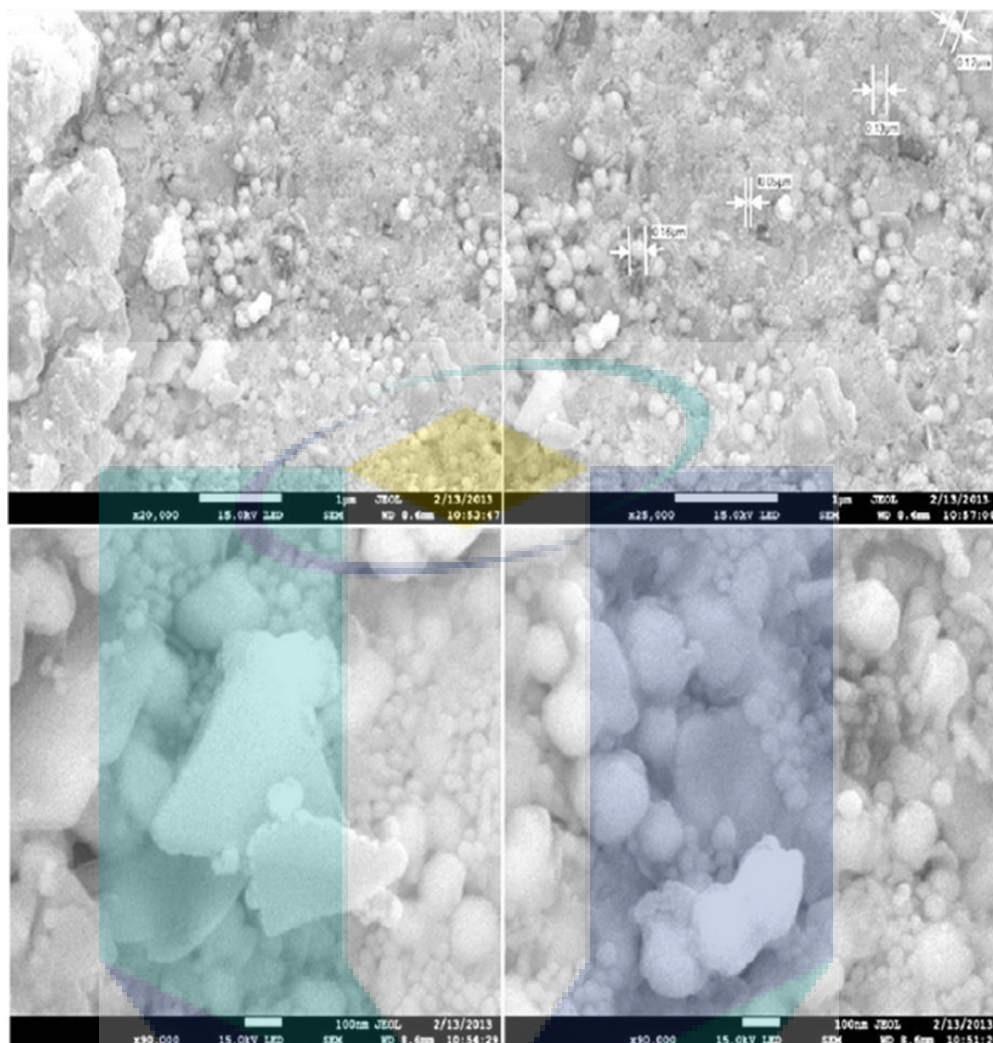


Figure 4.3: FESEM micrograph shows the different structure of gold nanoparticles synthesized using *Commelina nudiflora* extract

The presences of carbon and oxygen elements along with gold were seen in the EDX spectrum. Thus, this result leads to the evidence that the different elements act as stabilizing molecules on nanoparticles biosynthesis (Reveendran et al., 2003).

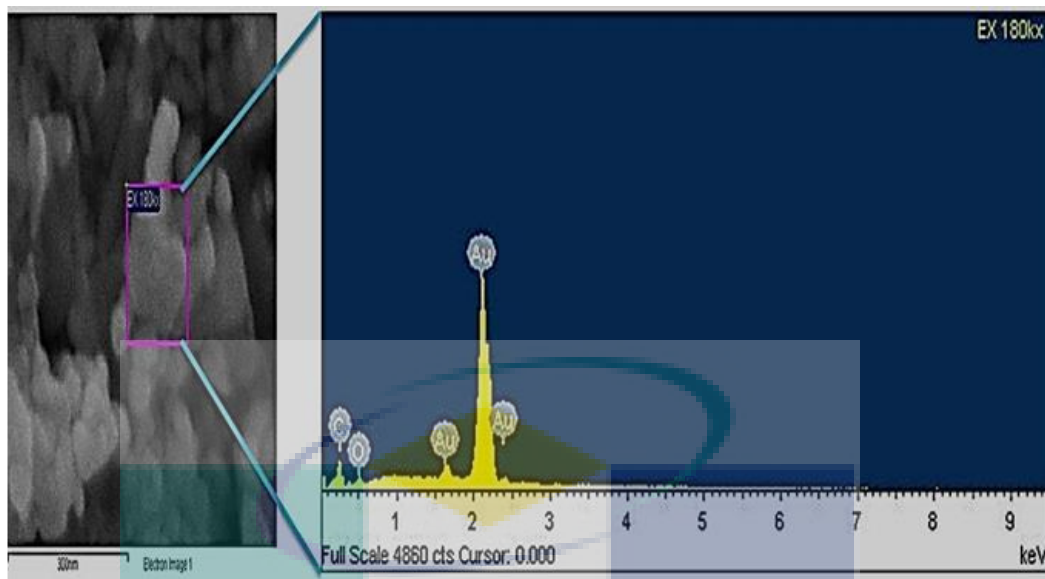


Figure 4.4: EDX graph expresses the presence of gold metal synthesized using *C. nudiflora* extract

Table 4.2: Summary of different bio-substrates used for metallic nanoparticles synthesis

Substrates	Nanoparticles	References
Sun light	Gold	Ganeshkumar et al., 2012
Melanin	Gold	Apte et al., 2013
Polysaccharides	Silver	Sathiyarayanan et al., 2013
Protein	Gold	Ravindra, 2009
Phospholipid	Gold	Chow et al., 1996
Counter ions	Gold	Sneha et al., 2010
Plant waste (POME, banana peel)	Gold	Bankar et al., 2010 Gan et al., 2012
Water	Gold	Li et al., 2011
Sucrose ester	Silver	Huang et al., 2010

Table 4.2 shows the different biological precursors used to synthesize gold and silver nanoparticles by biological method. Interestingly, some agro and industrial wastes

have been synthesizing metallic nanoparticles in eco-friendly ways. Based on that, the *C. nudiflora* common edible weed synthesizes metallic nanoparticles in a biological route with less cost and is environmental friendly.

Figure 4.5 XRD result shows the crystalline nature of synthesized AuNPs. The XRD graph reveals that the four different peaks correspond to (111), (200), (220) and (311) at $2\theta = 38.4^\circ$, 46.5° , 66.6° and 78.6° of metallic gold nanoparticle respectively. The peaks (111), (200), (220) and (311) have specific lattice spacing which expresses the different morphology and crystalline in the structure of the gold nanoparticles.

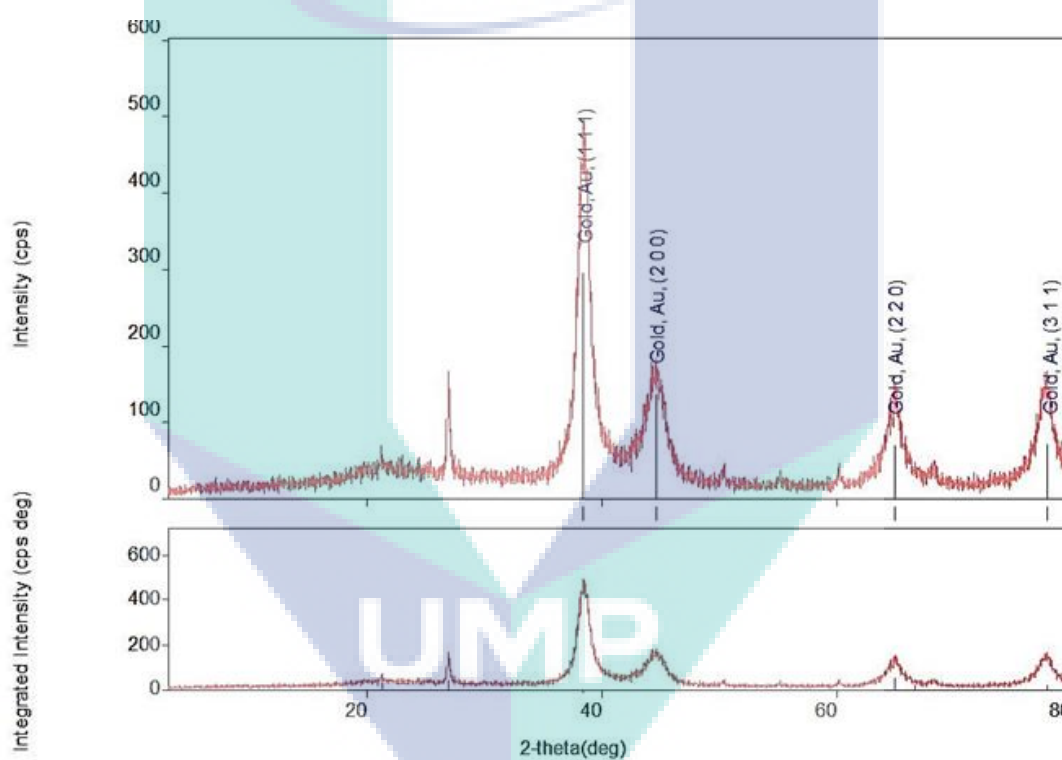


Figure 4.5: Powder XRD of biosynthesized gold nanoparticles using *C. nudiflora* extract

Similarly, 2θ values of 38.21° , 44.34° , 64.78° and 77.67° broad peaks indirectly represent the nanoparticles crystalline nature. The major shift in the peak positions (111) indicates the presence of crystal structure of metallic gold nanoparticles (Banupriya et al., 2010). Also, the *N. arbortristis* synthesized gold nanoparticles exhibit four prominent AuNPs peaks indexed as (111), (200), (220) and (311) which

correspond to 38.1° , 44.4° , 64.8° and 78.1° respectively, it express the nanoparticles are of single crystalline nature (Das et al., 2011). In contracts, the green synthesis of gold nanoparticles using aqueous extract of citrus fruits (*C.limon*, *C.reticulata*, *C.sinensis*) shows the (111) plane is more intense than the other indexed planes. Thus, the (111) plane has a predominant angle which is exactly equals to the standard database of gold material (Sujitha and Kannan, 2011).

4.1.4 Confirmation of functional groups from metallic gold nanoparticles

FT-IR spectra shows the different functional groups involved in the gold nanoparticles synthesis (Figure 4.6a). The FT-IR spectra confirmed strong absorbance bands in the region at 3401.29 cm^{-1} (N-H stretch – amides, alcohols), 1651.31 cm^{-1} (C=O stretch, amides) and medium range at 1539.07 cm^{-1} (N-H bends, amide) and 1032.17 cm^{-1} (C-N stretch, aliphatic amines). Among them, 850.40 cm^{-1} , 797.20 cm^{-1} signs indicate the presence of R-CH group; the metabolites predominantly involved in the reduction of Au^{III} into Au^0 . Overall, the FT-IR studies concluded that the amide, phenolic acids, sugar moieties and aliphatic amines are intensely contributed to the bioreduction mechanisms (Figure 4.6b). The well-known signature of these molecules is represented by the strong binding with ionic compound and reduced by metal nanoparticles.

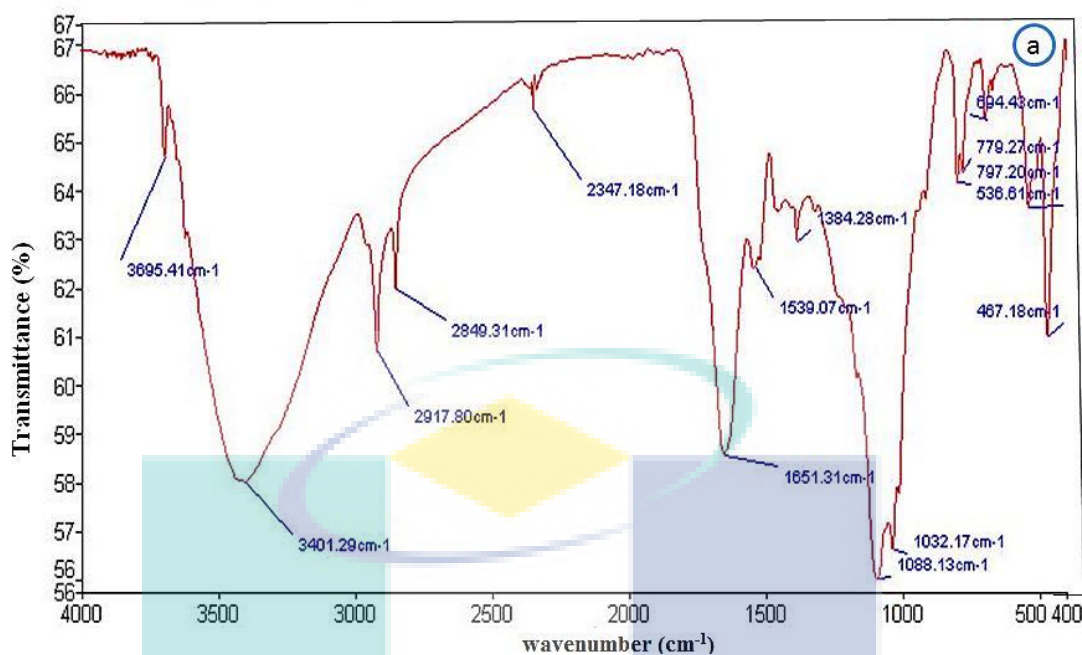


Figure 4.6a: The functional groups of plant extract are characterized by FT-IR

Similarly, the fenugreek seed extract contains various biological active compositions such as polysaccharides (sugar) and protein which cap and reduce gold nanoparticles from free gold ions (Aromal, 2012). Ravindra et al. (2003) reported the Fourier Transform Infrared (FT-IR) spectra result expressed the specific functional groups involved in the gold nanoparticles synthesis mechanism. There is a clear signal at 1405.28 cm^{-1} which exposes symmetric stretching of COO^- from amino group and the medium signal at 1719.03 cm^{-1} hydroxyl functional metabolites successfully converted ionic into metallic Au nanoparticles. Additionally, Jayaseelan et al. (2013) studied strong band at 1321 and 1388 cm^{-1} which are characteristics of C-N stretching vibration of aromatic amines and 1047 and 1064 cm^{-1} are identified as C-OH stretching of secondary alcohols which are identified in *A. esculentus* seed extract synthesized Au nanoparticles. So, these kinds of nutraceuticals/ metabolites also could be liable for the stabilization of gold nanoparticles.

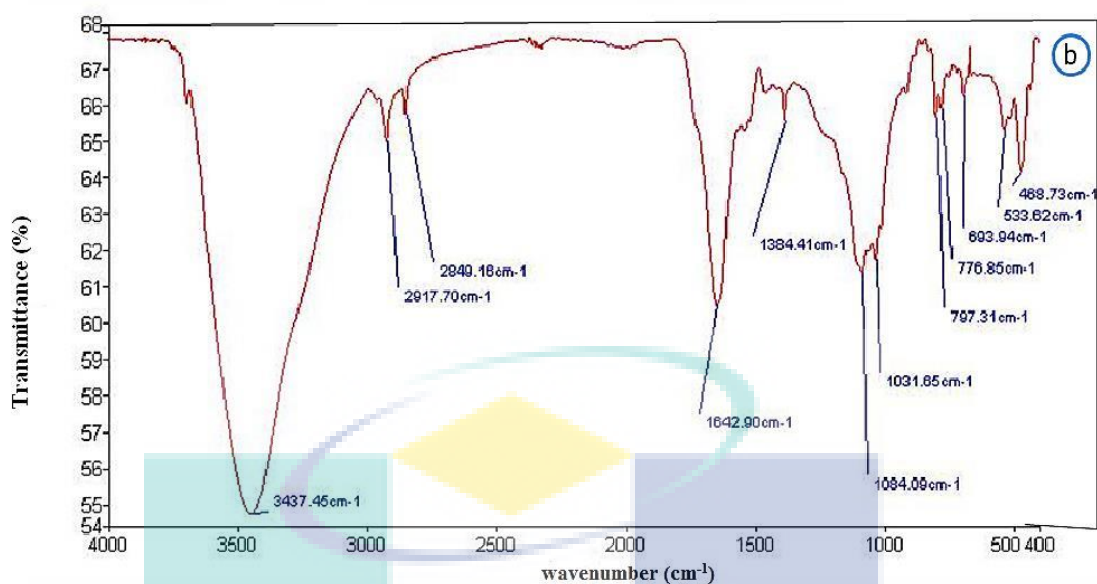


Figure 4.6b: Functional groups characterized by FT-IR spectra from gold nanoparticles sample

4.1.5 Analysis of particles size distribution and zeta potential studies

Figure 4.7 shows the average size distribution of gold nanoparticles in biosynthesized colloidal solution. The average size of gold nanoparticles was observed at 230 ± 20.09 nm. A negative zeta potential of -29.0 ± 0.77 mV was found in the synthesized gold nanoparticles. It expresses the potential surface charge of the synthesized gold nanoparticles. Sankar et al. (2013) says that the high absolute value of zeta potential expresses high electrical charge of the nanoparticles which can cause high stabilization of nanosuspension. The polydispersity indexes (PI) of gold nanoparticles are shown to be more than 400.

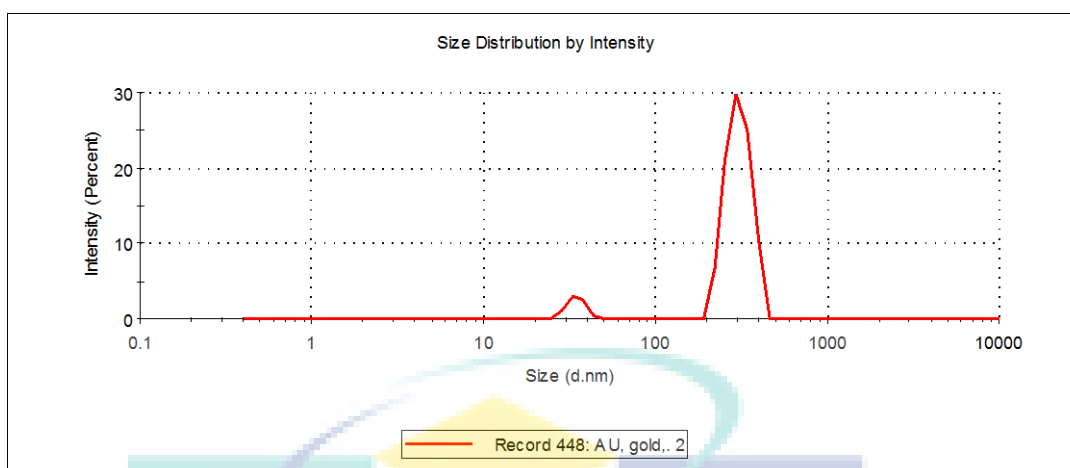


Figure 4.7: Particle size distribution of plant synthesized gold nanoparticles

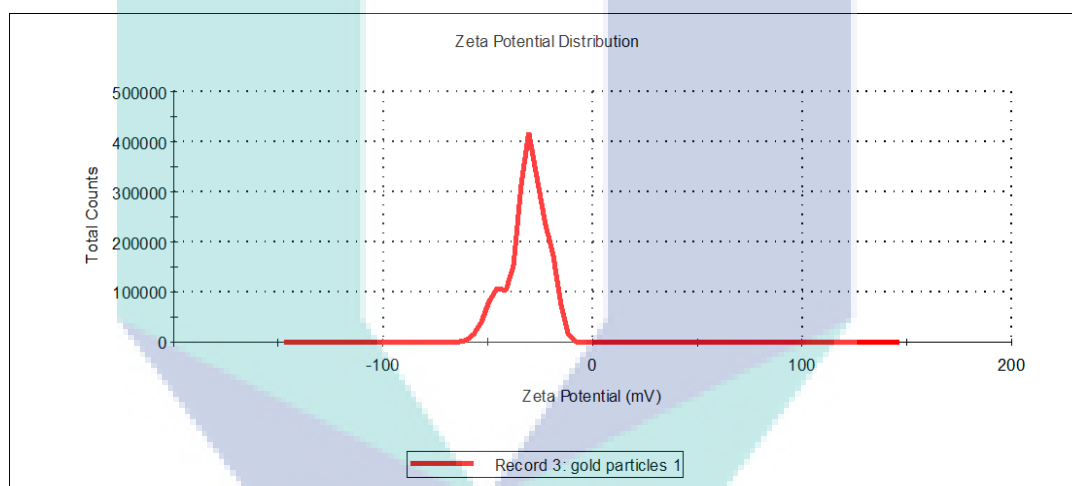


Figure 4.8: Zeta potential analyses of biosynthesized gold nanoparticles

The zeta potential (ZP) values reveal the information of the surface charge and stability of biosynthesized AuNPs. Adavallan et al. (2014) showed the average ZP value (-16 mV), and the highest negative value suggested the higher stability of colloidal AuNPs. The negative charge was also one of the indicators of particles size in the sample. The lower amount of negative charges in DLS indicates the nanoparticles diameters of less than 100 nm (Tabrizi et al., 2009).

4.1.6 TGA and BET analyses of biosynthesized gold nanoparticles

Figure 4.9 shows the thermograms of the biosynthesized gold nanoparticles. Interestingly, two main weight losses are observed in the TGA graph which are recorded in the temperature range of 50 °C to 700 °C. The first weight loss was recorded at 100 °C which was due to the loss of water molecules present in the samples. Next, the second weight loss was observed at the temperature between 300 to 350 °C. This weight loss was measured to be 50 % from the total weight of the gold nanoparticles sample.

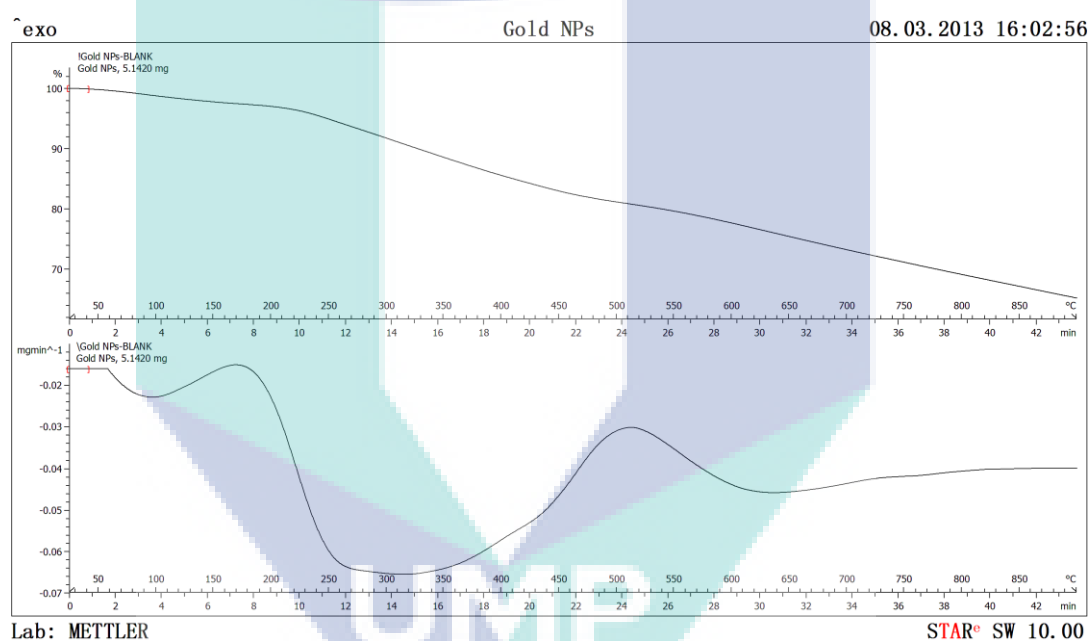


Figure 4.9: TGA thermogram of *C. nudiflora* synthesized gold nanoparticles

Figure 4.10 shows the BET plot of synthesized gold nanoparticles from *C. nudiflora* plant extract. Ahmad et al. (2013) reported that the BET plot of biosynthesized gold nanoparticles specific surface area was 18.9 m²/g. The biosynthesized metal nanoparticles have a significant surface area which can be useful in different biomedical applications.

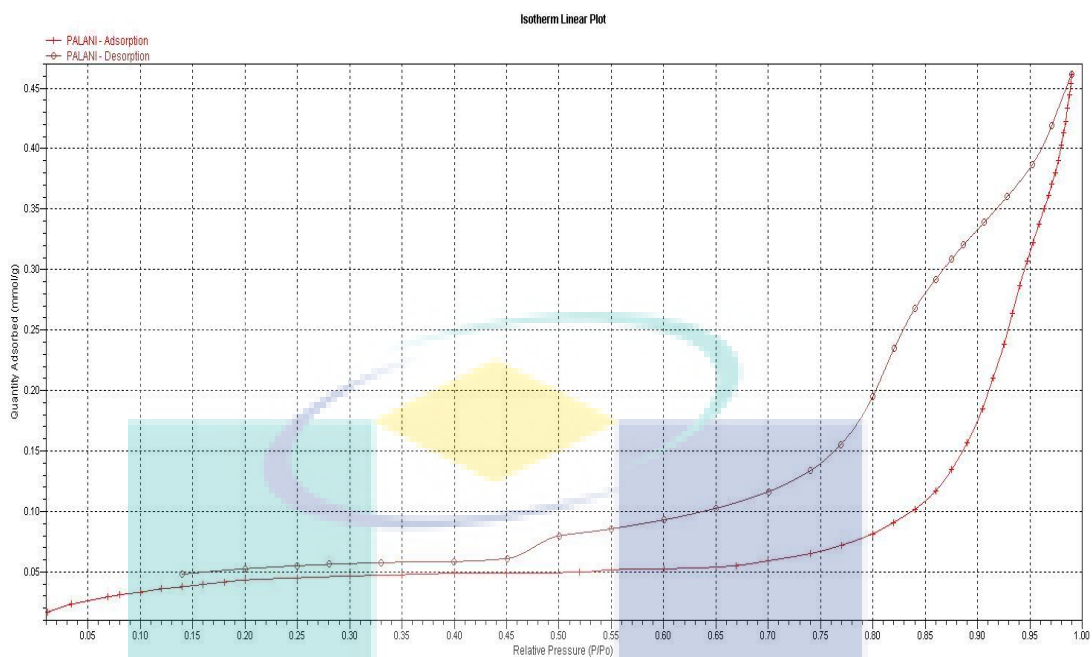


Figure 4.10: BET plot of the synthesized gold nanoparticles from *C. nudiflora* extract

4.1.7 Antibacterial activities of GNPs

The biosynthesized gold nanoparticles have strongly acted against different clinically harmful pathogens. The authentic bacterial strains were inoculated in corresponding MHA plates treated with 100, 75 and 50 $\mu\text{g/ml}$ /well concentrations of gold nanoparticles as shown in Figure 4.11. The higher concentration of gold nanoparticles (100 $\mu\text{g/ml}$) shows the highest zone of inhibition against *Staphylococcus aureus* and *E.coli*. Besides, the moderate growth of inhibition was observed in *Pseudomonas aurogenosa* and *S.typhi*. Further, the zone of inhibition (ZOI) of gold nanoparticles was observed in both pathogenic groups which were gram positive and gram negative bacteria. The highest clearing zones were shown in *E.coli* and *Staphylococcus aureus* with 16 and 13 mm respectively. The moderate growth inhibition was *Pseudomonas aurogenosa* and *S.typhi* which showed 12 and 11mm respectively, at the same concentration of 100 $\mu\text{g/ml}$.

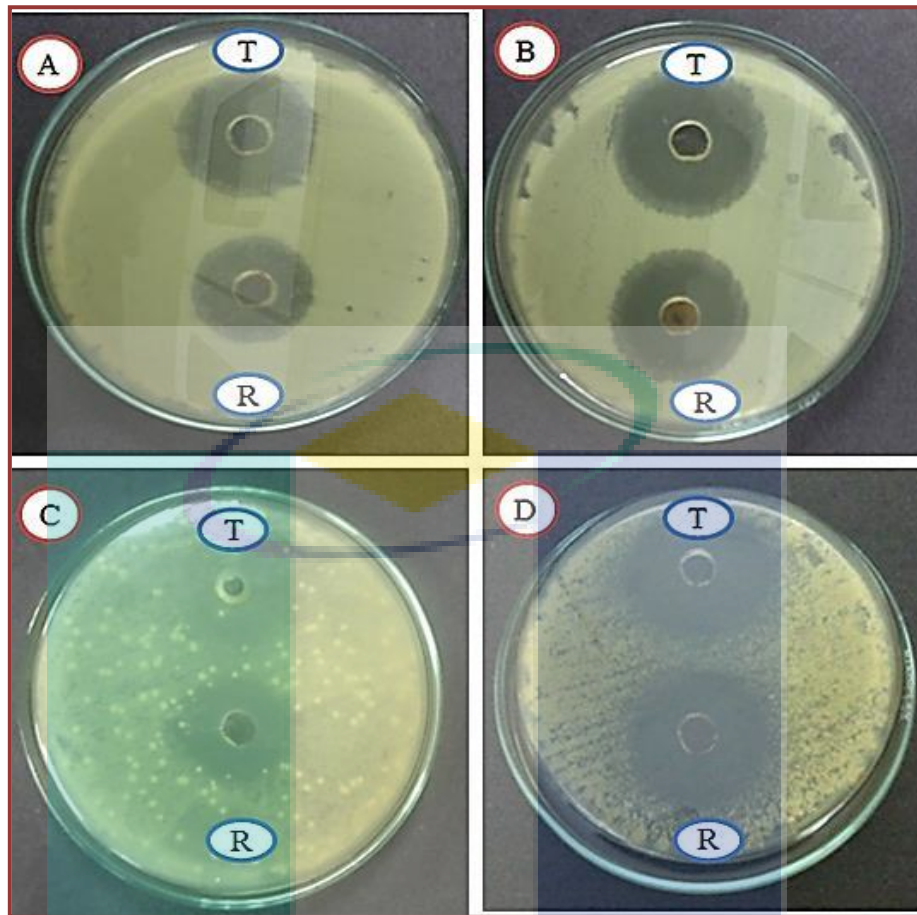


Figure 4.11: Antibacterial activity of AuNPs against different human pathogens a) *E.coli* b) *Bacillus subtilis* c) *Salmonella typhi* d) *Staphylococcus aureus* (T- test compound (AuNPs), R- Reference drug (streptomycin))

Lim et al. (2013) explored the biosynthesized gold nanoparticles which act as antimicrobial agents against *E.coli* and *Salmonella typhi*. The nanoparticles have a specific site of action in pathogenic microorganism compared with commercial antimicrobial drugs. The gold nanoparticles possess larger surface area, high stability and a smaller size making them easier to interact with microorganisms. Also, the smaller particles can easily interact with the outer membrane of cells and might cause structural changes and finally degrade the cells. The AuNPs stimulate biofilm production and each biofilm produces microorganisms that are bound closely on the surface. The biofilm producing bacteria trapped on that biofilm surface, it allows strongly bind with gold nanoparticles and eventually distort the cell wall of organisms (Geethalakshmi and Sarada, 2013).

4.1.8 Antioxidant activities of GNPs

Gold nanoparticles are more capable to control the free radical formation in cells due to the potent physico-chemical properties. The DPPH radical scavenging activity was monitored by DPPH color reaction, the purple DPPH changed into cherry red DPPH₂ molecules depending on the gold nanoparticles that bind with the excess free radicals from the reaction mixture. The DPPH scavenging activity of gold nanoparticles increased from 14 % to 35 % and the IC₅₀ value was found to be 20 µg/ml of AuNPs. Similarly, Dauthal et al. (2013) reported that the quenching effect of free radical scavenging of the nanoparticles increased from 15 % to 35 % in the gold nanoparticles treated samples, due to the plant extract combination in the synthesized solution.

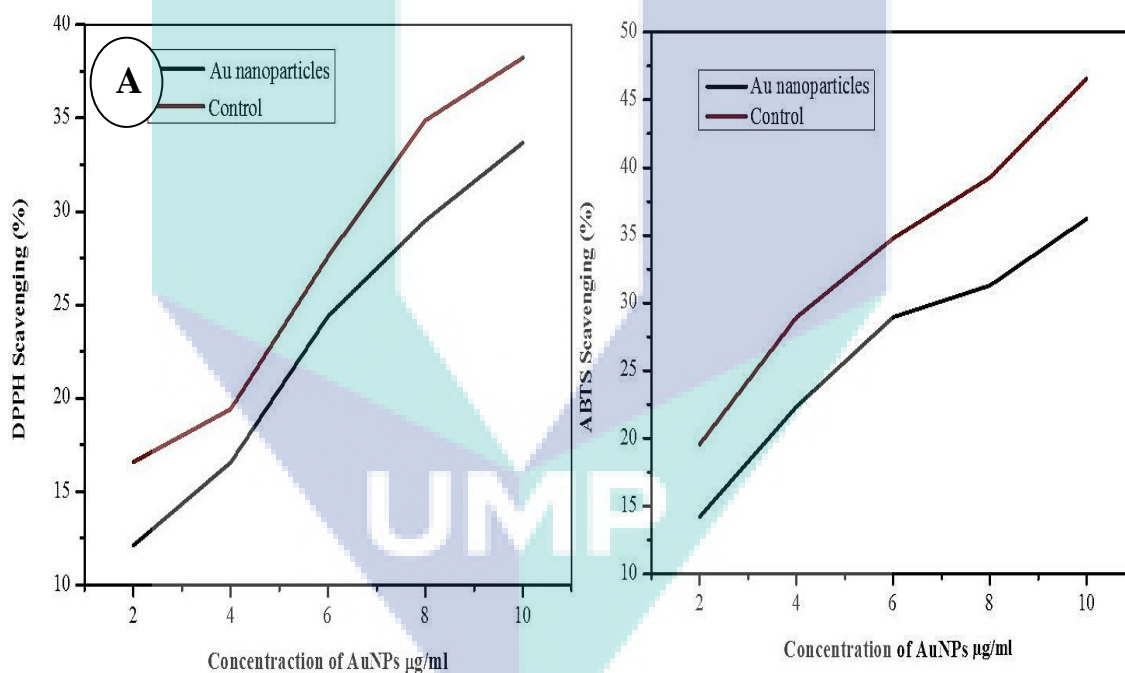


Figure 4.12: A) DPPH free radical scavenging activity of different concentrations of gold nanoparticles B) ABTS free radical scavenging activity of different concentrations of gold nanoparticles

The IC₅₀ values of ABTS were found in 40 µg/ml of gold nanoparticles. The lowest concentration of gold nanoparticles has a moderate activity in the DPPH assay compared to ABTS scavenging activity (Figure 4.12). This study evaluates the free

radical scavenging activity of gold nanoparticles and it could be a major impact in pharmaceutical industries as a free radical controlling agents.

Moreover, the existing antioxidant compounds are complicated to control the free radical scavenging activity. The development of bio-nanoparticles effectively acts as pro-oxidant control. The AuNPs are alternative antioxidant agents in free radical scavenging (Kalishwaralal et al., 2009). However, these antioxidant compounds were fascinated biomolecules onto the active surface of nanoparticles. The surface reaction phenomenon and large surface area of nanomaterials may generate a higher affinity to bind with the scavenged free radicals (Ganeshkumar et al., 2011).

Gold nanoparticles exhibit a high catalytic activity in redox reaction such as oxidative stress and cellular respiration. It is effectively interactive with free radicals and control oxidative damage. GNPs could prevent the oxidative DNA damage by the inter conversion of oxidative states from Au^0 to Au^{+1} . However, the electron acceptance/donating mechanism of metallic nanoparticles does not affect the plant metabolites (Yakimovich et al., 2008, and Ramamurthy et al., 2013).

4.2 BIOSYNTHESIS, CHARACTERIZATION AND BIOLOGICAL APPLICATIONS OF AgNPs

4.2.1 Biosynthesis of silver nanoparticles

The *C. nudiflora* aqueous extract was used as a reducing and stabilizing agent for the reduction of silver ions into metallic silver nanoparticles. The redox reaction was confirmed by the color changes in the synthesized solution.

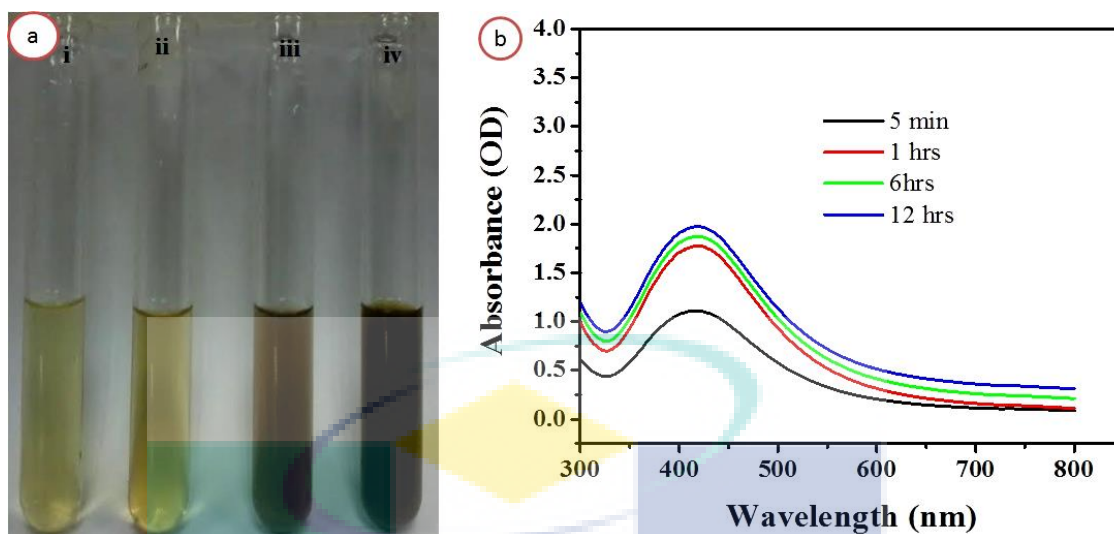


Figure 4.13: a) Colour formation after reduction of AgNO_3 using *Commelina nudiflora* aqueous extract i) 5 min ii) 30min iii) 1 hrs iv) 2 hrs. b) UV-Vis absorption spectra of biosynthesized silver nanoparticles with different time intervals

The pale yellow colour that changed into brown colour indicates that the reduction occurred in the mixture solution as shown in Figure 4.13a. The intensity of colour changed at different time intervals due to the increasing concentration of AgNPs in the sample. The unique colours of AgNPs were indirectly shown in several sizes and shapes of the nanoparticles formed in the synthesized medium.

4.2.2 UV-Vis spectra confirmation of biosynthesized AgNPs

Figure 4.13b shows UV-Vis spectra of silver nanoparticles using *C. nudiflora* aqueous extract. The maximum absorption band occurred in 435 nm and gradually increased as a function of time. The UV-Vis absorption spectrum is a strong evidence that the metal nanoparticles formed in different sizes and shapes in the medium.

The particle size was possibly controlled by the fluctuating temperature, leaf broth and metal ion concentration. For instance, the *Magnolia* plant extract concentration may control the particles size and reduction time by slowly increasing the concentration from 5% to 50% (Song and Kim, 2009). The higher concentration of plant extract produces bigger size nanoparticles and it may take longer reaction time. Similarly, the increasing concentrations of olive leaf extract shows the absorption peak is sharper and high SPR at 458nm. The sharper narrow peak indicates spherical shapes of nanoparticles and a homogeneous distribution in the solution. Therefore, the biosynthesis of silver nanoparticles requires a suitable concentration of metal ion and plant extract that could be responsible for the complete reduction of silver ions into metallic silver nanoparticles and size differences (Gopinath et al., 2012).

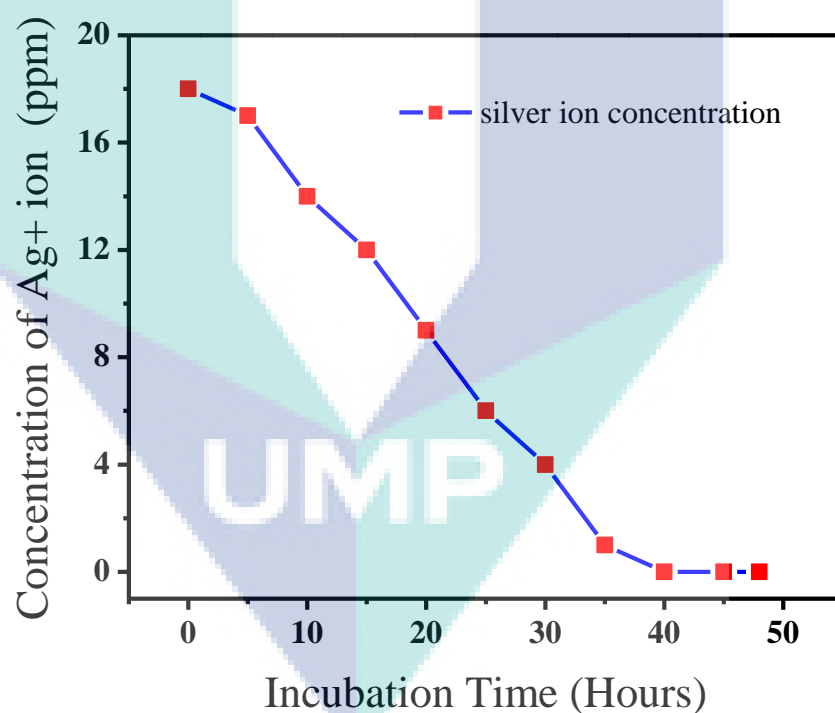


Figure 4.14: Quantification of Ag⁺ ions in the silver nanoparticles synthesized medium using ICP-MS

The presence of Ag ion in colloidal solutions was confirmed by the inductively coupled plasma mass spectrometry (ICP-MS) which revealed that there were Ag⁺ ions in the colloidal solutions anymore after 18 hours. The Ag⁺ ions were completely

reduced into bulk AgNPs by *C.nudiflora* extract. Figure 4.14 illustrates the ICP-MS quantification of Ag⁺ ions in the biosynthesized SNPs solution.

4.2.3 Structural characterization of AgNPs using FESEM with EDX

The morphology of the biosynthesized silver nanoparticles is presented in Figure 4.15. The obtained silver nanoparticles were spherical in shape with partial aggregates due to the sample being dried at a high temperature. The silver nanoparticles average size ranges from 30 to 45nm, calculated in the electron microscope.

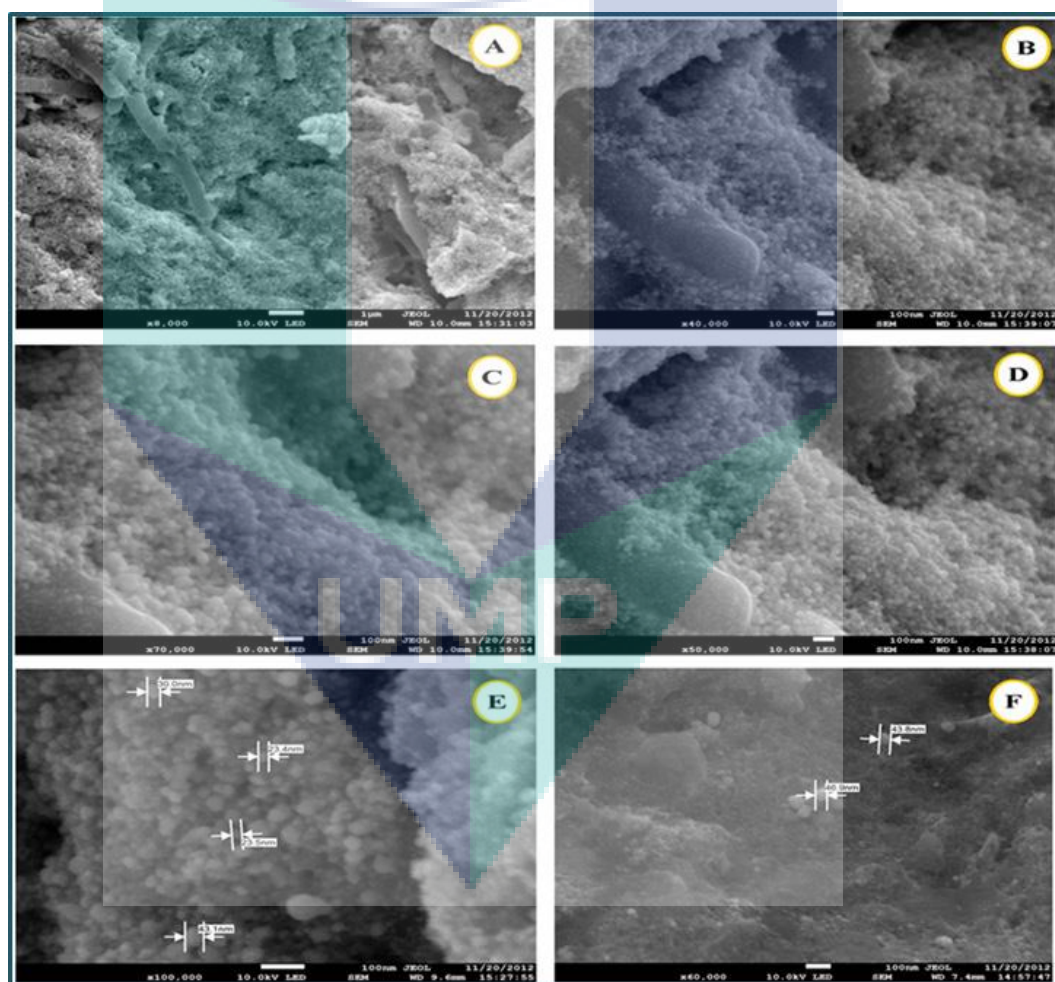


Figure 4.15: FESEM images of biosynthesized silver nanoparticles from *C. nudiflora* extract with different magnification powers (A-F)

FESEM micrograph was well documented to be spherical and less irregular shapes. The smaller size of particles was measured of about 25 nm and larger particle size is 47 nm and are spherical in shape. Similarly, the *Iresine herbstii* leaf extract synthesized a high density of silver nanoparticles at room temperature, the size ranges between 44 to 64 nm. The biosynthesis medium contains a high amount of flavonoids and terpenoids secondary metabolites which may exhibit the different sizes of the nanoparticles and reduction rate of metal ions (Dipankar and Murugan, 2012).

Figure 4.16 shows EDX spectrum of the synthesized silver nanoparticles. The EDX spectra is authentically expressed where the silver composition is nearly 80% in the synthesized sample. Thus, the strong signal energy peaks of silver atoms shown are in the range between 2 to 4 keV. Other weaker signals such as carbon, chloride and oxygen elements were also exhibited in the EDX spectra which is prevalent in the secondary metabolites of the plant extract.

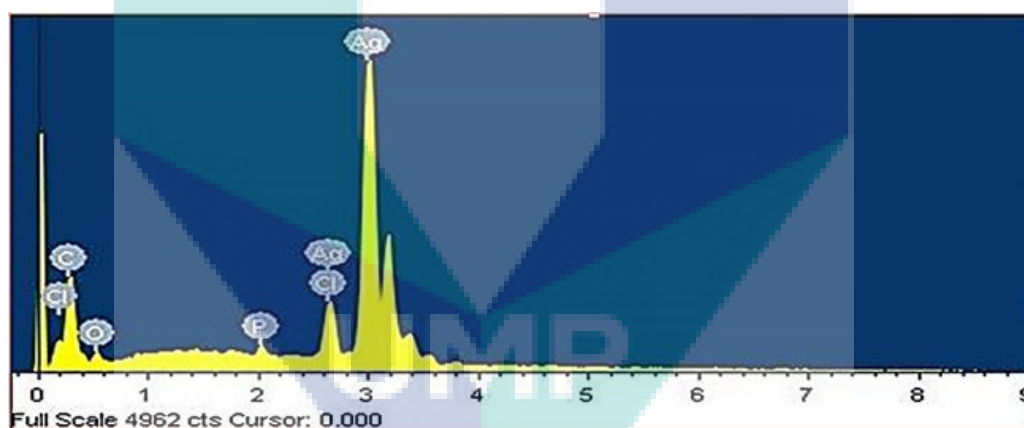


Figure 4.16: EDX spectrum of synthesized silver nanoparticles using *C.nudiflora*

4.2.4 Determination of crystalline nature of AgNPs using XRD

The XRD pattern of the synthesized silver nanoparticles is shown in Figure 4.17. The prominent intense peaks are observed at 38.1° , 77.6° and 81.9° which are assigned to (111), (220) and (311) respectively. Thus, the broadening of peaks confirms that the biosynthesized silver nanoparticles are crystalline in nature.

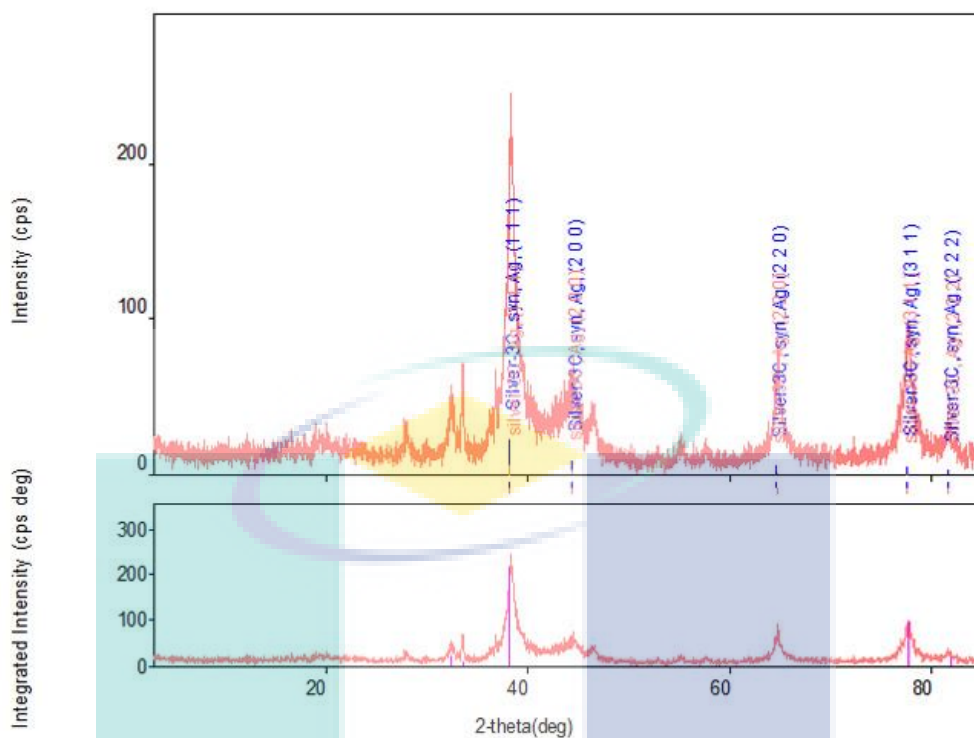


Figure 4.17: Powder XRD spectra of silver nanoparticles synthesized using *C. nudiflora* extract

The XRD graph typically shows some additional noise peaks which are unassigned peaks that may be due to the crystals of bioorganic phase present in the *C. nudiflora* plant extract. Similarly, the diffracted peaks are observed at 38.19° , 44.36° , 64.70° and 77.50° corresponding to the (111), (200), (220) and (311) facets of fcc lattice of silver nanoparticles obtained. These peak positions indicate the presence of silver nanocrystalline in the sample (Jain et al., 2006). Also, XRD smooth spectrum shows three intense peaks at 37.11° , 43.54° and 74.35° corresponding to the (111), (220), and (333) planes indicating the silver nanoparticles in the sample. Also, the undefined peak at 46° might have the crystalline nature of a reducing agent which is present in the synthesized plant mixture (Khan et al., 2011).

4.2.5 Particles size analyzer and zeta potential studies

The particle size distribution of SNPs is depicted in Figure 4.18. The silver nanoparticles average size distribution was found to be 185 ± 10.09 nm. The size of silver nanoparticles varies over a wide range due to agglomeration and polydispersity. The zeta potential value is -27.0 ± 0.77 mV, calculated in the synthesized silver nanoparticles which give the ideal surface charge of the synthesized silver nanoparticles (Lin et al., 2008).

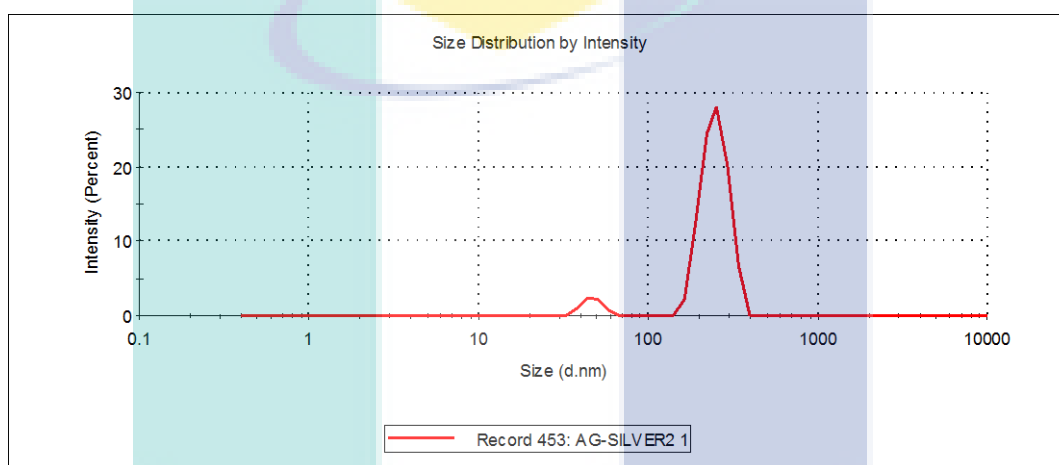


Figure 4.18: Particle size distributions in the synthesized silver nanoparticles using particle size analyzer

Similarly, the zeta potential value of SNPs calculated is -15.8 mV \pm 0.65 and the moderate negative charge exhibited a high stability of the biosynthesized nanoparticles (Figure 4.18). Generally, the biosynthesized metal nanoparticles have an absolute negative value with the increased pH of the synthesized medium (Gopalakrishnan and Raghu, 2014).

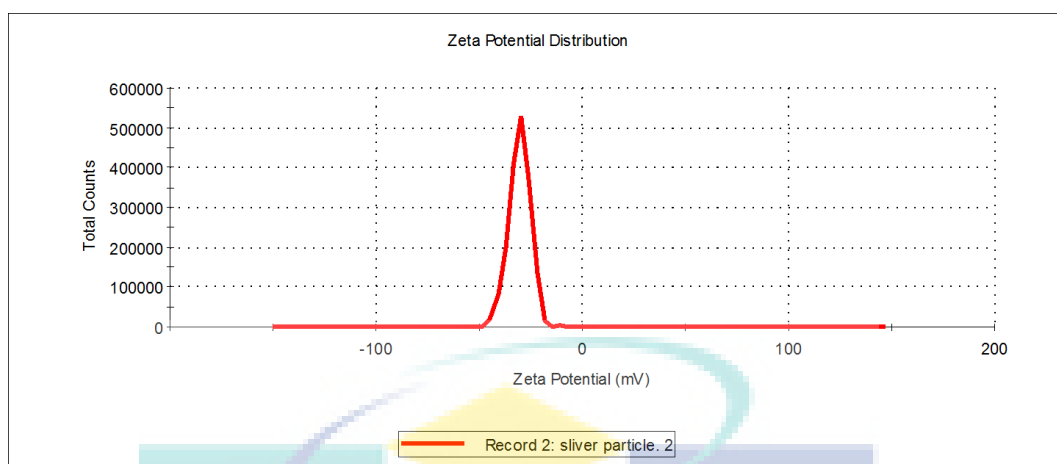


Figure 4.19: Zeta potential analysis of biosynthesized silver nanoparticles from *C. nudiflora* extract

4.2.6 Thermal gravimetric analysis and BET study of AgNPs

Figure 4.20 shows the TGA curve of the silver nanoparticles synthesized using *C. nudiflora* extract. Here, the sample weight loss was observed at the temperature between 260°C and 380°C. There is almost no weight loss below 250°C and above 380 °C. Overall, TGA results show adsorbed Ag nanoparticles of 11.1% below 260 °C. The dominant weight loss was occurred between 200 °C and 300 °C in the synthesized Ag nanoparticles sample.

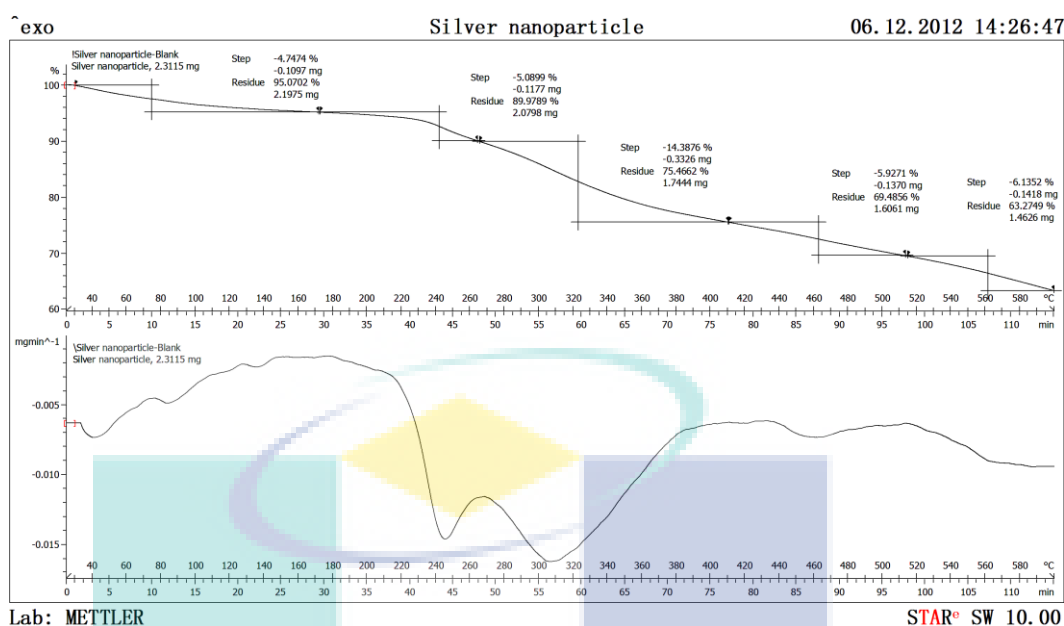


Figure 4.20: TGA thermogram of *C. nudiflora* synthesized silver nanoparticles

Similarly, Raja et al. (2012) determined the dominant weight loss occurred at the temperatures of 250 and 350 °C in plant mediated nanoparticles sample. There is almost no weight loss below 200°C and above 350 °C. Also, the result shows the highest weight loss of 14.58% at 300 °C. According to that, the biosynthesized metal nanoparticles have good thermal stability compared with chemically synthesized nanoparticles.

Figure 4.21 shows BET adsorption isotherm of the plant synthesized silver nanoparticles. The specific surface area of the silver nanoparticles was found to be at 3.0627 m²/g. The synthesized AgNPs have good surface energy when degassing at high temperature which may lead to grain diffusion and form relatively bigger particles. This study greatly influence on the particle distribution and cellular uptake. A negative value of zeta potential also indicates a high electric charge on the surface of the NPs (Baharara et al., 2014).

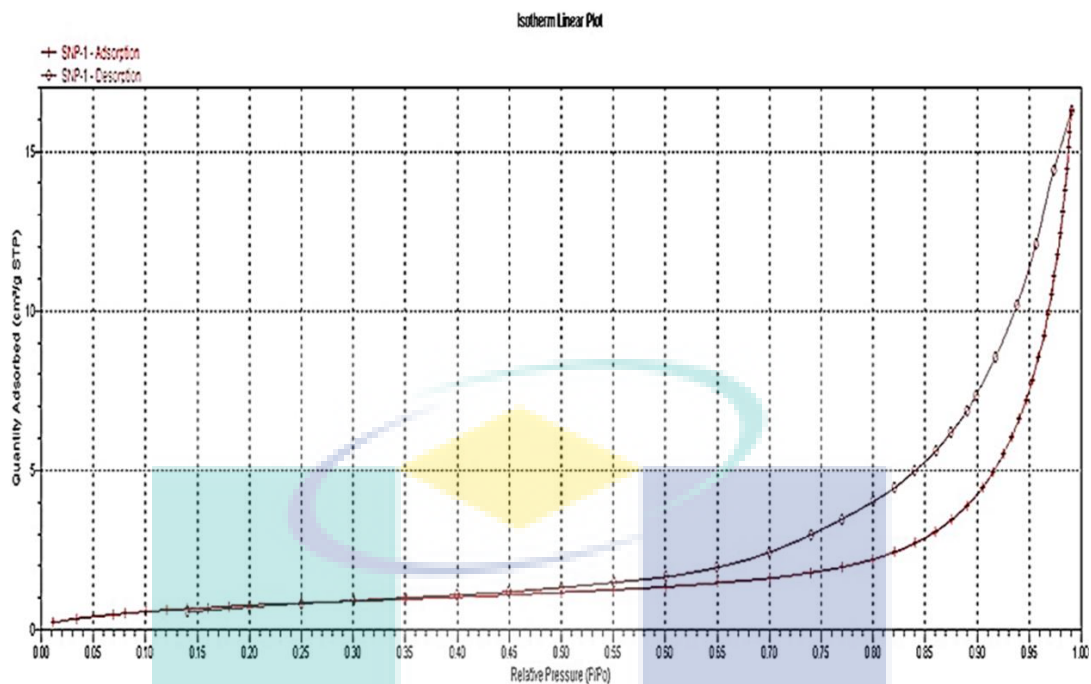


Figure 4.21: BET plot of the synthesized silver nanoparticles using *C. nudiflora* extract

The surface area of the AgNPs produces $78.59 \text{ m}^2 \text{ g}^{-1}$, whereas the higher surface area of the nanoparticles indicates better uniform pore distribution. Therefore, the BET plot shows the silver nanoparticles possessing a relatively large pores range in the sample (Rostamizadeh et al., 2013).

4.2.7 FT-IR analysis

Figure 4.22 shows FT-IR spectra of the biosynthesized silver nanoparticles. It expresses strong absorption bands at 1088 cm^{-1} and the stretching vibration (C-O, COO^- , ether and carboxylic acid), 1638 cm^{-1} (N-H, amide) of amino acid residue from protein and high absorption bands was observed in 3447 cm^{-1} which indicates how deforming vibration could be (phenols -O-H , amine R-NH_2). The presence of different clusters of secondary metabolites such as phenols, alcohol, carboxylic acid and protein could act as stabilizing and capping agents for the reduction of ionic compounds into the corresponding metal nanoparticles.

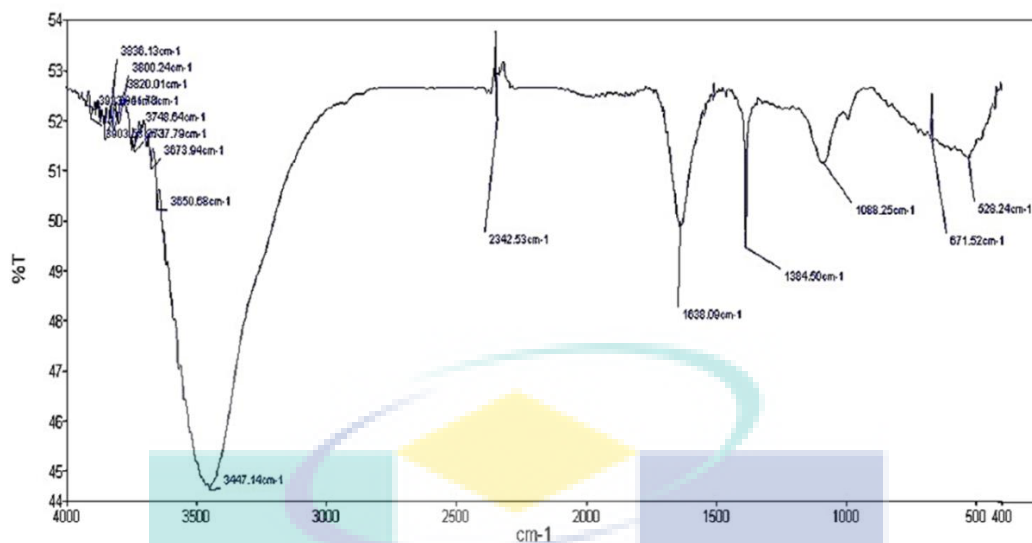


Figure 4.22: FT-IR spectra of synthesized AgNPs using *C. nudiflora* extract

FT-IR bands were confirmed as functional groups of secondary metabolites which are involved in the metallic nanoparticles synthesis. The secondary metabolites are mainly involved in the formation of pure metallic nanoparticles. The plant derived natural products such as terpenoids and polysaccharides possibly assisted the reduction reaction (MubarakAli et al., 2011). FTIR spectra exhibits a strong band at 2928 cm^{-1} (C-H stretching, aldehyde) and 1041 cm^{-1} (C-O-C stretching) which attributed to the reduction of Ag^+ into metallic Ag^0 . These prominent peaks were represented as flavonoids, phenolic, enzymes and terpenoids (Prakash et al., 2012).

4.2.8 Antibacterial study using AgNPs

In the present study, *C.nudiflora* mediated silver nanoparticles (50, 75 and 100 $\mu\text{g/ml}$) were tested against *E. coli*, *P. gingivalis* and *S. aureus* by disc diffusion method. The silver nanoparticles show an effective zone of inhibition at a higher concentration (100 $\mu\text{g/ml}$) which are 11 mm and 12 mm against *P. gingivalis* and *E.coli* respectively (Table 4.3). *S. aureus* showed moderate activity which is 9mm of ZOI. Figure 4.23 shows different concentrations of silver nanoparticles against pathogenic bacteria by agar disc diffusion method.

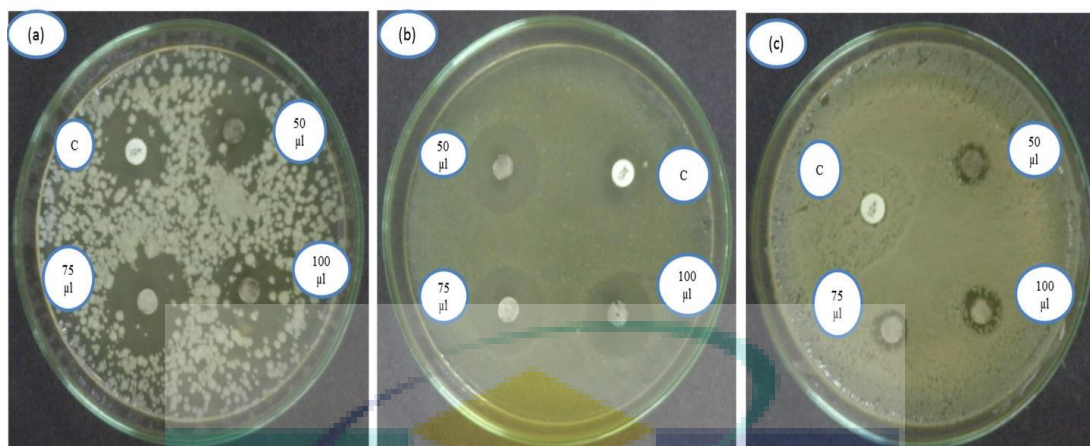


Figure 4.23: The efficacy of *C. nudiflora* synthesized silver nanoparticles against oral pathogenic bacteria (a) *S. aureus* (b) *E. coli* (c) *P. gingivalis*

The minimum inhibitory concentration (MIC) was conducted using two fold serial dilution method as different concentrations of silver nanoparticles were used against the same bacterial strain that are *E. coli* and *P. gingivalis*. The minimal inhibitory concentration was found to be 1.25 mg/l against *P. gingivalis* and *E. coli*. These results exhibit that the optimal concentration of AgNPs controls tested organisms.

Table 4.3: Antibacterial activity of biosynthesized silver nanoparticles against oral pathogenic bacteria

Bacterial strains	Zone of inhibition (mm)				MIC (mg/l)
	Control (Streptomycin)	50 µl	75 µl	100 µl	
<i>S. aureus</i>	5 ± 0.57	5 ± 0.56	7 ± 0.58	8 ± 0.60	ND
<i>E. coli</i>	7 ± 0.58	8 ± 0.57	9 ± 0.53	11 ± 0.28	125
<i>P. gingivalis</i>	6 ± 0.60	7 ± 0.59	9 ± 0.55	12 ± 0.29	125

ND- Not Detected

Over the past two decades, the increase in drug resistance pathogens has been the key challenge to control and it is harmful for the environment and human health (Ujowundu et al. 2008). Furthermore, the existing antibiotics have lack of activity

against resistance strains. As a result, novel drugs are needed to control the multi drug resistance pathogens (MDRP). The biological synthesized AgNPs have the highest antimicrobial activity against gram positive and gram negative bacteria. Feng et al. (2000) study confirmed that AgNPs are effective for multidrug resistance bacteria, where they act on the bacterial membrane proteins and control the replication of DNA. The surface of the cell membrane contains peptidoglycon, sugar, sulphur and phosphorus moiety and it strongly binds with the silver nanoparticles and controls pathogen replications. Kim et al. (2007) reported abacterial growth inhibition of around 56% in 18 hours, when using the concentration of 100mg/l of Ag nanoparticles. The gram negative bacterium *E.coli* was found to have maximum inhibitory zone at 10.75 mm in 100mg/ml of AgNPs. The cell wall of gram positive bacterium is made up of thick peptidoglycon layer which consists of a linear polysaccharide chain along with peptide linkages. The high concentration of metallic silver nanoparticles can effectively break the peptide consisted cell wall of gram positive compared with gram negative bacteria.

4.2.9 Antioxidant activity of silver nanoparticles

The DPPH and ABTS antioxidant activity of silver nanoparticles are shown in figure 4.24. The different concentrations of AgNP scavenged the DPPH free radicals moderately compared with the control (BHA). The higher concentration of AgNPs shows less than 30% efficiency of scavenging. On the other hand, ABTS activity of synthesized silver nanoparticles is also shown to be moderate at the highest concentration. However, the control (ascorbic acid) shows more activity than the SNPs which are 60% and 50% in DPPH and ABTS respectively. Similarly, the plant extract capped silver nanoparticles were found to be a potent free radical scavenger when compared to ascorbic acid standard.

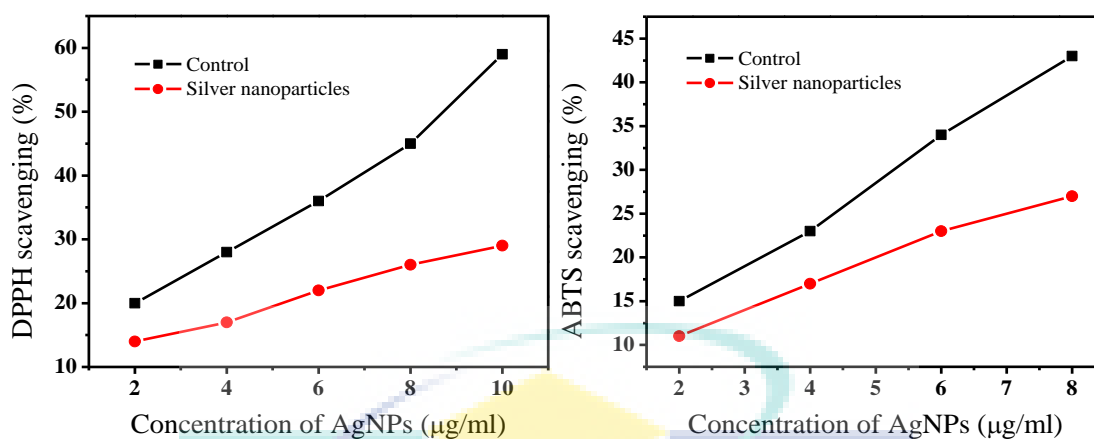


Figure 4.24: A) DPPH free radical scavenging activity of different concentrations of silver nanoparticles B) ABTS free radical scavenging activity of different concentrations of silver nanoparticles

The antioxidant activity of nanoparticles is due to the capping precursors such as bioactive metabolites present in plant extracts and also on the metal surface (El-Rafie and Abdel-Aziz Hamed, 2014). The plant synthesized AgNPs have the ability to control DPPH free radical scavenging activity at the lowest concentration of 5 µg/ml. The BHA has less than 10% efficiency, whereas AgNP has more than 10% inhibition of free radicals (Raghunandan et al., 2011).

The DPPH scavenging exhibited the inhibition activity of both AgNPs and the plant extract compared with the ascorbic acid (standard). However, the AgNPs with the plant extract exhibited the highest inhibition which was more than 70% scavenging activity of DPPH than the plant extract alone (Dipankar and Murugan, 2012). Similarly, Abdel-Aziz et al. (2014) studied plant mediated AgNPs and found that they possessed a higher DPPH scavenging activity compared with the plant extract alone. The results show that the lowest concentration of the aqueous extract (5 mg/l) had 12% activity and this value increased at 20mg/l where the activity was more than 50%.

4.3 PHYTOCHEMICALS CHARACTERIZATION OF *C.nudiflora* EXTRACTS

4.3.1 Identification of secondary metabolites from *C. nudiflora* extracts

Table 1 shows the identified phytochemical constituents from *C. nudiflora* extracts. The preliminary phytochemicals analysis was carried out on selected solvent extracts such as hexane, ethyl acetate, chloroform, ethanol and aqueous. These crude extracts show positive results of alkaloids, flavonoids, terpenoids and phenolics compounds in chloroform, ethanol and aqueous extracts. Saponins are present in all solvent extracts. On the other hand, terpenoids is absent in chloroform extract and it is present in other solvent extracts.

Table 4.4: Preliminary identification of phytochemical constituents from *C. nudiflora* extracts

Secondary metabolites	Chloroform	Ethanol	Hexane	Aqueous	Ethyl acetate
Alkaloids	+	+	-	+	-
Flavonoids	+	+	+	+	+
Saponins	+	+	+	+	+
Sterols	-	-	-	-	+
Terpenoids	+	+	-	+	+
Volatile oils	+	-	+	-	+
Tannins	+	+	+	-	+
Phenolics	+	+	+	+	+
Carbohydrates	-	+	-	+	-

‘+’ denotes present, ‘-’denotes absent

The different phytochemicals such as alkaloids, flavonoids, saponins, carbohydrates, phenolics, tannins, terpenoids and volatile oils were detected in the *C.nudiflora* extracts. Furthermore, the total phenolic content in the aqueous extract was found to have the highest activity (63.4 mg GAE/g) among other extracts. Also, the hexane plant extract had 59.7 mg GAE/g and ethanol had 31.6 mg GAE/g and a considerable total phenolic content was detected in the *C. nudiflora* extract. The total flavonoid content of the ethanol extract was calculated at 55.3 mg/g while water and the

ethyl acetate extract have a moderate activity in total flavonoid content which are 53.4 mg/g and 43.1 mg/g respectively (Table 4.5).

Table 4.5: Quantitative analysis of phenolic and flavonoid contents from *C. nudiflora* crude extracts

Plant extract	Total phenolic content (mg/GAE)	Total flavonoids content (mg/ g)
Water	63.4±0.05	53.40±0.06
Hexane	59.7±0.11	43.15±0.04
Ethyl acetate	14.6±0.05	23.40±0.11
Chloroform	18.2±0.08	24.56±0.02
Ethanol	31.6±0.05	55.30±0.05
Standard	74.4±0.04*	78.1±0.05 [#]

(*Gallic acid, [#] α -BHT)

These ethno pharmacological importance chemical constituents have a wide range of pharmacological activities to control microbial infections and also enhance the human immune functions (Ahameethunisa, 2012).

Table 4.6: Antioxidant activities of *C. nudiflora* crude extracts

Antioxidant assay	Aqueous	Hexane	Ethyl acetate	Chloroform	Ethanol	Standard
DPPH assay ^{a, b}	43.40±0.05	31.63±0.04	22.79±0.02	32.70±0.05	33.29±0.05	67.29±0.04*
ABTS assay ^{a, b}	46.64±0.03	30.14±0.03	29.46±0.04	34.80±0.05	26.20±0.05	69.23±0.05*

*- ascorbic acid

^aThe values are mean (n=3) with the significantly difference at p<0.05. ^bPercentage of inhibition at extract concentration of 100 µg/ml.

4.3.2 GC-MS characterization of *C. nudiflora* crude extracts

Figure 4.25 and 4.26 show GC-MS chromatogram of *C. nudiflora* extracts. The different classes of organic chemical constituents were identified by GC-MS analysis. The GC-MS result shows medicinally valued phytochemicals are present in the plant extracts.

Table 4.7: Summary of organic constituents identified by GC-MS from *C. nudiflora* extracts

S.No	Plant extract	Retention time	Area %	Chemical constituents
1	Ethyl acetate extract	33.144	1.16	Benzoic acid
		33.763	3.04	Ethanedioic acid
		36.339	0.97	2-pyrimidine
		43.125	4.14	Phytol
		43.808	3.89	n-decanoic acid
		53.743	2.78	phthalic acid
2	Chloroform extract	4.402	7.13	Acetic acid
		4.522	1.52	1-propanol
		7.827	14.88	Ethane
		8.976	2.08	Oxalic acid
		33.769	1.98	Phosphonic acid
		31.283	1.00	Muscimol
3	Aqueous extract	31.281	2.41	2-H- azepin- 2- one
		32.785	0.44	Difluorobenzoic acid
		33.771	1.22	1-butanamine
		36.786	0.81	N-ethyl formamide
		40.250	6.19	Hexadecanoic acid
4	Ethanol extract	4.522	0.40	Carbonic acid
		30.408	0.57	Ethanedioic acid
		34.549	0.27	Cystamine
		40.718	0.28	Isobutylamine
		41.796	20.34	Tridecanoic acid
		39.476	0.29	3,8 dioxo- 2,9 disilade -5-ene
5	Hexane extract	4.339	0.56	Cyclopentane
		4.743	5.76	Heptane
		14.524	1.79	Toluene
		17.644	0.47	Octane
		23.452	7.05	Oxalic acid

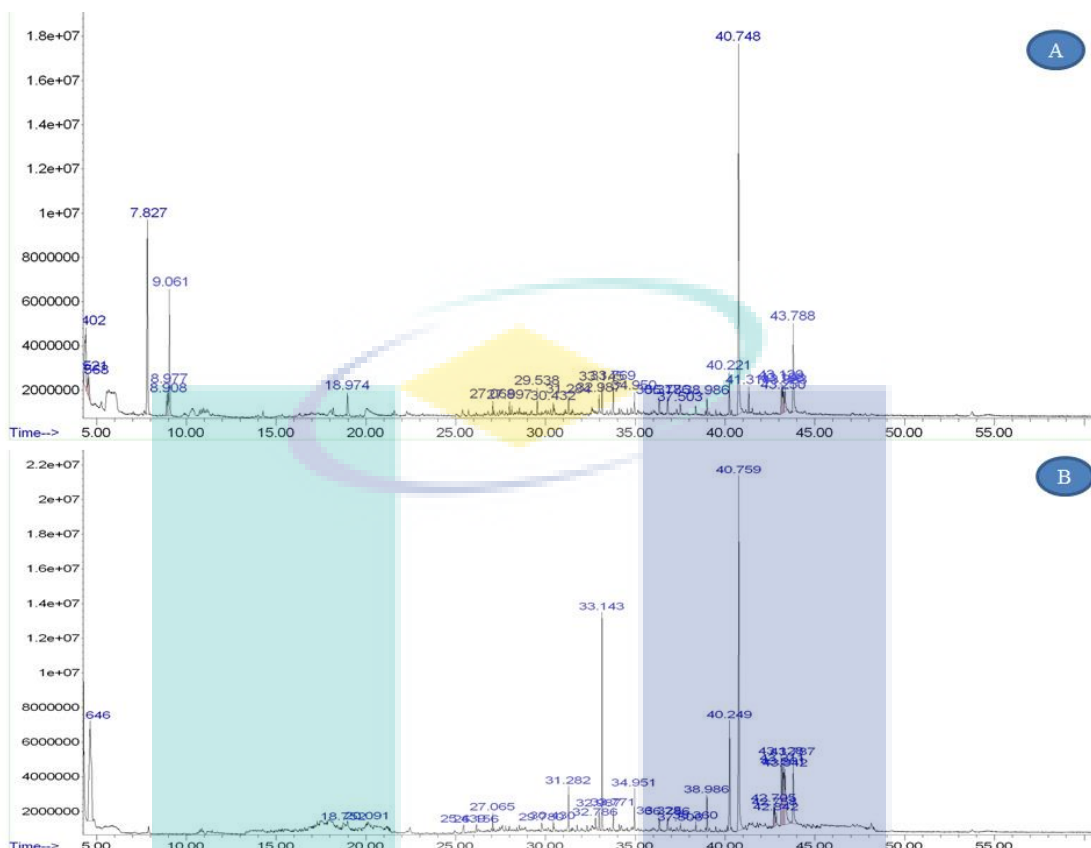


Figure 4.25: GC-MS chromatogram of different solvent extracts from *C. nudiflora* A) Ethanol B) Aqueous

The *C. nudiflora* extracts contains different secondary metabolites as tabulated in Table 4.7. The chemically synthesis antibiotics have their disadvantages such as less active site action and harmful to human. Therefore, the development of natural antimicrobial agents could act as a specific active site and also trigger the primary immune system and metabolic functions. The identified major clinically useful compounds such as phytol and hexadecanoic acid from *C. nudiflora* extracts are commercially and clinically important therapeutic agents.

Phytol is a chemical form of acyclic diterpene alcohol that is used as a precursor for the synthesis of synthetic vitamin E and vitamin K. Phytol is likely to have acyclic isoprenoid compound and it is present in the biosphere of the environment. The

degradation products of phytol have been used as a biogeochemical tracer in aquatic environments.

The palmitic acid is known as hexadecanoic acid. It is the most common saturated fatty acid found in plants, animals and microorganisms. It is a major source from palm trees and also found in meats, cheeses, butter, and dairy products. A 20% of palmitic acid diet in animal feeds could alter the central nervous system and insulin secretion in *in-vivo* studies.

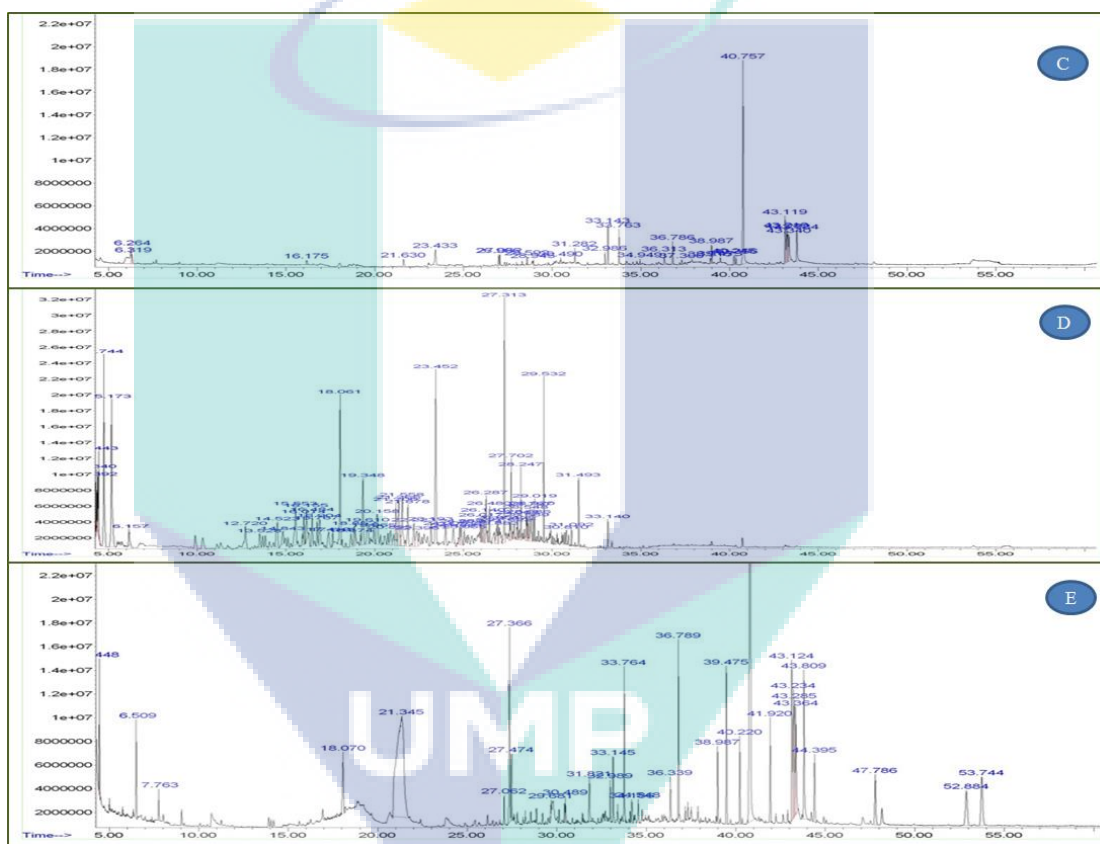


Figure 2.26: GC-MS chromatogram of different solvent extracts from *C. nudiflora* C) Hexane D) DCM E) Chloroform

4.3.3 Antibacterial activities of *C. nudiflora* extract

The antibacterial activities of the aqueous extract of *C. nudiflora* are presented in Figure 4.27. The aqueous plant extract showed the highest inhibitory activity against *P. aurogenosa* (13 mm) followed by the *E. coli* and *S. typhi*. The least activity was

measured in *Bacillus subtilis* and *Staphylococcus aureus* with 11 mm and 9 mm respectively. Overall, the aqueous *C. nudiflora* extract showed promising antibacterial activities against food borne pathogenic bacteria. The MIC range was calculated at 12.25 mg/ml as the minimum inhibitory concentration of aqueous plant extract against *P. aeruginosa*.

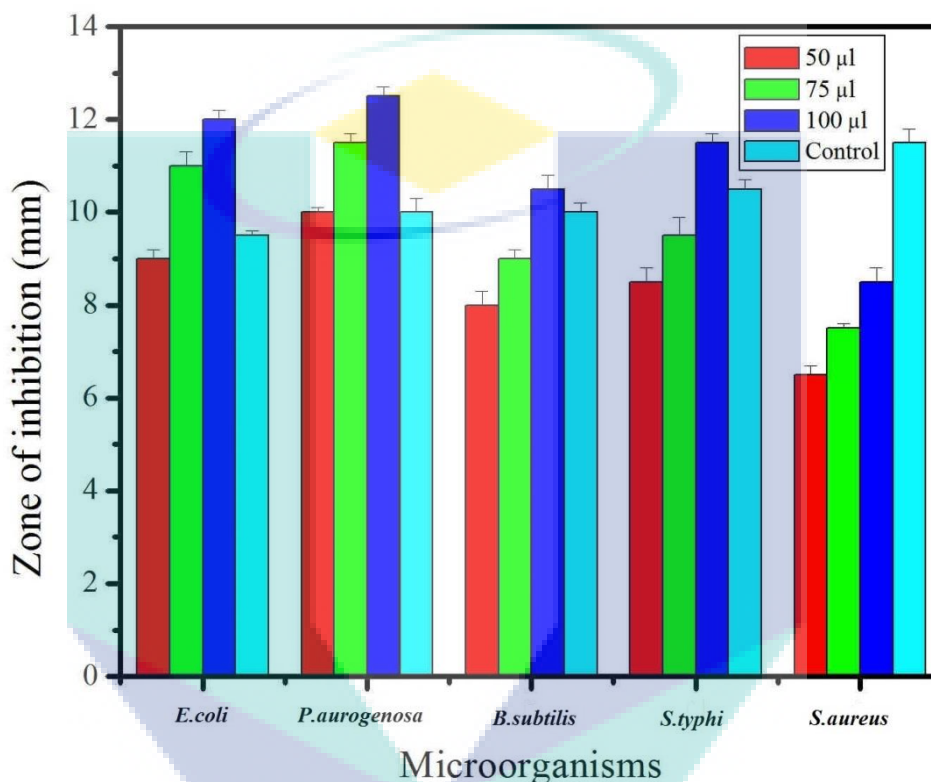


Figure 4.27: Antibacterial activity of *C. nudiflora* aqueous extract against pathogenic bacteria

Recently, the increasing resistance rate of bacterial strains is a big challenge that needs to be controlled. The plant extract effectively inhibits the growth of pathogens even though the multidrug resistance pathogens are found to be less sensitive to the crude plant extracts. For instance, the clinically challenging *Staphylococcus aureus* strain is a major cause of community and hospital-associated infections with an estimated mortality rate of around 7 to 10% (Tamokou et al., 2012). The methanolic *H. rhamnoides* extract exhibited the highest activity against gram positive bacteria such as *B. subtilis* and *S. aureus*. The plant contains bioflavonoids and phenolics which acted as marker compounds for the antimicrobial and antioxidant activities (Jeong et al., 2010).

4.3.4 Free radical scavenging activity on *C. nudiflora* extracts

The DPPH and ABTS radical scavenging activities of plant extracts are shown in table 4.6. The aqueous extract of *C. nudiflora* showed significant DPPH scavenging activity (43.4%) compared with gallic acid standard. The hexane and ethanol extracts showed moderate scavenging properties of 31.63% and 33.29% respectively. In addition, the ethyl acetate has the lowest radical scavenging activity (22.79%). ABTS free radical scavenging activity was analyzed using BHT as a standard. The aqueous plant extract revealed significant ABTS radical scavenging activity (46.64%), followed by chloroform (34.8%), and hexane (30.14%). In ABTS scavenging assay, the aqueous extract exhibited the highest percentage and it controlled the free radicals formation in *in-vitro*.

The excess free radicals caused cellular damage and induced many dysfunctions in human such as atherosclerosis, myocardial infarction, cancer and neurogenerative disorders. The natural antioxidant compounds are useful to repair the free radical formation in the cells (Fakruddin et al., 2012). For instance, *C. heptaphylla* plant extract plays a significant role in DPPH radical scavenging activity with the IC₅₀ value of 3.11 µg/ml. The plant extracts have major natural compounds such as saponin, flavonoids, iridoid glycosides, steroid and spermine. These chemical groups mainly participate in the antioxidant activities (Ozcan et al., 2011). Yildirim et al. (2001) studied the percentage of DPPH scavenging activities of *Rumex crispus* extracts. *R. crispus* seed extracts were prepared in different concentrations of 50 to 400 µg, and exposed better scavenging activities at the highest concentration. The amount of phenolic content in the extract could increase the DPPH free radical scavenging activity. Also, the activity is relatively correlated with the amount of phenolic content in the extract.

Bazzaz et al. (2011) proved the antioxidant capacity is based on the composition of different phenolic contents in the *S. litwinowii* extracts. The antioxidant tests have high specificity and sensitivity for temperature and incubation time. In this study, the aqueous extract has shown significant antioxidant activities in DPPH and ABTS scavenging. The highest activity shows the relation between abundant quantities of

phenolic, flavonoids in the plant extract. Mohamed et al. (2013) revealed the high polarity solvents using *S.cumini* extraction are more effective to control free radical scavenging compared with the non-polar solvent extracts. The *S.cumini* extract contains essential oils and other bioactive metabolites which actively participate in the antioxidant mechanisms and prevent the cellular damages. According to that, the study successfully defends the commonly available weed plant, *C.nudiflora*, which could control the oxidative damage in *in-vitro*.

4.4 IN-VITRO ANTICANCER STUDIES OF BIOSYNTHESED GOLD AND SILVER NPs

4.4.1 *In-vitro* MTT assay

In-vitro methods are the ideal model to study human diseases and possess a high degree of transparency and ability to find the drug concentration choice for *in vivo* experiments. Also, the *in-vitro* method is rapid and has high throughput to study the effectiveness of drugs for clinical analysis.

Figure 4.28 shows *in-vitro* MTT assay against HCT-116 cells treated with gold and silver nanoparticles and plant extract alone. The cytotoxicity of biosynthesized gold and silver nanoparticles was evaluated against HCT-116 cells at different concentrations (200, 100, 50, 25, 12.5 and 6.25 $\mu\text{g/ml}$). The stock samples were prepared at 1mg/ml. The *in-vitro* cytotoxicity analysis of the biosynthesized nanoparticles shows a direct dose-response relationship and cytotoxicity increases at increasing concentrations. *C.nudiflora* plant mediated gold and silver nanoparticles showed potent cytotoxicity against HCT-116 cells. The inhibitory concentration (IC_{50}) of AuNPs and AgNPs were 200 $\mu\text{g/ml}$ and 100 $\mu\text{g/ml}$ respectively showed significant cytotoxicity after 24 hours treatment. Figure 4.29 and Figure 4.30 show the cell viability percentage of treated gold and silver nanoparticles samples respectively.

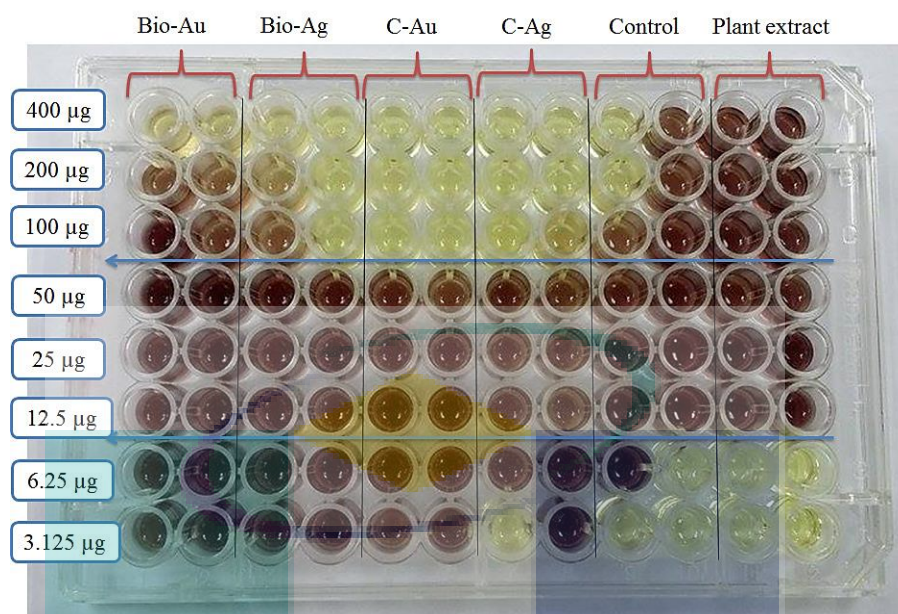


Figure 4.28: The HCT-116 cells treated with biosynthesized gold and silver nanoparticles

The IC_{50} concentrations of gold and silver nanoparticles achieved 50% of growth inhibition in HCT-116 cells. The biosynthesized AuNPs induced over 90% cell death at the highest concentration of 400µg/ml. On the other hand, the silver nanoparticles have less toxicity against HCT-116 cells compared with gold nanoparticles. The IC_{50} concentration of AgNPs was calculated at 100 µg/ml.

UMP

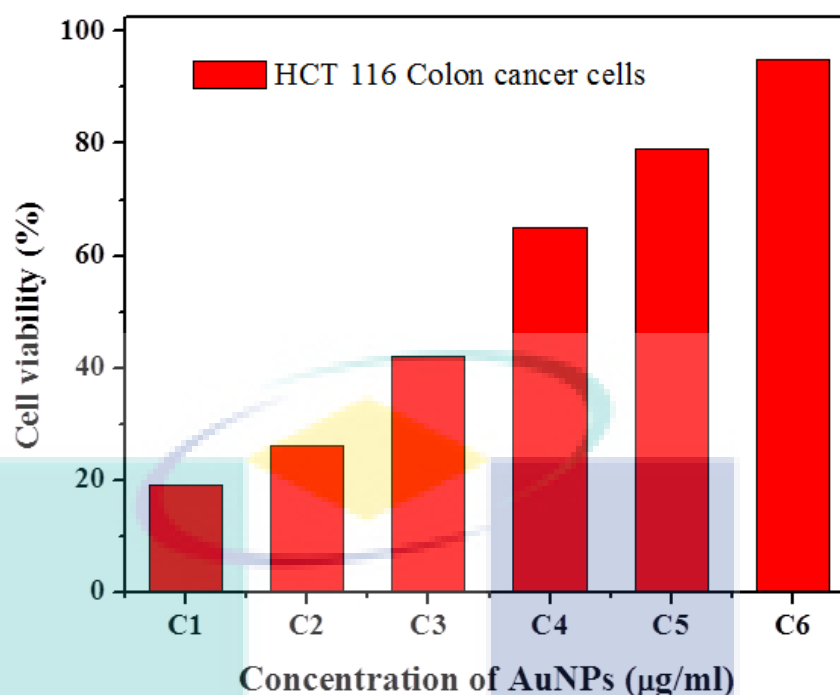


Figure 4.29: Effect of HCT-116 cell viability in treated with biosynthesized gold nanoparticles using MTT assay (C1-C6 increasing concentration from 12.5-400 µg/ml)

The biosynthesized gold and silver nanoparticles are promising agent acting against HCT-116 cells. The activity of NPs is based on their size, shapes and concentration. The biological mediated nanoparticles usually show better activity compared with plant extract alone. In the present study, the plant extract and commercial gold and silver nanoparticles were evaluated. The aqueous plants extract exposed less activity compared with biomediated gold and silver nanoparticles. On the other hand, chemically synthesized gold and silver nanoparticles (purchased from Sigma, USA, Molecular formulae: Au, Ag) were dissolved with 1% saline and the *in-vitro* cytotoxicity properties were evaluated. There was no major significant difference compared with the biosynthesized nanoparticles. However, the green synthesized NPs showed reduced cell number in the treated samples.

The plant metabolites acted as a reducing and capping agent in the synthesis of metal nanoparticles. Identifying the specific roles of bioactive compounds in the biosynthesis procedure was challenging and quite difficult. Hence, to address this issue

the efficacy of plant extract alone should be evaluated which may give a clear evidence of the nanoparticles function. The plant mediated gold and silver nanoparticles are shown to be more effective than only the plant extract. In this study, the *in-vitro* cytotoxicity results showed the biosynthesized gold and silver nanoparticles induced the cell death compared with the crude plant extract which was proven by the MTT assay.

According to Mohtashami et al. (2012), the chemically synthesized silver nanoparticles had high monodispersity and smaller in size, but biosynthesized nanoparticles had higher polydispersity and high aggregates. The chemical preparation of NP may be harmful to use in clinical studies due to the use of extranal chemical stabilizing and capping agents in the synthesis procedure. The biosynthesis method uses plant or bacterial supernatant as a substrate. Sudhasree et al. (2014) studied the biological activity of metal nanoparticles synthesized by chemical and green routes. The chemical synthesis of NPs was mediated by polyethylene glycol and hydrazine hydrate as the stabilizing and reducing agent. On the other hand, the *desmodium gangeticum* aqueous root extract was used to prepare NP without any stabilizing and reducing agent. The free radical scavenging activities and antibacterial activities of NiNP were evaluated, and the study suggests that the green route possesses reliable antioxidant and antibacterial activity. Also, the study proves that the green route was nontoxic in animal and cell line. Therefore, the biologically synthesized nanoparticles could be a more efficient material in clinical studies than chemical based nanomaterials.

Table 4.8: Summary of pros and cons of chemical and biological syntheses of metal nanoparticles

Properties	Physical-chemical synthesis of nanoparticles	Biological synthesis of nanoparticles
Stability	<ul style="list-style-type: none"> The additional chemical stabilizing agents is necessary e.g: NaHB₄, citrate etc. It is less specific and has high adverse effect 	<ul style="list-style-type: none"> The plant extract acts as a reducing, stabilizing agent Highly specific and it has lower side effects
Properties	<ul style="list-style-type: none"> It is smaller in size and produces different shapes Good thermal stability and more molecule is rigid 	<ul style="list-style-type: none"> The native confirmation is crucial It is eco-friendly and can be used clinically
Manufacturing	<ul style="list-style-type: none"> A lot of vaccum techniques is essential Longest and complicated synthesis procedure Expensive 	<ul style="list-style-type: none"> Less expensive One pot synthesis Easy method
Metabolism	<ul style="list-style-type: none"> The nanoparticles are chemically converted (oxidation, conjugation) into nano forms which is tough to excrete from the body 	<ul style="list-style-type: none"> Chemically degraded into monomers, which can be easily excreted from the body through faces and urine
Portion on the market	<ul style="list-style-type: none"> Majority of experiments, more than 90% using the synthesis of nanomaterials 	<ul style="list-style-type: none"> Less than 1% experiment using the synthesis of nanomaterials

Recently, Vasanth et al. (2014) proposed the cancer cells to be treated with various concentrations of silver nanoparticles which affect the percentage of cell viability. The highest concentration of AgNPs (250 $\mu\text{g/ml}$) shows 94% cell death after 24 hours of treatment. The nanoparticles treated cancer cells underwent membrane blebbing and morphological alterations and eventually involved in the apoptosis. Also, the GNPs treated MDA-MB-231 cells revealed the slightly higher cytotoxic effects at increasing different concentrations of nanoparticles such as 1, 10 and 50 mg/ml . However, both silver and gold nanoparticles of 100 mg/ml showed toxic effects ($\sim 40\%$) in the treated cells. On the other hand, the HAuCl_4 , AgNO_3 and *A. indica* leaves extract which were used as a positive control did not show toxic effects in the treated cells. It is shown that more than 60% of cell viability was at the highest concentration that was 100 mg/ml (Krishnaraj et al., 2014).

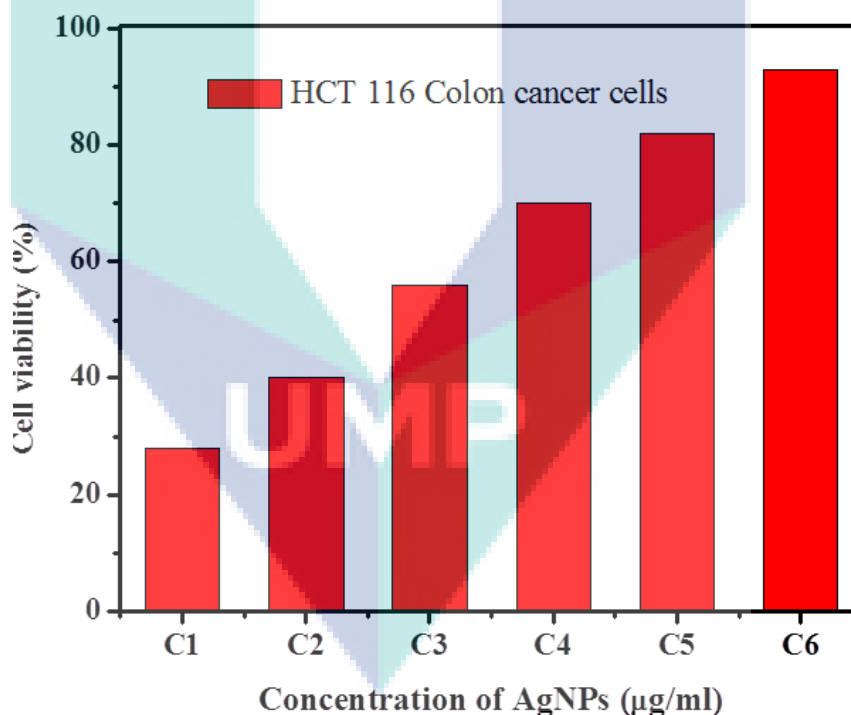


Figure 4.30: Effect of cell viability in different concentrations of biosynthesized silver nanoparticles using MTT assay

Similarly, Mittal et al. (2014) reported the Ag–Se bimetallic nanoparticles reduced the viability of dalton lymphoma (DL) cells in 48 hours of treatment. The DL

cell viability was 20% at 50 $\mu\text{g/ml}$ Ag–Se NPs. The minimum cytotoxicity concentration of the nanoparticles in tumor cells was found at 50 $\mu\text{g/mL}$ and above. The size of the nanoparticles is also one of the key factors in cytotoxic activity. The cell viability considerably decreased with the increasing concentration of nanoparticles from 25 to 300 $\mu\text{g/ml}$. Also, the rate of mortality predicted the cytotoxic effect of drugs and also can be considered as the tumor reduction rate (Dipankar and Murugan, 2012). The AuNPs and AgNPs have been reported in various IC_{50} concentrations of 100 to 300 $\mu\text{g/ml}$ and 5 to 10 $\mu\text{g/ml}$, against different cell lines. Therefore, the metal nanoparticles toxicity may vary according to the types of cell lines and their physico-chemical properties.

4.4.2 Flow cytometry analysis

The cell cycle progression in HCT-116 cells was studied using flow cytometry. The IC_{50} concentrations of Au and AgNPs treated HCT-116 cells cycle is shown in Figure 4.31. The cell cycle analysis explored the distribution changes occurred in the treated Au, Ag nanoparticles samples. The proportion of the sub G1 phase increased in all treated samples compared with the control. The Au, Ag nanoparticles treated samples decreased in the G0/G1 phase and increased in the S/(G2/M) compared with the positive control (cisplatin). Also, the DNA content or amount of the fragmented DNA significantly increased in both gold and silver nanoparticles treated cells.

The obtained result suggests that the biological synthesized gold and silver nanoparticles could induce the sub G0 phases in the cell cycle. Also, the histogram results show that the DNA content reduces significantly in G1 phases and makes them appear in the sub-G0 region which is indicative of apoptosis that occurs in the treated samples. However, the consequent loss of cells in the G1 phase clearly indicates that the programmed cell death is induced by nanoparticles. The plant mediated metal nanoparticles induce cell death through apoptosis mechanism neither necrosis factor.

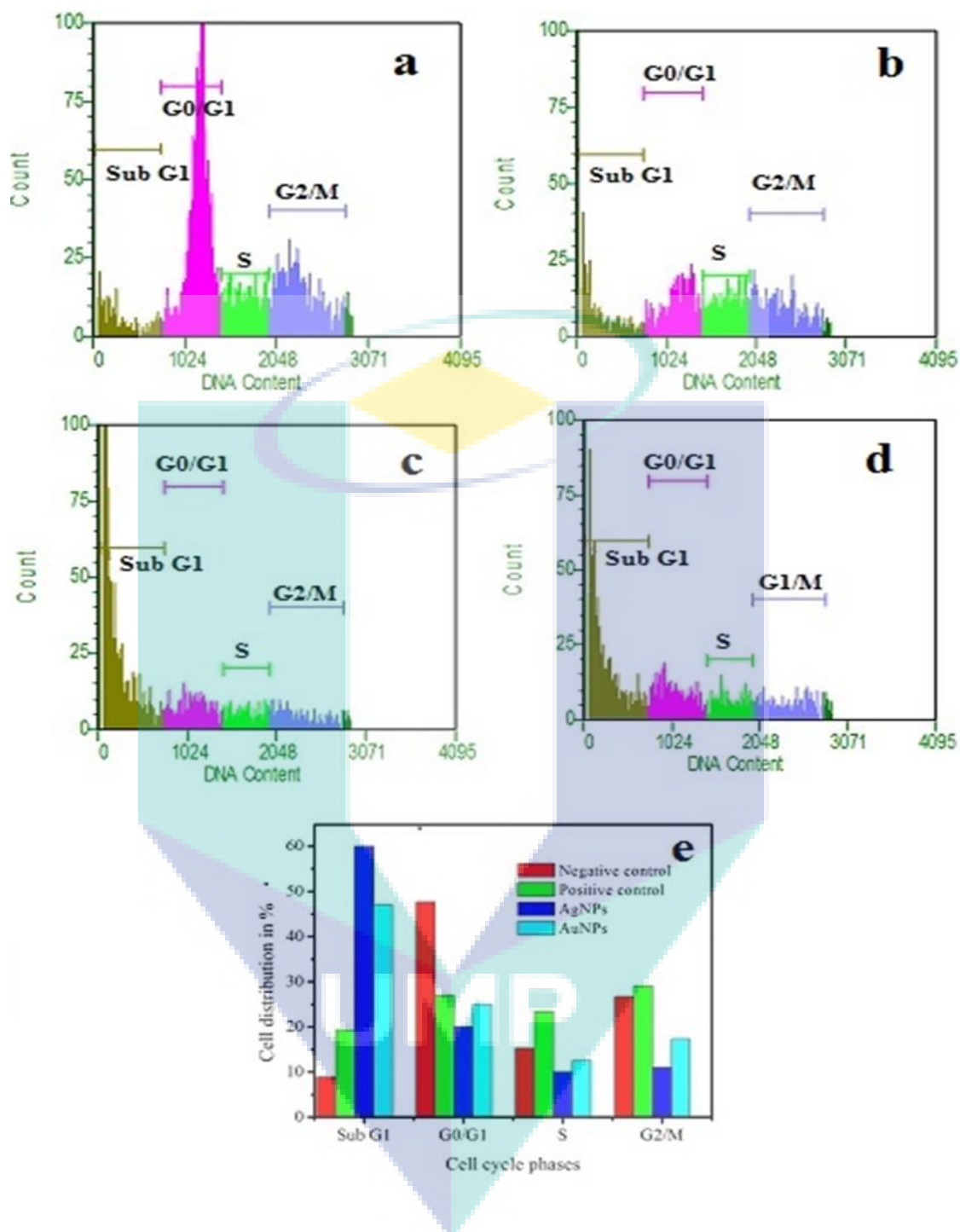


Figure 4.31: Flow cytometry histogram shows cell cycle phases of HCT-116 cells treated with IC_{50} concentration of gold and silver nanoparticles a) P.Control b) N.Control c) AuNPs d) AgNPs e) Bar diagram shows DNA content in cell cycle phases

Kerr and et al. (1972) proposed the apoptosis is evident by the morphological changes in the cellular organelles including DNA content and cell membranes.

Apoptosis starts with various stages of cell degradation such as shrinkage of the cell structure and the nucleus, followed by the fragmentation of nuclear and chromatin materials. The activated nuclease enzymes are responsible for the DNA degradation and fragmentation of an approximately 180 to 200 base pairs (bp). As a consequence, the experimental cells have less content of DNA and a large number of fragmented DNA which can be detected in subdiploid of the cell cycle by flow cytometry techniques.

The cell cycle covers four distinct phases: G1 phase, S phase, G2 phase and mitosis including two checkpoints: G0/G1 and G2/M. The series of cell cycle phases takes place when the genetic materials duplicate into daughter cells and there seems to not be any DNA damage while divided into two cells. Besides, sometimes in the gene regulation or signaling pathway, error will occur and leads to cancer. Interestingly, the recent discoveries of the biosynthesized gold and silver metallic nanoparticles could arrest all stages of the cell cycle in the experimental samples. Thirnavukarasu et al. (2014) found that the gold nanoparticles arrest all stages of the cell cycle and increase the DNA fragmentation in the treated samples. The gold NPs treated samples have varying percentages in each phase of the cell cycle. Therefore, the gold nanoparticles effectively regulate the cell cycle in G0/G1 phase. The HepG2 cells treated with IC₅₀ concentration of gold nanoparticles showed a significant reduction of the DNA content in the cell cycle phases. The fragmented DNA appeared in sub-G1 region which indicates apoptosis occurred in the cells. In addition, the subsequent loss of cells in the G1 phase expressed the survivability of cancer cells that significantly reduced.

Similarly, Prabhu et al. (2013) reported the biosynthesized silver nanoparticles inhibited the growth of HCT-15 colon cancer cells with an IC₅₀ concentration 20 µg/ml at 48 hours incubation period. The AgNPs arrested HCT-15 cell growth at G0/G1 cycle phase. The AgNPs suppress the colon cancer cell growth in terms of reducing DNA synthesis and arresting the G1 phase activity. Therefore, AgNPs can act as an alternative apoptosis inducer as seen by the nuclear condensation and morphological changes in the propidium iodide staining cells. Gajendran et al. (2014) studied the antiproliferative effect of biosynthesized AgNPs. The treated MCF-7 cells were stained with PI showed apoptotic changes and nuclear condensation in the sample. Thus, the

treated cancer cells showed nearly the least number of cell population in G1 phase and there were no changes seen in the G2/M phase in the treated sample.

4.4.3 Morphological characterization of nanoparticles treated HCT-116 cells

The cytomorphological changes of treated HCT-116 cells were studied by an optical microscope. The HCT-116 cells were treated with IC_{50} concentration of newly synthesized AuNPs and AgNPs. The treated cells were incubated for 48 hours at 37 °C in 5% CO_2 atmosphere. After treatment, the morphological changes were observed under an optical microscope (Nikon, Japan). The metal nanoparticles treated cells clearly showed the apoptotic mechanisms that started through the altered cell membranes and nuclear condensation. The cell morphological changes in the treated HCT-116 cells are shown in Figure 4.32.

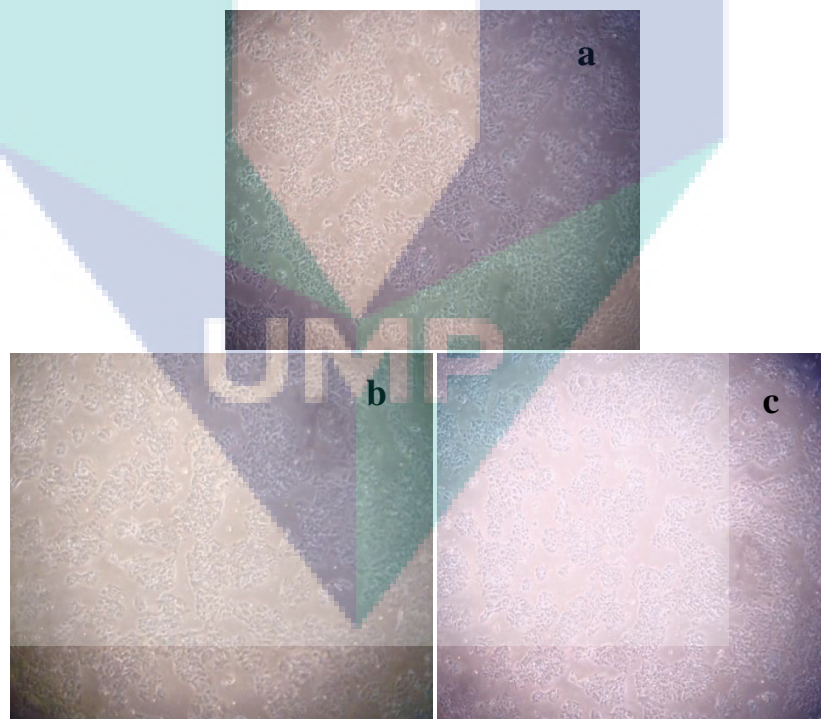


Figure 4.32: Typical microscopic images (40x magnifications) of nanoparticles treated HCT-116 colon cancer cells a) control, b) gold nanoparticles c) silver nanoparticles

4.4.4 Quantitative real time polymerase chain reaction studies

Reverse transcription polymerase chain reaction (RT-qPCR) is a novel technique to identify the different patterns of gene expression in cancer and normal cells. The RT-qPCR technique is highly sensitive and can measure samples of very low amount. Table 4.6 shows the concentration of RNA in the samples measured by a spectrophotometer.

Table 4.9: Calculated RNA concentrations from experimental samples

Name of sample	Concentration of RNA at 260/280 (OD)
PC	1.98
NC	1.90
S1	1.96
S2	1.97

The mRNA relative expression of four different genes such as PUMA, Caspase-3, Caspase-8 and Caspase-9 was studied. These genes are mainly involved in the programmed cell death. The PUMA, Caspase-3 and Caspase-8 gene expression shows significant changes in gold nanoparticles treated samples compared with the control ($p < 0.05$).

The PUMA gene was moderately expressed in the silver nanoparticles treated sample. The caspase-9 was significantly upregulated in gold nanoparticles treated samples but it was not a considerable expression in the silver nanoparticles treated samples ($p < 0.05$). The gold nanoparticles treated samples increased expression was more than two folds as noticed in Caspase-8, Caspase-3 compared with the positive control (cisplatin). Also, the negative control did not show significant changes in their mRNA expression of all samples. The RT-qPCR studies clearly showed the induction of apoptosis through the activation of PUMA, Caspases-3, -8, and -9 genes which are pro-apoptotic genes involved in the mitochondrial dependent apoptotic pathway. Ledgerwood and Morison (2007) reported that, the activation of caspase proteases is

fundamental for triggering apoptotic cell death. Caspases have different subgroups, among those classes, caspase-3 is an important factor. It can induce the apoptotic machinery by initiating DNA fragmentation and membrane cleavages. Figure 4.33 shows the relative quantification of PUMA mRNA expression in HCT-116 cells treated with AuNPs and AgNPs.

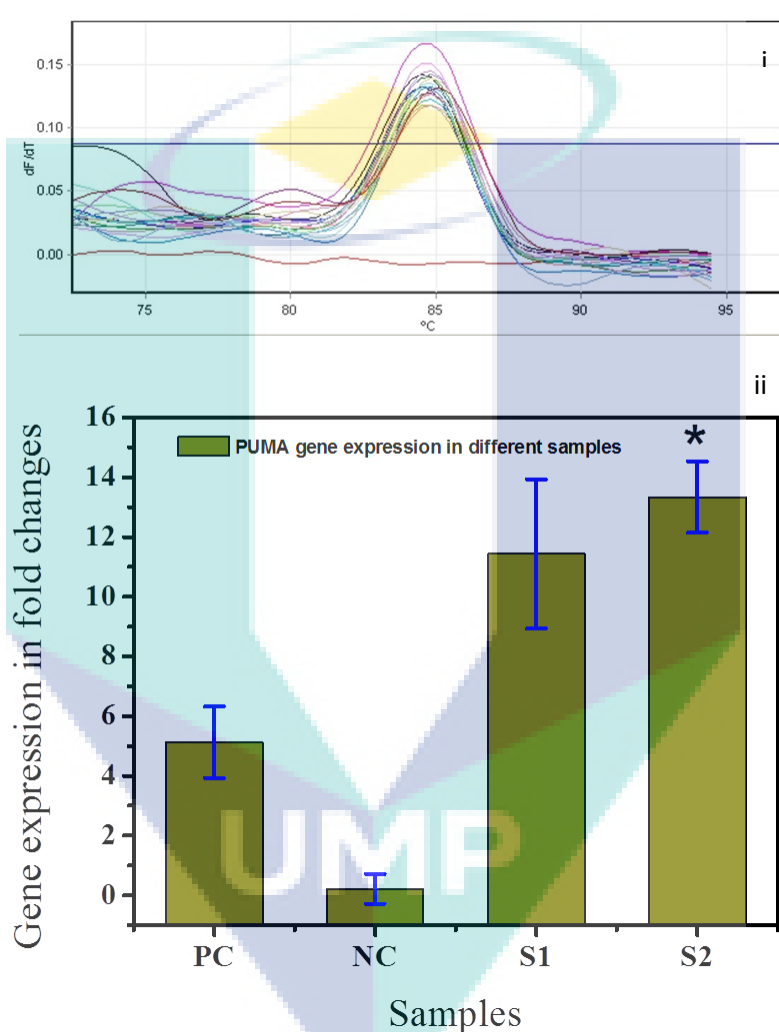


Figure 4.33: The relative quantification of mRNA expression in HCT-116 cells treated with IC₅₀ concentration of AuNPs and AgNPs and control (cisplatin). i) Melt curve from RT-qPCR of PUMA gene ii) PUMA mRNA gene expression treated with IC₅₀ concentration of AuNPs and AgNPs. The data are presented as the means \pm SD of three replicates

These genes treated with gold and silver nanoparticles were up-regulated. Hence, the mRNA expression levels slightly changed between these two nanoparticle

samples. Figure 4.34 shows the Caspase-3 mRNA genes expression treated with gold and silver nanoparticles. The gold nanoparticles treated groups have significantly elevated in all gene expressions including PUMA, Caspase-3, and Caspase-9. Nevertheless, both samples certainly upregulated the pro-apoptotic genes in HCT-116 cells. Also, it shows that there is not much variation in the qPCR amplification efficiencies of the experiments. Figure 4.35 shows the Caspase-8 mRNA gene expression treated by gold and silver nanoparticles. Figure 4.36 shows the mRNA expression of Caspase-3 genes treated by gold and silver nanoparticles.

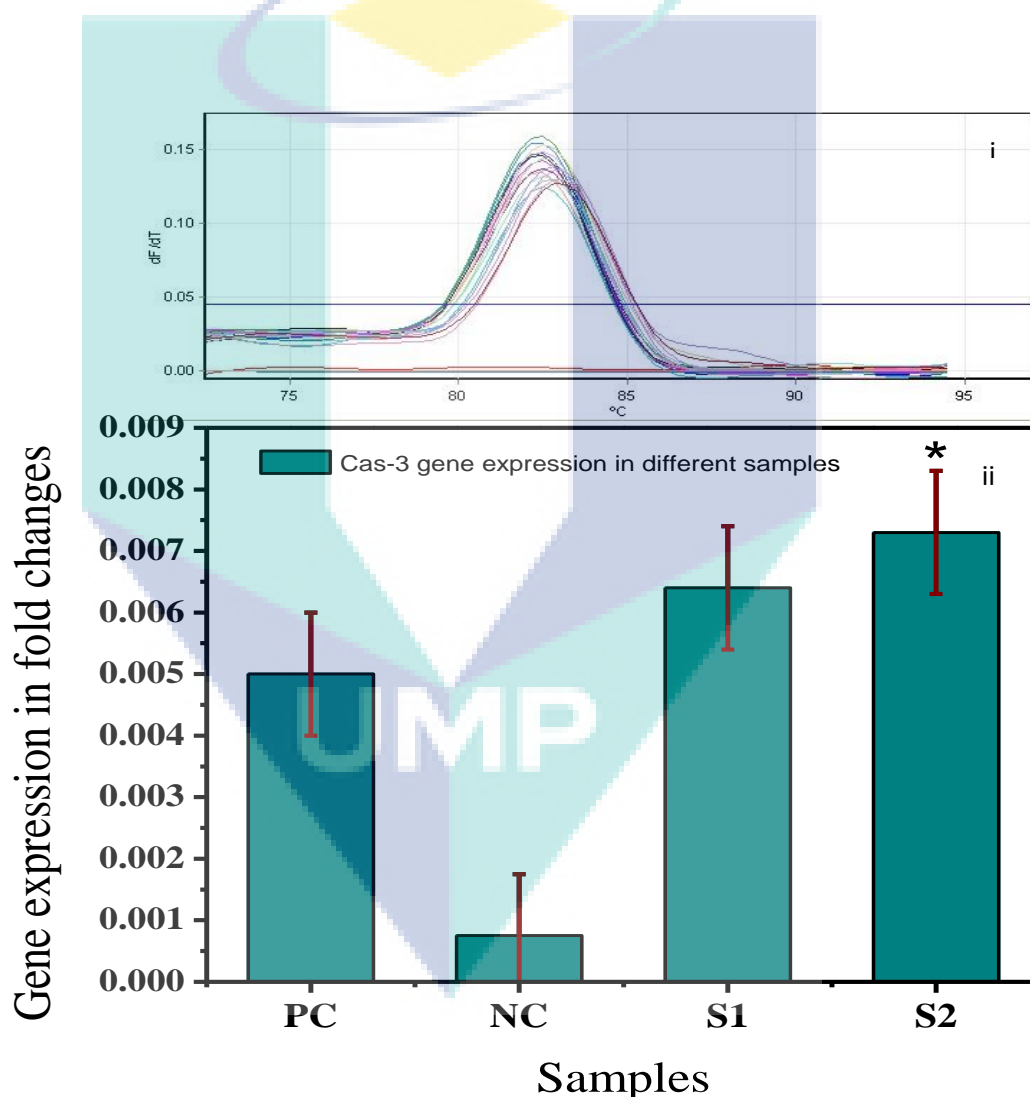


Figure 4.34: i) Melt curve from qPCR of Cas-3 gene ii) mRNA expression of Cas-3 gene treated with AuNPs and AgNPs

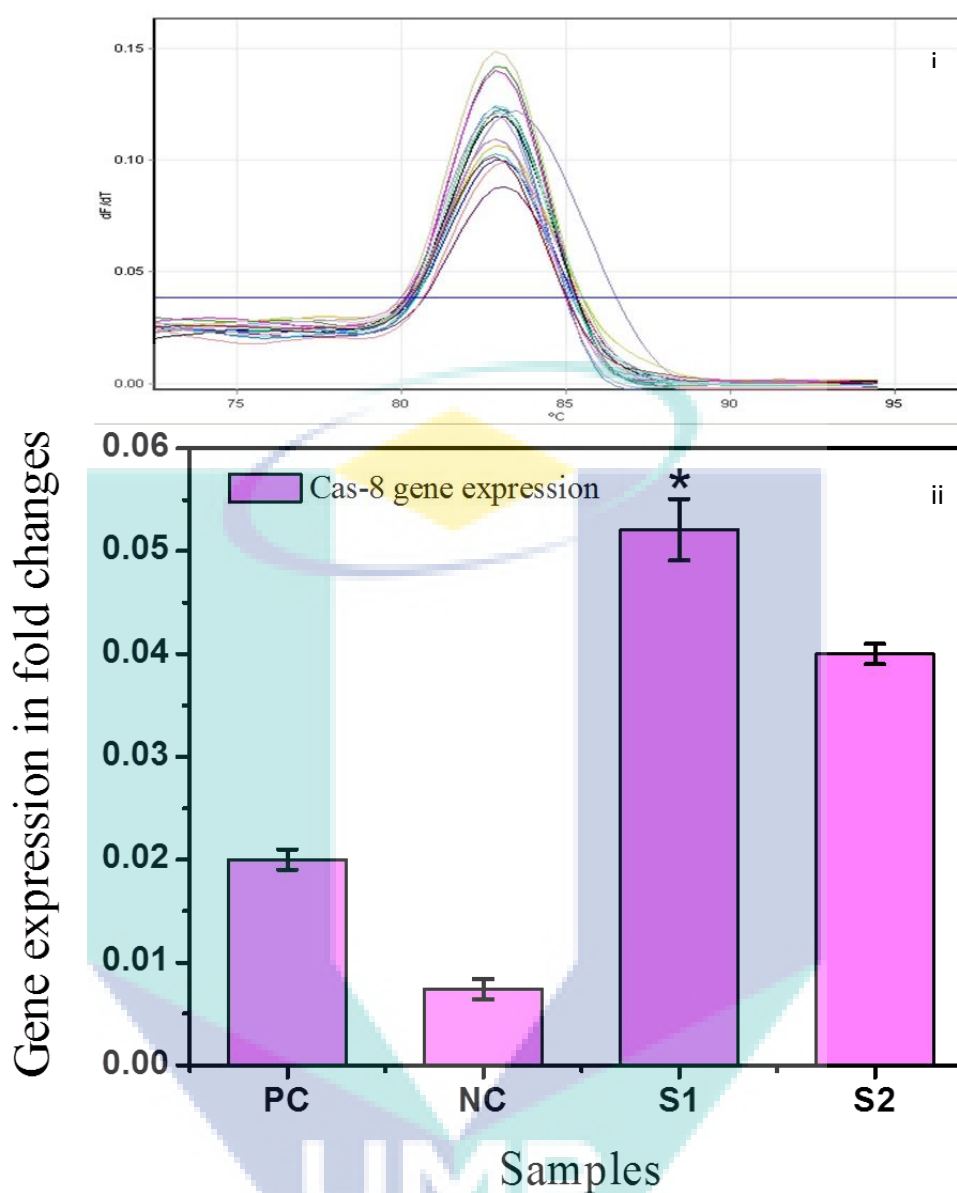


Figure 4.35: i) Melt curve from qPCR of Cas-8 gene ii) mRNA expression of Cas-8 gene treated with AuNPs and AgNPs

Recently, the metal nanoparticles have been the primary concern for the development of new drugs for cancers. Many studies reported the different metal nanoparticles could control the harmful diseases with limited dose concentrations.

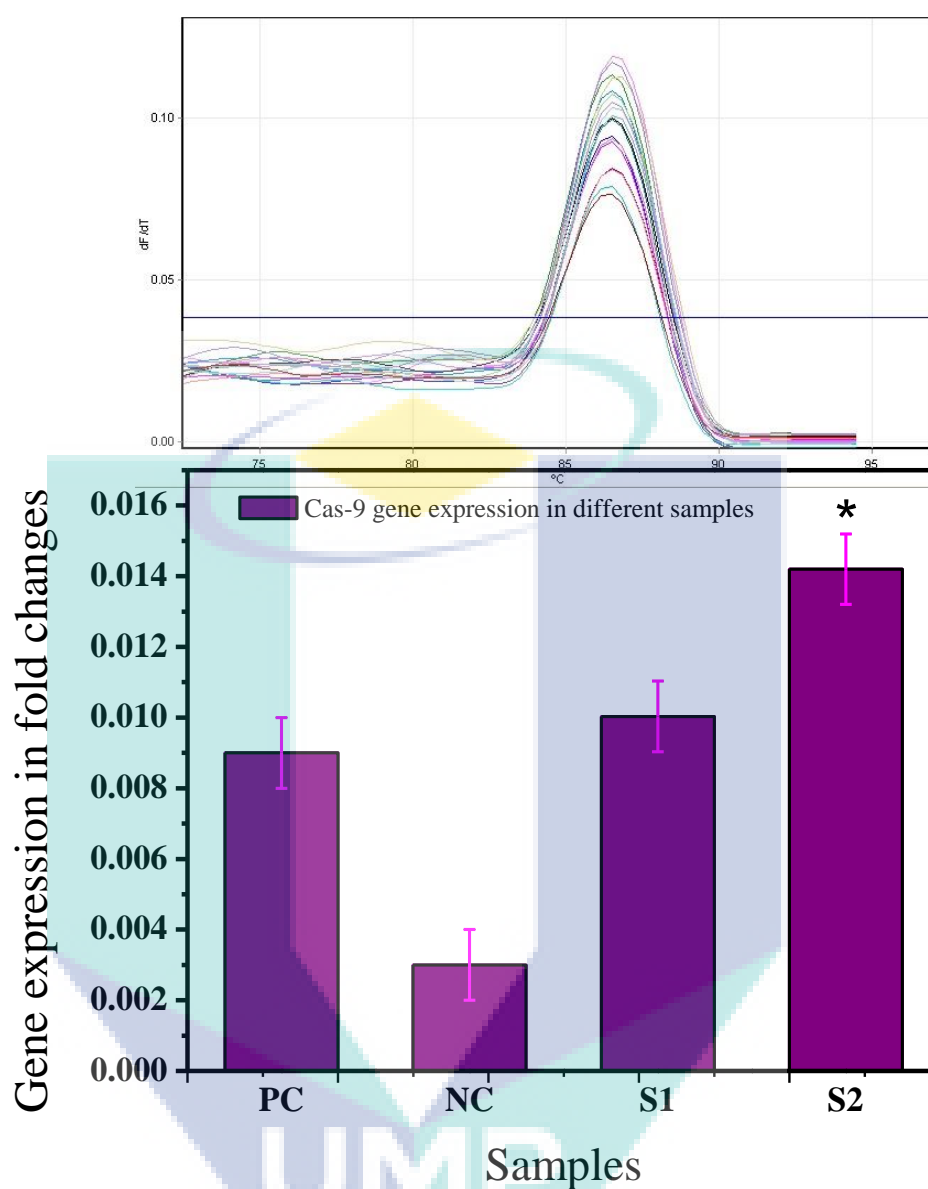


Figure 4.36: i) Melt curve from RT-qPCR of Cas-9 gene ii) mRNA expression of Casp-9 gene treated with AuNPs and AgNPs. (Note: *Statistically shows significant difference compared to the control ($p < 0.05$ for each))

Mustata et al. (2011) explained the PUMA (p53 upregulated modulator of apoptosis) induces apoptosis through a Bax and mitochondria-dependent manner in colon cancer. Also, the effect on apoptosis is regulated through PUMA in DLD1 cells, which is inserted with adenovirus expressing PUMA. Caspase-3 mediated apoptosis was evaluated in colo 205 cells treated with and without CG extract. The results show

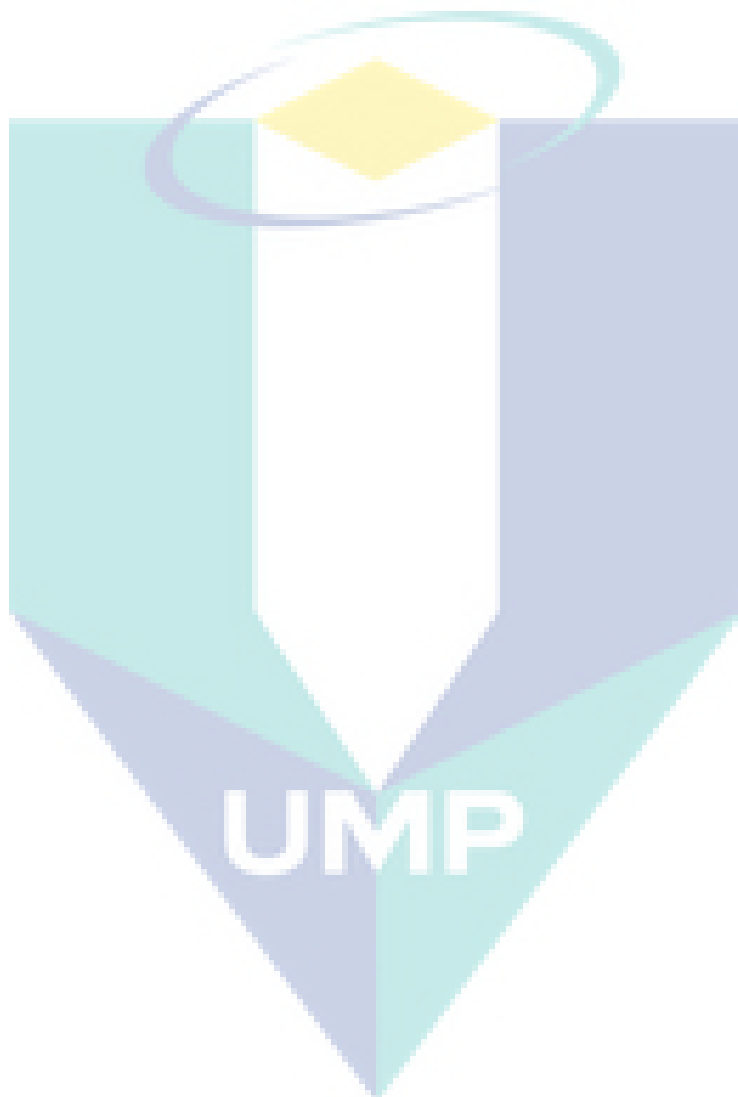
that CGE increases the Caspase-3 activity in colo 205 cells and eventually it controls the cell proliferation in colon cells.

Antiangiogenic process is a one of the main tumor growth factors that could be controlled by the use of GNPs. The angiogenesis factors have been inhibited by GNP which are demonstrated in *in-vitro* and *in vivo* studies. The gold nanoparticles enhance the apoptosis in the chronic lymphocytic leukemia cells (Mejía-Jaramillo et al., 2011). Caspase enzymes play an important role in the programmed cell death mechanisms. Karthik et al. (2014) noticed that the nanoparticles treated groups have significantly increased the Caspase-3, -8 expressions in A549 NSCLC cells. Caspase-3 and -7 are called effector caspases which generally have small pro-domains. These pro-domains are responsible for disrupting the cells after the initiation of apoptosis.

The C2C12 cells were incubated with AuNPs (1000 ng/ml) for 24 hours. After incubation, the relative mRNA expression was measured by RT-qPCR. The mRNA levels of apoptotic markers (e.g., Caspase-3 and Caspase-7) were found to be up-regulated in the AuNPs treated samples compared with the untreated control. The up-regulation of Caspases might activate apoptosis in cancer cells and initiation and execution of apoptosis (Wahab et al., 2014). Caspases (cysteine-aspartic acid proteases) trigger apoptosis in cancer cells through cellular DNA fragmentation. Similarly, Gopinath et al. (2010) observed that caspase-3 gene expression was upregulated in silver nanoparticles treated cells. The caspases-3 gene expression profile indirectly expressed the apoptosis induced by AgNP treated samples of both BHK21 and HT29 cells.

The different apoptotic genes such as C-myc, caspase-3 expressions were analyzed in various cancer models. Interestingly, it was observed to up regulate in the NPs treated samples. The anti-apoptotic genes, such as bcl- 2 and bcl-XL expression were down-regulated in the reaction. The housekeeping gene β -actin acted as an internal control where it remained stable even given any external stress or stimuli. Jayaraj et al. (2013) proposed the apoptotic regulators been measured in AgNPs treated cancer cells. The mRNA expressions of the Caspase-3, -8 and -9 genes were upregulated in the

AgNPs treated cells and no alterations were seen in the positive control (cisplatin). Hence, the AgNPs have the ability to trigger the apoptosis through the activation of the caspase cascades. The results demonstrated that the AuNPs and AgNPs induce the apoptosis by activating the proapoptotic genes such as PUMA, Caspase-3, Caspase-8 and Caspase-9. Therefore, the AuNPs and AgNPs activate the cell death through intrinsic apoptotic pathway.



CHAPTER 5

CONCLUSIONS AND RECOMENDATIONS

5.0 CHAPTER OVERVIEW

The different experiments used throughout the research produced many outcomes and to be concluded and listed below. In addition, the research findings recommend some essential work which is needed for the near future.

5.1 CONCLUSIONS

In this study, the biosynthesis reaction has optimized and controlled the size of the synthesized gold and silver nanoparticles using *C. nudiflora* aqueous extract. The gold and silver nanoparticles were synthesized successfully without adding any external chemicals as stabilizing and capping agents. The plant broth itself acts as natural stabilizing and capping agent to reduce the Au^+ and Ag^+ ions to Au^0 and Ag^0 respectively. *C. nudiflora* aqueous extract was used to synthesize the gold and silver nanoparticles at room temperature at the optimum pH of 6.5. Therefore, the biological synthesis method is simple, clean, a one-step method, reproducible and fast.

The physico-chemical characteristics of the synthesized gold nanoparticles have been demonstrated using a few analytical techniques such as UV-Vis spectrophotometer, FESEM, EDX, XRD, FT-IR and DLS. The biosynthesized GNPs have shown consistent yields with spherical, triangular in shapes and sizes that range between 50 to 85 nm. Thus, the synthesized gold nanoparticles have the potential to control clinical pathogenic bacteria activity and free radicals.

Also, the *C. nudiflora* aqueous extract synthesized silver nanoparticles by biosynthesis approaches. The aqueous plant extract acted as an economically reducing and stabilizing agent to produce stable silver nanoparticle with the size of < 50 nm. *C. nudiflora* extract contains a cluster of secondary metabolites such as alkaloids, saponins, polyphenols and flavonoids. It may act as a reducing and stabilizing agent for the reduction of Ag^+ to AgNPs. The biosynthesized silver nanoparticles effectively acted against oral pathogenic bacteria with the highest inhibition zone recorded. The biosynthesized gold and silver nanoparticles have effectively controlled the *E.coli* and *S.typhi* oral pathogenic bacteria. The results explored the potential of the synthesized silver nanoparticles to act as potential antibiotics against oral pathogenic bacteria. In addition, the synthesized Au, Ag nanoparticles exhibited moderate radical scavenging activity in DPPH and ABTS assays, but the metal nanoparticles activity was relatively lower than the ascorbic acid activity.

This study also demonstrated the edible weed plant, *C. nudiflora* possessing various bioactive compounds in different solvent extracts. The *C. nudiflora* extracts controlled the activity of food borne pathogens such as *E.coli* and *P. aurogenosa*. Also, the aqueous extract of *C. nudiflora* showed a significant activity in free radical scavenging properties.

Finally, the *in-vitro* cytotoxicity of synthesized gold and silver nanoparticles was demonstrated against HCT-116 colon cancer cells. The cell cycle pattern of treated HCT-116 cells clearly showed that the cell cycle phases were altered through DNA fragmentation. Also, the qRT-PCR analysis showed that the apoptotic genes such as PUMA, caspase-3, caspase-8 and caspase-9 were significantly expressed and eventually induced programmed cell death in colon cancer cells through intrinsic apoptotic pathway. This study demonstrated the *in-vitro* antibacterial, antioxidant and anticancer activity of synthesized gold and silver nanoparticles using *C. nudiflora* aqueous plant extract. Thus, by designing these metallic nanoparticles drugs, abnormal growths of colon cancer cells could be targeted and it promises a new strategy for treating colon cancer.

5.2 RECOMMENDATIONS

The research successfully investigated the synthesis of metallic Au, Ag nanoparticles using *C. nudiflora* plant extract. The plant extract acts in dual functions which are reducing and stabilizing agent in the redox-reaction. The synthesized gold and silver nanoparticles have been evaluated by a series of bioactivity assays such as *in-vitro* antibacterial, antioxidant and anticancer activities. The biosynthesis of nanoparticles was carried out at room temperature with no external addition of stabilizing and reducing agents. However, there is still no report available where the assembly of metal ions and plant extracts produce nano-sized metal nanoparticles. The greatest challenge is perhaps the biochemical redox-reaction between the metal ions and secondary metabolites and also the stability of the metals in the assembly process. Though, it is a widely accepted concept, it is limited in applications due to the lack of available technologies and process of validation as anticancer drugs. However, some additional findings are also needed for this study; hence, the recommendations that may enhance the whole research are listed below.

1. For further research, the *in-vivo* studies should be conducted to test the effectiveness of Au, Ag nanoparticles against colon cancer and others.
2. There is a need to figure out the specific secondary metabolites in the plant extracts which are fully/partially involved in the reduction reaction.
3. Laboratory scale production of metallic nanoparticles should be extended to a large scale production, and their functional mechanism against the pathogenic organisms needs to be elucidated.

REFERENCES

- Abdel-Aziz, M.S., Shaheen, M.S., El-Nekeety, A.A. and Abdel-Wahhab, M.A. 2014. Antioxidant and antibacterial activity of silver nanoparticles biosynthesized using *Chenopodium murale* leaf extract. *Journal of Saudi Chemical Society*. **18**: 356–363.
- Adavallan, K. and Krishnakumar, N. 2014. Mulberry leaf extract mediated synthesis of gold nanoparticles and its anti-bacterial activity against human pathogens. *Advanced Natural Sciences: Nanoscience and Nanotechnology*. **5**: 025018.
- Ahameethunisa, A.R. and Hopper, W. 2012. *In vitro* antimicrobial activity on clinical microbial strains and antioxidant properties of *Artemisia parviflora*. *Annals of Clinical Microbiology and Antimicrobials*. **11**: 30.
- Ahmad, A., Mukherjee, P., Senapati, S., Khan, M.I., Kumar, R. and Sastry, M. 2005. Extra-/intracellular biosynthesis of gold nanoparticles by an alkalotolerant fungus *Trichothecium* sp. *Journal of Biomedical Nanotechnology*. **1**: 47–53.
- Ahmad, T., Wani, I.A., Manzoor, N., Ahmed, J. and Asiri, A.M. 2013. Biosynthesis, structural characterization and antimicrobial activity of gold and silver nanoparticles. *Colloids and Surfaces B: Biointerfaces*. **107**: 227– 234.
- Akamatsu, K., Ikeda, S., Nawafune, H. and Deki, S. 2003. Surface modification-based synthesis and microstructural tuning of nanocomposite layers: Monodispersed copper nanoparticles in polyimide resins. *Chemistry of Materials*. **15**(13): 2488–2491.

- Andeani, J.K., Kazemi, H., Mohsenzadeh, S. and Safavi, A. 2011. Biosynthesis of gold nanoparticles using dried flowers extract of *Achillea Wilhelmsii* plant. *Digest Journal of Nanomaterials and Biostructures*. **6**: 1011-1017.
- Ankamwar, B., Damle, C., Ahmad, A. and Sastry, M. 2005. Biosynthesis of gold and silver nanoparticles using *Emblica officinalis* fruit extract, their phase transfer and trans-metallation in an organic solution. *Journal of Nanoscience and Nanotechnology*. **10**: 1665–1671.
- Anshup, J., Venkataraman, S., Subramaniam, C., Kumar, R.R., Priya, S., Kumar, T.R.S., Omkumar, R.V., John, A. and Pradeep, T. 2005. Growth of gold nanoparticles in human cells. *Langmuir* **21**: 11562-11567.
- Antony, J.J., Sivalingam, P., Siva, D., Kamalakkannan, S., Anbarasu, K. and Sukirtha, R. 2011. Comparative evaluation of antibacterial activity of silver nanoparticles synthesized using *Rhizophora apiculata* and glucose. *Colloids and Surfaces B: Biointerfaces*. **98**: 65-72.
- Apte, M., Girme, G., Nair, R., Bankar, A., Kumar, A.R. and Zinjarde, S. 2013. Melanin mediated synthesis of gold nanoparticles by *Yarrowia lipolytica*. *Materials Letters*. **95**: 149-152.
- Aromal, S.A. and Philip, D. 2012. Green synthesis of gold nanoparticles using *Trigonella foenum-graecum* and its size dependent catalytic activity. *Spectrochimica Acta Part A: Molecular and Biomolecular spectroscopy*. **97**: 1-5.
- Aromal, S.A., Vidhu, V.K. and Philip, D. 2012. Green synthesis of well-dispersed gold nanoparticles using *Macrotyloma uniflorum*. *Spectrochimica Acta Part A: Molecular and Biomolecular Spectroscopy*. **85**: 99-104.
- AshaRani, P.V., Hande, M.P. and Valiyaveetil, S. 2009. Anti-proliferative activity of silver nanoparticles. *BMC Cell Biology*. **10**: 65.

- Asmathunisha, N., Kathiresan, K., Anburaj, R. and Nabeel, M.A. 2010. Synthesis of antimicrobial silver nanoparticles by callus and leaf extracts from saltmarsh plant, *Sesuvium portulacastrum* L. *Colloids and Surfaces B: Biointerfaces*. **79**: 488-493.
- Asmathunisha, N. and Kathiresan, K. 2013. A review on biosynthesis of nanoparticles by marine organisms. *Colloids and Surfaces B: Biointerfaces*. **103**: 283–287.
- Astruc, D., Lu, F. and Aranzaes, J.R. 2005. Nanoparticles as recyclable catalysts: The frontier between homogeneous and heterogeneous catalysis. *Angewandte Chemie International Edition*. **44**(48): 7852–7872.
- Baharara, J., Namvar, F., Ramezani, T., Hosseini, N. and Mohamad, R. 2014. Green synthesis of silver nanoparticles using *Achillea biebersteinii* flower extract and its anti-angiogenic properties in the rat aortic ring model. *Molecules*. **19**: 4624-4634.
- Baker, S., Rakshith, D., Kavitha, K.S., Santosh, P., Kavitha, H.U., Rao, Y. and Satish S. 2013. Plants: Emerging as nanofactories towards facile route in synthesis of nanoparticles. *Bioimpacts*. **3**(3): 111–117.
- Bankar, A., Joshi, B., Kumar, A.R. and Zinjardea, S. 2010. Banana peel extract mediated novel route for the synthesis of silver nanoparticles. *Colloids and Surfaces A: Physicochemical and Engineering Aspects*. **368**: 58–63.
- Banupriya, A.R., Sathishkumar, M. and Yun S.-I. 2010. Biocrystallization of silver and gold ions by inactive cell filtrate of *Rhizopus stolonifer*. *Colloids and Surfaces B: Biointerfaces*. **79**: 531-534.

- Bar, H., Bhui, D.K., Sahoo, G.P., Sarkar, P., De, S.P. and Misra, A. 2009. Green synthesis of silver nanoparticles using latex of *Jatropha curcas*. *Colloids and Surfaces A: Physicochemical Engineering Aspects*. **339**: 134–139
- Bazzaz, B.S.F., Khayat, M.H., Emamic, S.A., Asili, J., Sahebkar, A. and Neishabory, E.J. 2011. Antioxidant and antimicrobial activity of methanol, dichloromethane, and ethyl acetate extracts of *Scutellaria litwinowii*. *Science Asia*. **37**: 327-334.
- Begum, N.A., Mondal, S., Basu, S., Laskar, R.A. and Mandal D. 2009. Biogenic synthesis of Au and Ag nanoparticles using aqueous solutions of black tea leaf extracts. *Colloids and surfaces B: Biointerfaces*. **71**: 113-118.
- Bhainsa, K.C. and D'Souza, S.F. 2006. Extracellular biosynthesis of silver nanoparticles using the fungus *Aspergillus fumigatus*. *Colloids and Surface B: Biointerfaces*. **47**(2): 160-164.
- Bhattacharya, D. and Gupta, R.K. 2005. Nanotechnology and potential of microorganisms. *Critical Reviews in Biotechnology*, **25**: 199–204.
- Bigall N.C. and Eychmuller A. 2010. Synthesis of noble metal nanoparticles and their non-ordered superstructures, *Philosophical Transactions of the Royal Society*. **368**: 1385–1404.
- Birla, S.S., Tiwari, V.V., Gade, A.K., Ingle, A.P., Yadav, A.P. and Rai, M.K. 2009. Fabrication of silver nanoparticles by *Phoma glomerata* and its combined effect against *Escherichia coli* *Pseudomonas aeruginosa* and *Staphylococcus aureus*. *Letters in Applied Microbiology*. **48**: 173–179.
- Boopathi, S., Gopinath, S., Boopathi, T., Balamurugan, V., Rajeshkumar, R. and Sundararaman, M. 2012. Characterization and antimicrobial properties of silver and silver oxide nanoparticles synthesized by cell-free extract of a mangrove

associated *Pseudomonas aeruginosa* M6 using two different thermal treatments. *Industrial Engineering Chemistry Research*. **34**: 231-235.

- Canizal, G., Ascencio, J.A., Gardea-Torresday, J. and Jose-Yacaman, M. 2001. Multiple twinned gold nanorods grown by bio-reduction techniques. *Journal of Nanoparticle Reserach*. **3**: 475-481.
- Chaloupka, K., Malam, Y. and Seifalian, A.M. 2010. Nanosilver as a new generation of nanoprodukt in biomedical applications. *Trends in Biotechnology*. **28**(11): 580-588.
- Chandran, S.P., Chaudhary, M., Pasricha, R., Ahmad, A. and Sastry, M. 2006. Synthesis of gold nanotriangles and silver nanoparticles using *Aloe vera* plant extract. *Biotechnology Progress*. **22**: 577-583.
- Chen, C.-W. and Akashi, M. 1997. Synthesis, characterization, and catalytic properties of colloidal platinum nanoparticles protected by poly (*N*-isopropylacrylamide). *Langmuir*. **13**(24): 6465-6472
- Chen, S., Zhao, M., Wu, G., Yao, C. and Zhang, J. 2012. Recent advances in morphological cell image analysis. *Computational and Mathematical Methods in Medicine*. **101536**: 1-10.
- Chimentao, R., Kirm, I., Medina, F., Rodri'guez, X., Cesteros, Y., Salagre, P., Sueiras, J., 2004. Different morphologies of silver nanoparticles as catalysts for the selective oxidation of styrene in the gas phase. *Chemical Communications*. **4**: 846-847.
- Chithrani, B.D., Ghazani, A.A. and Chan, W.C.W. 2006. Determining the size and shape dependence of gold nanoparticle uptake into mammalian cells. *Nano Letters*. **6**: 662-668.

- Choi, Y., Ho, N. and Tung, C. 2007. Sensing phosphatase activity by using gold nanoparticles. *Angewandte Chemie International Edition*. **46**(5): 707-709.
- Chow, A.Y. 2010. Cell cycle control by oncogenes and tumor suppressors: driving the transformation of normal cells into cancerous cells. *Nature Education*. **3**(9): 7.
- Chow, G.M., Markowitz, M.A., Rayne, R., Dunn, D.N. and Singh, A. 1996. Phospholipid mediated synthesis and characterization of gold nanoparticles. *Journal of Colloids and Interface Science*. **183**: 135-142.
- Cuenya, B.R. 2010. Synthesis and catalytic properties of metal nanoparticles: Size, shape, support, composition, and oxidation state effects. *Thin Solid Films*. **518**: 3127–3150.
- Daisy, P. and Saipriya, K. 2012. Biochemical analysis of *Cassia fistula* aqueous extract and phytochemically synthesized gold nanoparticles as hypoglycemic treatment for diabetes mellitus. *International Journal of Nanomedicine* **7**: 1189–1202.
- Das, R.K., Gogoi, N. and Bora, U. 2011. Green synthesis of gold nanoparticles using *Nyctanthes arbortristis* flower extract. *Bioprocess Biosystems Engineering*. **34**: 615–619.
- Das, S., Das, J., Samadder, A., Bhattacharyya, S.S., Das, D. and Khuda-Bukhsh, A.R. 2013. Biosynthesized silver nanoparticles by ethanolic extracts of *Phytolacca decandra*, *Gelsemium sempervirens*, *Hydrastis canadensis* and *Thuja occidentalis* induce differential cytotoxicity through G2/M arrest in A375 cells. *Colloids and Surfaces B: Biointerfaces*. **101**: 325–336.
- Das, S.K., Dickinson, C., Laffir, F., Brougham, D.F. and Marsili, E. (2012) Synthesis, characterization and catalytic activity of gold nanoparticles biosynthesized with *Rhizopus oryzae* protein extract. *Green Chemistry*. **14**: 1322– 1344.

- Das, S.K., Liang, J., Schmidt, M., Laffir, F., and Marsili, E. (2012b) Biomineralization mechanism of gold by zygomycete fungi *Rhizopus oryzae*. *ACS Nano* **6**: 6165–6173.
- Dassenoy, F., Philippot, K., Ould Ely, T., Amiens, C., Lecante, P., Snoeck, E., Mosset, A., Casanove, M.-J. and Chaudret B. 1998. Platinum nanoparticles stabilized by CO and octanethiol ligands or polymers: FT-IR, NMR, HREM and WAXS studies. *New Journal of Chemistry*. **22**: 703-711.
- Dauthal, P. and Mukhopadhyay, M. 2013. *In-vitro* free radical scavenging activity of biosynthesized gold and silver nanoparticles using *Prunus armeniaca* (apricot) fruit extract. *Journal of Nanoparticle Research*. **15**: 1366-1372.
- Dipankar, C. and Murugan, S. 2012. The green synthesis, characterization and evaluation of the biological activities of silver nanoparticles synthesized from *Iresine herbstii* leaf aqueous extracts. *Colloids and Surfaces B: Biointerfaces*. **98**: 112–119.
- Dong, S.A., Yang, S.C. and Tang, C. 2007. Rapid synthesis of size-controlled gold nanoparticles by complex intramolecular photoreduction. *Chemical Research in Chinese Universities*. **5**: 500-504.
- Douglas-Kinghorn, A. 2001. Pharmacognosy in the 21st century. *Journal of Pharmacy and Pharmacology*. **53**: 135-148.
- Dreaden, E.C., Mackey, M.A., Huang, X., z Bin Kangy, and El-Sayed M.A. 2011. Beating cancer in multiple ways using nanogold. *Chemical Society Reviews*. **40**: 3391–3404.
- Dubey, S.P., Lahtinen, M. and Sillanpaa, M. 2010. Tansy fruit mediated greener synthesis of silver and gold nanoparticles. *Process Biochemistry*. **45**: 1065-1071.

- Durán, N., Marcato, P.D, Alves, O.L., Souza, G.I. and Esposito, E. 2005. Mechanistic aspects of biosynthesis of silver nanoparticles by several *Fusarium oxysporum* strains. *Journal of Nanobiotechnology*. **3**: 8.
- Dykman, L.A. and Khlebtsov, N.G. 2011. Gold nanoparticles in biology and medicine: recent advances and prospects. *Acta Naturae*. **3**(2): 9.
- Elavazhagan, T. and Arunachalam, K.D. 2011. *Memecylon edule* leaf extract mediated green synthesis of silver and gold nanoparticles. *International Journal of Nanomedicine*. **6**: 1265–1278.
- El-Nour, A., Kholoud, M.M., Eftaiha, A., Al-Warthan, A. and Ammar, R.A.A. 2010. Synthesis and applications of silver nanoparticles. *Arabian Journal of Chemistry*. **3**(3): 135–140.
- El-Rafie, H.M. and Abdel-Aziz Hamed M. 2014. Antioxidant and anti-inflammatory activities of silver nanoparticles biosynthesized from aqueous leaves extracts of four *Terminalia* species. *Advanced Nature Science: Nanoscience and Nanotechnology*. **5**: 035008-0350019.
- Fakruddin, M., Mannan, K.S., Mazumdar, R.M. and Afroz, H. 2012. Antibacterial, antifungal and antioxidant activities of the ethanol extract of the stem bark of *Clausena heptaphylla*. *BMC Complementary and Alternative Medicine* **12**: 232.
- Fayaz, A.M., Balaji, K., Girilal, M., Yadav, R., Kalaichelvan, P.T. and Venketesan, R. 2010. Biogenic synthesis of silver nanoparticles and their synergistic effect with antibiotics: a study against gram-positive and gram-negative bacteria. *Nanomedicine*. **6**: 103–109

- Fayaz, A.M., Girilal, M., Rahman, M., Venkatesan, R. and Kalaichelvan, P.T. 2011. Biosynthesis of silver and gold nanoparticles using thermophilic bacterium *Geobacillus stearothermophilus*. *Process Biochemistry*. **46**: 1958-1962.
- Feng, Q., Wu, J., Chen, G., Cui, F., Kim, T. and Kim, J. 2000. A mechanistic study of the antibacterial effect of silver ions on *Escherichia coli* and *Staphylococcus aureus*. *Journal of Biomedical Materials Research*. **52**: 662-668.
- Ford, C. 1986. *Inorganic Reactions and Methods*, VCH, Deerfield Beach, Florida.
- Gade, A.K., Bonde, P., Ingle, A.P., Marcato, P.D., Duran, N. and Rai, M.K. 2008. Exploitation of *Aspergillus niger* for synthesis of silver nanoparticles. *Journal of Biobased Materials and Bioenergy*. **2**: 243-247.
- Gajendran, B., Chinnasamy, A., Durai, P., Raman, J. and Ramar, M. 2014. Biosynthesis and characterization of silver nanoparticles from *Datura innoxia* and its apoptotic effect on human breast cancer cell line MCF7. *Materials Letters*. **122**: 98-102.
- Gan, P.P., Ng, S.H., Huang, Y. and Li, S.F.Y. 2012. Green synthesis of gold nanoparticles using palm oil mill effluent (POME): A low-cost and eco-friendly viable approach. *Bioresource Technology*. **113**: 132-135.
- Ganeshkumar, M., Sathishkumar, M., Ponrasu, T., Dinesh, M. and Suguna, L. 2013. Spontaneous ultra fast synthesis of gold nanoparticles using *Punica granatum* for cancer targeted drug delivery. *Colloids and Surfaces B: Biointerfaces*. **106**: 208-216.
- Ganeshkumar, M., Sastry, T.P., Kumar, M.S., Dinesh, M.G., Kannappan, S. and Suguna, L. 2012. Sun light mediated synthesis of gold nanoparticles as carrier for 6-mercaptopurine: Preparation, characterization and toxicity studies in zebrafish embryo model. *Materials Research Bulletin*. **47**: 2113-2119.

- Ganeshkumar, V., Gokavarapu, S.D., Rajeswari, A., Dhas, T.S., Karthick, V., Kapadia, Z., Shrestha, T., Barathy, I.A., Roy A. and Sinha S. 2011. Facile green synthesis of gold nanoparticles using leaf extract of antidiabetic potent *Cassia auriculata*. *Colloids and surfaces B: Biointerfaces*. **87**: 159-163.
- Gardea-Torresdey, J.L., Parsons, J.G., Gomez, E., Peralta-Viddeca, J., Troiani, H.E., Santiago, P. and Jose Yacaman, M. 2002. Formation and growth of Au nanoparticles inside live Alfalfa plants. *Nano Letters*. **2**: 397–401.
- Gardea-Torresdey, J.L., Gomez, E., Jose-Yacaman, M., Parsons, J.G., Peralta-Videa, J.R. and Tioani, H. 2003. Alfalfa sprouts: a natural source for the synthesis of silver nanoparticles. *Langmuir*. **19**: 1357–1361.
- Geethalakshmi, R. and Sarada, D.V.L. 2013. Characterization and antimicrobial activity of gold and silver nanoparticles synthesized using saponin isolated from *Trianthema decandra*. *Industrial Crops Products*. **51**: 107-115.
- Ghosh, S., Patil, S., Ahire, M., Kitture, R., Kale, S., Pardesi, K., Cameotra, S.S. and Bellare, J., Dhavale, D.D., Jabgunde, A. and Chopad, B.A. 2012. Synthesis of silver nanoparticles using *Dioscorea bulbifera* tuber extract and evaluation of its synergistic potential in combination with antimicrobial agents. *International Journal of Nanomedicine*. **7**: 483–496.
- Gingrich, J. et al. 2006. Effect of RNA degradation on the data quality in quantitative PCR and microarray experiments. *Bio-Rad Bulletin*. **5452**: 1-11.
- Gopalakrishnan, R. and Raghu, K. 2014. Biosynthesis and characterization of gold and silver nanoparticles using milk thistle (*Silybum marianum*) seed extract. *Journal of Nanoscience*. **905404**: 1-8.

- Gopinath, P., Gogoi, S.K., Sanpui, P., Paul, A., Chattopadhyay, A. and Ghosh, S.S. 2010. Signaling gene cascade in silver nanoparticle induced apoptosis. *Colloids and Surfaces B: Biointerfaces*. **77**: 240–245.
- Gopinath, V., MubarakAli, D., Priyadarshini, S., Priyadharsshini, N.M., Thajuddin, N. and Velusamy, P. 2012. Biosynthesis of silver nanoparticles from *Tribulus terrestris* and its antimicrobial activity: a novel biological approach. *Colloids and Surfaces B: Biointerfaces*. **96**: 69-74.
- Govindaraju, K., Khaleel Basha, S., Ganesh Kumar, V. and Singaravelu, G. 2008. Silver, gold and bimetallic nanoparticles production using single-cell protein (*Spirulina platensis*) Geitler. *Journal of Material Sciences*. **34**: 322-329.
- Gurunathan, S., Kalishwaralal, K. and Vaidyanathan, R. et al. 2009. Biosynthesis, purification and characterization of silver nanoparticles using *Escherichia coli*. *Colloids and Surfaces B: Biointerfaces*. **74**(1): 328–335.
- Hanauer, M., Lotz, A., Pierrat, S., Sonnichsen, C., Zins, I. 2007. Separation of nanoparticles by gel electrophoresis according to size and shape. *Nano Letters*. **7**(9): 2881–2885.
- Harborne JB (1998) *Phytochemical methods*. 3rd ed. Chapman and Hall Publication, 34-88.
- Hengartner, M.O. 2000. The biochemistry of apoptosis. *Nature*. **407**: 770–776.
- Howes, D.P., Chandrawati, R. and Stevens, M. M. 2014. Colloidal nanoparticles as advanced biological sensors. *Science*. **346** (6205): 1247390-10.
- Huang, N.M., Lim, H.N., Radiman, S., Khiew, P.S., Chiu, W.S., Hashim, R. and Chia, C.H. 2010. Sucrose ester micellar-mediated synthesis of Ag nanoparticles and

the antibacterial properties. *Colloids and Surfaces A: Physicochemical and Engineering Aspects*. **35**: 69-76.

Hutter, E. and Fendler, J.H. 2004. Exploitation of localized surface plasmon resonance. *Advanced Materials*. **16**(19): 1685-1706.

Inbakandan, D., Venkatesan, R. and Ajmal Khan, S. 2010. Biosynthesis of gold nanoparticles utilizing marine sponge *Acanthella elongata* (Dendy, 1905). *Colloids and Surfaces B: Biointerfaces*. **81**(2): 634-639.

Ingelsten, H.H., Bagwe, R., Palmqvist, A., Skoglundh, M., Svanberg, C., Holmberg, K. and Shah, D.O. 2001. Kinetics of the Formation of Nano-Sized Platinum Particles in Water-in-Oil Microemulsions. *Journal Colloid Interface Science*. **241**: 104-111.

Jain, P.K., Lee, K.S., El-Sayed ,I.H. and El-Sayed, M.A. 2006. Calculated absorption and scattering properties of gold nanoparticles of different size, shape, and composition: applications in biological imaging and biomedicine. *Journal of Physical Chemistry B*. **110**: 7238-7243.

Jain, P.K., Huang, X., El Sayed, L.H. and El Syed, M.A. 2007. Review of some interesting surface plasmon resonance enhanced properties of noble metal nanoparticles and their applications to biosystems. *Plasmonics* **2**: 107-118.

Jeyaraj, M., Sathishkumar, G., Sivanandhan, G., MubarakAli, D., Rajesh, M., Arun, R. et al. 2013. Biogenic silver nanoparticles for cancer treatment: An experimental report. *Colloids and surfaces B: Biointerfaces*. **106**: 86-92.

Jayaseelan, C., Ramkumar, R., Rahuman, A.A. and Perumal P. 2013. Green synthesis of gold nanoparticles using seed aqueous extract of *Abelmoschus esculentus* and its antifungal activity. *Industrial Crops and Products*. **45**: 423-429.

- Jeong, J.H., Lee, J.W., Kim, K.S., Kim, J-S., Han, S.N., Yu, C.Y., Lee, J.K., Kwon, Y.S. and Kim, M.J. 2010. Antioxidant and antimicrobial activities of extracts from a medicinal plant sea buckthorn. *Journal of Korean Society of Applied Biological Chemistry*. **53**: 33-38.
- Jha, A.K., Prasad, K., Prasad, K. and Kulkarni, A.R. 2009. Plant system: Nature's nanofactory. *Colloids and Surfaces B: Biointerfaces*. **73**: 219–223.
- Kaliswaralal, K., Babu, R.S., Venkataraman, D., Bilal, M. and Gurunathan, S. 2009. Biosynthesis of silver nanocrystals by *Bacillus licheniformis*. *Colloids and Surfaces B: Biointerfaces*. **65**(1): 150–153.
- Karthik, S., Sankar, R., Varunkumar, K. and Ravikumar, V. 2014. Romidepsin induces cell cycle arrest, apoptosis, histone hyperacetylation and reduces matrix metalloproteinases 2 and 9 expression in bortezomib sensitized non-small cell lung cancer cells. *Biomedicine & Pharmacotherapy*. **68**: 327–334.
- Kasthuri, J., Kathiravan, K. and Rajendiran, N. 2009. Phyllanthin-assisted biosynthesis of silver and gold nanoparticles: a novel biological approach. *Journal of Nanoparticle Research*. **11**: 1075–1085.
- Kathiresan, K., Manivannan, S., Nabeel, M.A. and Dhivya, B. 2009. Studies on silver nanoparticles synthesized by a marine fungus, *Penicillium fellutanum* isolated from coastal mangrove sediment. *Colloids and Surfaces B: Biointerfaces*. **71**(1): 133-137.
- Katz, E. and Willner, I. 2004. Integrated nanoparticle–biomolecule hybrid systems: synthesis, properties, and applications. *Angewandte Chemie International Ed.* **43**: 6042-6108.
- Kaviya, S., Santhanalakshmi, J., Viswanathan, B., Muthumary, J. and Srinivasan, K. 2011. Biosynthesis of silver nanoparticles using *Citrus sinensis* peel extract and

its antibacterial activity. *Spectrochimica Acta Part A: Molecular and Biomolecular spectroscopy*. **79**: 594-598.

Kerr, J.F. 2000. History of the events leading to the formulation of the apoptosis concept. *Toxicology*. **181**: 471-474.

Khan, M.A.M., Kumar, S., Ahamed, M., Alrokayan, S.A. and Alsalhi, M.S. 2011. Structural and thermal studies of silver nanoparticles and electrical transport study of their thin films. *Nanoscale Research Letters*. **6**: 434-439.

Khomutov, G. and Gubin, S. 2002. Interfacial synthesis of noble metal nanoparticles. *Materials Science and Engineering C*. **22**(2): 141-146.

Kim, J.S., Kuk, E., Yu, K.N., Kim, J.H., Park, S.J. and Lee, H.J et al. 2007. Antimicrobial effects of silver nanoparticles. *Nanomedicine* **3**: 95-101.

Klabunde, K.J. and Mulukutla, R.S. 2001. Chap: 7. Chemical catalytic aspects of nanocrystals. In *Nanoscale Materials and chemistry*; Ed: John Wiley & Sons, Inc. 223-261.

Kokura, S., Handa, O., Takagi, T., Ishikawa, T., Naito, Y. and Yoshikawa, T. 2010. Silver nanoparticles as a safe preservative for use in cosmetics. *Nanomedicine*. **5**: 1-5.

Kouvaris, P., Delimitis, A., Zaspalis, V., Papadopoulos, D., Tsipas, S.A. and Michailidis, N. 2012. Green synthesis and characterization of silver nanoparticles produced using *Arbutus unedo* leaf extract. *Materials Letters*. **76**: 18-20.

Krishnaraj, C., Jagan, E.G., Rajasekar, S., Selvakumar, P., Kalaichelvan, P.T. and Mohan, N. 2010. Synthesis of silver nanoparticles using *Acalypha indica* leaf

extracts and its antibacterial activity against water borne pathogens. *Colloids and Surface B: Biointerfaces*. **76**: 50–56.

Krishnaraj, C., Muthukumaran, P., Ramachandran, R., Balakumaran, M.D. and Kalaichelvan, P.T. 2014. *Acalypha indica* Linn: Biogenic synthesis of silver and gold nanoparticles and their cytotoxic effects against MDA-MB-231, human breast cancer cells. *Biotechnology Reports*. **4**: 42–49.

Krug, J.T., Wang, G.D., Emory, S.R. and Nie, S. 1999. Efficient Raman enhancement and intermittent light emission observed in single gold nanocrystals. *Journal of American Chemical Society*. **121**(39): 9208–9214.

Kumar, C.S.S.R. 2007. Nanomaterials for cancer diagnosis. Wiley, Weinheim, Germany.

Kumar, S.A., Abyaneh, M.K., Gosavi, S.W., Kulkarni, S.K., Pasricha, R., Ahmad, A. and Khan, M.I. 2007a. Nitrate reductase-mediated synthesis of silver nanoparticles from AgNO₃. *Biotechnology Letters*. **29**: 439–445.

Kumar, V. and Yadav, S.K. 2008. Plant-mediated synthesis of silver and gold nanoparticles and their applications. *Journal of Chemical Technology and Biotechnology*. **84**: 151–157.

Labouta, H.I. and Schneider, M. 2010. Tailor-made biofunctionalized nanoparticles using layer-by-layer technology. *International Journal of Pharmaceutics*. **365**: 236–242.

Law, N., Ansari, S., Livens, F.R., Renshaw, J.C., Lloyd, J.R. 2008. The formation of nano-scale elemental silver particles via enzymatic reduction by *Geobacter sulfurreducens*. *Applied Environmental Microbiology*. **74**: 7090–7093.

- Ledgerwood, E.C. and Morison, I.M. 2009. Targeting the apoptosome for cancer therapy. *Clinical Cancer Research*. **15**(2): 245-255.
- Lekeufack, D.D. and Brioude, A. 2012. One pot biosynthesis of gold NPs using red cabbage extracts. *Dalton Transactions*. **41**: 1461-1464.
- Lengke, M.F., Fleet, M.E. and Southam, G. 2006. Morphology of gold nanoparticles synthesized by filamentous cyanobacteria from gold (I)-thiosulfate and gold (III)-chloride complexes. *Langmuir*. **22**: 2780–2787.
- Li, C., Li, D., Wan, G., Xu, J. and Hou, W. 2011. Facile synthesis of concentrated gold nanoparticles with low size-distribution in water: temperature and pH controls. *Nano Scale Research Letters*. **6**: 440.
- Lim, E., Guerra, R., Lara, V. and Guzmán, A. 2013. Gold nanoparticles as efficient antimicrobial agents for *Escherichia coli* and *Salmonella typhi*. *Chemistry Central Journal*. **7**: 11-19.
- Lim, G.C.C., Halimah, Y. and Lim, T.O. 2008. The first report of National Cancer Registry, Cancer Incidence in Malaysia. <http://www.acrm.org.my/ncr>
- Lin, L., Qiu, P., Cao, X. and Jin, L. 2008. Colloidal silver nanoparticles modified electrode and its application to the electroanalysis of Cytochrome c. *Electrochimica Acta*. **53**(16): 5368-5372.
- Lisec, J., Schauer, N., Kopka, J., Willmitzer, L. and Fernie, A.R. 2006. Gas chromatography mass spectrometry–based metabolite profiling in plants. *Nature Protocols*. **1**: 387-396.
- Liu, J. and Hurt, R.H. 2010. Ion release kinetics and particle persistence in aqueous nano-silver colloids. *Environmental Science and Technology*. **44**: 2169–2175.

- Liu, W.T. 2006. Nanoparticles and their biological and environmental applications. *Journal of Bioscience and Bioengineering*. **102**(1): 1–7.
- Loannou, Y.A. and Chen, F.W. 1996. Quantitation of DNA Fragmentation in Apoptosis. *Nucleic Acids Research*. **24**(5): 992–993.
- Logeswari, P., Silambarasan, S. and Abraham, J. 2011. Synthesis of silver nanoparticles using plants extract and analysis of their antimicrobial property. *Journal of Saudi Chemical Society*. **22**: 34-39.
- Malik, M.A., O'Brien, P. and Revaprasadu, N.A. 2002. Simple route to the synthesis of core/shell nanoparticles of chalcogenides. *Chemistry of Materials*. **14**(5): 2004–2010.
- Manian, R., Anusuya, N., Siddhuraja, P. and Manian, S. 2008. The antioxidant activity and free radical scavenging potential of two different solvent extracts of *Comellia sinensis* (L.) O.Kuntz, *Ficus bengalensis* L. and *Ficus recemosa* L. *Food Chemistry*. **107**: 1000-1007.
- Manikanth, S.B., Kalishwaralal, K., Sriram, M., Pandian, S.R.K., Hyung-seop, Y., Eom, S.H. and Gurunathan, S. 2010. Anti-oxidant effect of gold nanoparticles restrains hyperglycemic conditions in diabetic mice. *Journal of Nanobiotechnology*. **8**: 77-81.
- Manivannan, S., Nabeel, M.A. and Kathiresan, K. 2010. In vitro synthesis of silver nanoparticles by marine yeasts from coastal mangrove sediment. *Advanced Science Letters*, **3**: 428-433.
- Mata, Y.N., Torres, E., Blazquez, M.L., Ballester, A., Gonzalez, F. and Munoz, J.A. 2009. Gold(III) biosorption and bio-reduction with the brown alga *Fucus vesiculosus*. *Journal of Hazardous Materials*. **166**: 612-618.

- Mejía-Jaramillo, A.M., Fernández, G.J., Palacio, L. and Triana-Chávez, O. 2011. Gene expression study using real-time PCR identifies an NTR gene as a major marker of resistance to benznidazole in *Trypanosoma cruzi*. *Parasitology Vectors*. **5**: 4:169.
- Miller. M. 1972. Biochemical methods for agricultural sciences. pp. 6–40. Wiley Eastern Ltd, New Delhi.
- Mittal, A.K., Kumar, S. and Banerjee, U.C. 2014. Quercetin and gallic acid mediated synthesis of bimetallic (silver and selenium) nanoparticles and their antitumor and antimicrobial potential. *Journal of Colloid and Interface Science*. **431**: 194–199.
- Mohamed, A.A., Ali, S.I. and El-Baz, F.K. 2013. Antioxidant and antibacterial activities of crude extracts and essential oils of *syzygium cumini* leaves. *Plos One* **8**: e60269.
- Mohanpuria, P., Rana, N.K. and Yadav, S.K. 2008. Biosynthesis of nanoparticles: technological concepts and future applications. *Journal of Nanoparticle Research*. **10**: 507–517.
- Mohtashami, M., Sepehriseresht, S., Asli, E., Boroumand, M.A. and Ghasemi, A. 2012. Synthesis of silver nanoparticles through chemical reduction and biosynthesis methods and evaluation of their antibacterial effects. *Razi Journal of Medical Sciences*. **19**(103): 110-115.
- Mott, D., Thuy, N.T.B., Aoki, Y., Maenosono, S. 2010. Aqueous synthesis and characterization of Ag and Ag-Au nanoparticles: addressing challenges in size, monodispersity and structure. *Philosophical Transactions of the Royal Society A*. **368**: 1-8.

- MubarakAli, D., Thajuddin, N., Jeganathan, K. and Gunasekaran, M. 2011. Plant extract mediated synthesis of silver and gold nanoparticles and its antibacterial activity against clinically isolated pathogens. *Colloids and Surfaces B: Biointerfaces*. **85**: 360-365.
- Mukherjee, S., Chowdhury, D., Kotcherlakota, R., Patra, S., Vinothkumar, B, Bhadra, M.P., Sreedhar, B., Patra, C.R. 2014. Potential theranostics application of bio-synthesized silver nanoparticles (4-in-1 System). *Theranostics*. **4**(3): 316-335.
- Mukherjee, P., Senapati, S., Mandal, D., Ahmad, A., Khan, M.I., Kumar, R. and Sastry, M. 2001a. Bioreduction of AuCl₄⁻ ions by the fungus, *Verticillium* sp. and surface trapping of the gold nanoparticles formed. *Angewandte Chemie International Edition*. **40**: 3585– 3588
- Mukherjee, P., Senapati, S., Mandal, D., Ahmad, A., Khan, M.I., Kumar, R. and Sastry, M. 2001b. Fungus-mediated synthesis of silver nanoparticles and their immobilization in the mycelial matrix: a novel biological approach to nanoparticle synthesis. *Nano Letters*. **1**: 515–519
- Mukherjee, P., Senapati, S., Mandal, D., Ahmad, A., Khan, M.I., Kumar, R. and Sastry, M. 2002. Extracellular synthesis of gold nanoparticles by the fungus *Fusarium oxysporum*. *Chembiochem* **5**(3): 461–463.
- Mustata, R.C., Vasile, G., Fernandez-Vallone, V., Strollo, S., Lefort, A. and Libert, F. et al. 2013. Identification of lgr5-independent spheroid-generating progenitors of the mouse fetal intestinal epithelium. *Cell Reports*. **5**: 421–432.
- Murphy, C.J., Gole, A.M., Stone, J.W., Sisco, P.N., Alkilany, A.M., Goldsmith, E.C. and Baxter, S.C. Gold nanoparticles in biology: beyond toxicity to cellular imaging. *Accounts of Chemical Research A*. **12**: 322-329.

- Nagati, V.B., Alwala, J., Koyyati, R., Donda, M.R., Banala, R. and Padigya, P.R.M. 2012. Green Synthesis of plant-mediated silver nanoparticles using *Withania somnifera* leaf extract and evaluation of their anti microbial activity. *Asian Pacific Journal of Tropical Biomedicine*. **2**: 1-5.
- Nangia, Y., Wangoo, N., Sharma, S., Wu, J.-S., Dravid, V., Shekhawat, G.S., Suri, R.C. 2009. Facile biosynthesis of phosphate capped gold nanoparticles by a bacterial isolate *Stenotrophomonas maltophilia*. *Applied Physics Letters*. **94**: 233901-907.
- Narayanan, K.B. and Sakthivel, N. 2008. Coriander leaf mediated biosynthesis of gold nanoparticles. *Materials Letters* **62**: 4588–4590.
- Narayanan, K.B. and Sakthivel, N. 2010 Biological synthesis of metal nanoparticles by microbes. *Advanced Colloids and Interfaces Science*. **22**: 1-13.
- Narayanan, K.B. and Sakthivel, N. 2011a. Facile green synthesis of gold nanostructures by NADPH – dependent enzyme from the extract of *Sclerotium rolfsii*. *Colloids Surface A*. **380**: 156–161.
- Nath, D. and Banerjee, P. 2013. Green nanotechnology – A new hope for medical biology. *Environmental Toxicology and Pharmacology*. **36**: 997–1014.
- NCCLS. 1997. Performance standards for antimicrobial disk susceptibility tests: approved standard M2-A7. National Committee for Clinical Laboratory Standards, Wayne, PA, USA.
- Neutra, M.J. and Forstner, J.F. 1987. Gastrointestinal mucus: synthesis, secretion and function. In: *Physiology of the Gastrointestinal Tract*. Second edition, pp. 975-1009, L.R. Johnson (Ed.). Raven Press, New York.

- Niraimathi, K.L., Sudha, V., Lavanya, R. and Brindha, P. 2012. Biosynthesis of silver nanoparticles using *Alternanthera sessilis* (Linn.) extract and their antimicrobial, antioxidant activities. *Colloids and Surface B: Biointerfaces*. **88**: 34-39.
- Noruzi, M., Zare, D. and Davoodi, D. 2012. A rapid biosynthesis route for the preparation of gold nanoparticles by aqueous extract of cypress leaves at room temperature. *Spectrochimica Acta Part A. Molecular and Biomolecular Spectroscopy*. **94**: 84-88.
- Ozcan, B., Esen, M., Caliskan, M., Mothana, R.A., Cihan, A.C. and Yolcu, H. 2011. Antimicrobial and antioxidant activities of the various extracts of *Verbascum pinetorum* Boiss. O. Kuntze (Scrophulariaceae). *European Review of Medical Pharmacology*. **15**: 900-905.
- Pandey, S., Mewada, A., Thakur, M., Shinde S., Shah, R., Oza, G. and Sharon M. 2013. Rapid Biosynthesis of silver nanoparticles by exploiting the reducing potential of *Trapa bispinosa* peel extract. *Journal of Nanoscience*. **516357**: 1-7.
- Parial, D., Patra, H.K., Roychoudhury, P., Dasgupta, A.K. and Pal R. 2012. Gold nanorod production by cyanobacteria—a green chemistry approach. *Journal of Applied Phycology*. **24**: 55-60.
- Pawan Khanna, K. and Nair, C.K.K. 2009. Synthesis of silver nanoparticles using cod liver oil (fish oil): green approach to nanotechnology. *International Journal of Green Nanotechnology and Physical Chemistry*. **1**: P3.
- Philip, D. 2009. Honey mediated green synthesis of gold nanoparticles. *Spectrochimica Acta Part A: Molecular Biomolecular Spectroscopy*. **73**: 650-653.
- Philip, D. and Unni, C. 2011. Extracellular biosynthesis of gold and silver nanoparticles using Krishna tulsi (*Ocimum sanctum*) leaf. *Physica E*. **43**: 1318–1322.

- Pickup, J.C., Zhi, Z.L., Khan, F., Saxl, T. and Birch, D.J. 2008. Nanomedicine and its potential in diabetes research and practice. *Diabetes Metabolism Research*. **24**: 604-610.
- Prabhu, D., Arulvasu, C., Babu, G., Manikandan, R. and Srinivasan, P. 2013. Biologically synthesized green silver nanoparticles from leaf extract of *Vitex negundo* L. induce growth-inhibitory effect on human colon cancer cell line HCT15. *Process Biochemistry*. **48**: 317–324.
- Prakash, N.K.U., Bhuvanewari, S., Jahnvi, B., Abhinaya, K., Rajalin, A.G. and Kumar, M.P. et al. 2012. A study on antibacterial activity of common weeds in Northern Districts of Tamil Nadu, India. *Research Journal of Medicinal Plant*. **6**: 341-345.
- Prakash, S. and Urbanska, A.M. 2008. Colon-targeted delivery of live bacterial cell biotherapeutics including microencapsulated live bacterial cells. *Biologics*. **2**(3): 355–378.
- Qi, W.H. and Wang, M.P. 2005. Size and shape dependent lattice parameters of metallic nanoparticles. *Journal of Nanoparticle Research*. **7**(1): 51-57.
- Qu, L. and Dai, L. 2005. Substrate-enhanced electroless deposition of metal nanoparticles on carbon nanotubes. *Journal of American Chemical Society*. **127**(31): 10806–10807.
- Raghunandan, D., Borgaonkar, P.A., Bendegumble, B., Bedre, M.D., Bhagawanraju, M. and Yalagatti M.S. et al., 2011. Microwave-assisted rapid extracellular biosynthesis of silver nanoparticles using carom seed (*Trachyspermum copticum*) extract and *in vitro* studies. *American Journal of Analytical Chemistry*, **2**: 475-483.

- Rai, A., Singh, A., Ahmad, A. and Sastry, M. 2006. Role of halide ions and temperature on the morphology of biologically synthesized gold nanotriangles. *Langmuir*. **22**: 736–741.
- Rai, M. and Duran, N. (eds.), 2011. Metal nanoparticles in microbiology, pp-45-67, Springer-Verlag Berlin Heidelberg.
- Raja, K., Saravanakumar, A. and Vijayakumar, R. 2012. Efficient synthesis of silver nanoparticles from *Prosopis juliflora* leaf extract and its antimicrobial activity using sewage. *Spectrochimia Acta Part A. Molecular and Biomolecular Spectroscopy*. **97**: 490-494.
- Rajasekharreddy, P., Rani, P.U. and Sreedhar, B. 2010. Qualitative assessment of silver and gold nanoparticle synthesis in various plants: a photobiological approach. *Journal of Nanoparticle Research*. **12**: 1711–1721.
- Rajasree, R.S.R. and Suman, T.Y. 2011. Extracellular biosynthesis of gold nanoparticles using a gram negative bacterium *Pseudomonas fluorescens*. *Asian Pacific Journal of Tropical Diseases*. **3**: S795-S799.
- Raju, D., Mehta, U.J. and Hazra, S. 2011. Synthesis of gold nanoparticles by various leaf fractions of *Semecarpus anacardium* L. tree. *Trees Structure and Function*. **25**: 145–151.
- Ramamurthy, C.H., Padma, M., Samadanam, I.D.M., Mareeswaran, R., Suyavaran, A., Suresh Kumar, M., Premkumar, K. and Thirunavukkarasu, C. 2013. The extra cellular synthesis of gold and silver nanoparticles and their free radical scavenging and antibacterial properties. *Colloids and Surfaces B: Biointerfaces*. **102**: 808-815.
- Ravindra, P. 2009. Protein-mediated synthesis of gold nanoparticles. *Materials Science and Engineering B*. **163**: 93-98.

- Réthy, B., Zupkó, I., Minorics, R., Hohmann, J., Ocsóvszki, I. and Falkay, G. 2007. Investigation of cytotoxic activity on human cancer cell lines of arborinine and furanoacridones isolated from *Ruta graveolens*. *Planta Med.* **73**: 41-48.
- Reveendran, P., Wallen, S. and Fu, J. 2003. Complete green synthesis and stabilization of metal nanoparticles. *Journal of American Chemical Society.* **125**: 12940-945.
- Reza Ghorbani, H., Safekordi, A.A., Attar, H. and Sorkhabadi, S.M.R. 2011. Biological and non-biological methods for silver nanoparticles synthesis. *Chemical Biochemical Engineering Q.* **25**(3): 317–326.
- Richardson, A., Chan, B.C., Crouch, R.D., Janiec, A., Chan, B.C. and Crouch, R.D. 2006. Synthesis of silver nanoparticles: an undergraduate laboratory using green approach. *Chemical Education.* **11**: 331–333.
- Roco, M.C. 2003. Nanotechnology: convergence with modern biology and medicine. *Current Opinion in Biotechnology.* **14**: 337-346.
- Rodriguez-Moranta, F., Castells, A., Andreu, M., Pinol, V., Castellvi-Bel, S. and Alenda, C. 2006. Clinical performance of original and revised Bethesda guidelines for the identification of MSH2/MLH1 gene carriers in patients with newly diagnosed colorectal cancer: Proposal of a new and simpler set of recommendations. *American Journal of Gastroenterology.* **101**: 1104-1111.
- Rostamizadeh, K., Abdollahi, H. and Parsajoo, C. 2013. Synthesis, optimization, and characterization of molecularly imprinted nanoparticles. *International Nano Letters.* **3**: 20.
- Salata, O.V. 2004. Applications of nanoparticles in biology and medicine. *Journal of Nanobiotechnology.* **2**: 3

- Sanchez-Mendieta, V. and Vilchis-Nestor, A.R. 2012. Green synthesis of noble metal (au, ag, pt) nanoparticles, assisted by plant-extracts, noble metals, Dr. Yen-Hsun Su (Ed.), InTech, ISBN: 978-953-307-898.
- Sankar, R., Karthik, A., Prabu, A., Karthik, S., Shivashangari, K. S. and Ravikumar, V. 2013. *Origanum vulgare* mediated biosynthesis of silver nanoparticles for its antibacterial and anticancer activity. *Colloids and Surfaces B: Biointerfaces*. **108**: 80–84.
- Santhosh kumar, T., Rahuman, A.A., Rajakumar, G., Marimuthu, S., Bagavan, A., Jayaseelan, C., Zahir, A.A., Elango, G. and Kamaraj, C. 2011. Synthesis of silver nanoparticles using *Nelumbo nucifera* leaf extract and its larvicidal activity against malaria and filariasis vectors. *Parasitology Research*. **108**: 693–702.
- Sanvicens, N. and Marco, M.P. 2009. Multifunctional nanoparticles – properties and prospects for their use in human medicine. *Trends in Biotechnology*. **26**(8): 424–433.
- Sapsford, K.E., Algar, W.R., Berti, L., Gemmill, K.B., Casey, B.J., Oh, E., Stewart, M. H., and Medintz, I.L. 2013. Functionalizing nanoparticles with biological molecules: developing chemistries that facilitate nanotechnology. *Chemical Reviews*. **113**(3): 1904–2074.
- Sarkar, A., Parikh, N., Hearn, S.A., Fuller, M.T., Tazuke, S.I. and Schulz, C. 2007. Antagonistic roles of Rac and Rho in organizing the germ cell microenvironment. *Current Biology*. **17**(14): 1253--1258.
- Sathishkumar, M., Sneha, K., Won, S.W., Cho, C.W., Kim, S. and Yun, Y.S. 2009. *Cinnamon zeylanicum* bark extract and powder mediated green synthesis of nano-crystalline silver particles and its bactericidal activity. *Colloids and Surface B: Biointerfaces*. **73**: 332–338.

- Sathiyarayanan, G., Seghal Kiran, G. and Selvin, J. 2013. Synthesis of silver nanoparticles by polysaccharide bioflocculant produced from marine *Bacillus subtilis* MSBN17. *Colloids and Surfaces B: Biointerfaces*. **102**: 13–20.
- Satyavani, K., Gurudeeban, S., Ramanathan, T. and Balasubramanian, T. 2011. Biomedical potential of silver nanoparticles synthesized from calli cells of *Citrullus colocynthis* (L.) Schrad. *Journal of Nanobiotechnology*. **9**: 43-51.
- Satyavani, K., Ramanathan, T. and Gurudeeban, S. 2011. Plant mediated synthesis of biomedical silver nanoparticles by using leaf extract of *Citrullus colocynthis*. *Research Journal of Nanoscience and Nanotechnology*. **1**: 95-101.
- Sau, T.K. and Rogach, A.L. 2010. Nonspherical noble metal nanoparticles: colloid-chemical synthesis and morphology control. *Advanced Materials*. **22**(16): 1781–1804.
- Scherrer, P. 1918. Nachr. “Bestimmung der Grösse und der inneren Struktur von Kolloidteilchen mittels Röntgenstrahlen.” *Ges Wiss Göttingen*. **26**: 98-100.
- Schrofel, A., Kratošova, G., Krautova, M., Dobročka, E. and Vavra, I. 2011. Biosynthesis of gold nanoparticles using diatoms—silica-gold and EPS-gold bionanocomposite formation. *Journal of Nanoparticle Research*. **13**(8): 3207-3216.
- Seeman, N.C. 1982. Nucleic acid junctions and lattices. *Journal of Theoretical Biology*. **99**: 237-247.
- Seigneuric, R., Markey, L., Nuyten, D.S.A., Dubernet, C., Evelo, C.T.A., Finot, E. and Garrido, C. 2010. From nanotechnology to nanomedicine: applications to cancer research. *Current Molecular Medicine*. **10**: 640–652.

- Selvakannan, P.R., Swami, A., Srisathiyarayanan, D., Shirude, P.S., Pasricha, R., Mandale, A.B. and Sastry, M. 2004a. Synthesis of aqueous Au core–Ag shell nanoparticles using tyrosine as a pH-dependent reducing agent and assembling phase-transferred silver nanoparticles at the air–water interface. *Langmuir*. **20**: 7825–7836.
- Senapati, S., Mandal, D., Ahmad, A., Khan, M.I., Sastry, M. and Kumar, R. 2004. Fungus mediated synthesis of silver nanoparticles: a novel biological approach. *Indian Journal of Physics*. **78A**: 101–105.
- Senapati S., Ahmad A., Khan M.I., Sastry M. and Kumar R.. 2005. Extracellular biosynthesis of bimetallic Au-Ag alloy nanoparticles. *Small*. **1**: 517–520.
- Shankar, S.S., Ahmad, A., Pasricha, R. and Sastry, M. 2003a. Bioreduction of chloroaurate ions by geranium leaves and its endophytic fungus yields gold nanoparticles of different shapes. *Journal of Materials Chemistry*. **13**: 1822–1826.
- Shankar, S.S., Ahmad, A., Sastry, M. 2003b. Geranium leaf assisted biosynthesis of silver nanoparticles. *Biotechnology Progress*. **19**: 1627–1631.
- Shankar, S.S., Rai, A., Ankamwar, B., Singh, A., Ahmad, A. and Sastry, M. 2004a. Biological synthesis of triangular gold nanoprisms. *Nature Materials*. **3**: 482–488.
- Sheeba, J.M. and Thambidurai, S. 2009. Extraction, characterization, and application of seaweed nanoparticles on cotton fabrics. *Journal of Applied Polymer Science*. **113** (4): 2287-2292.
- Sheny, D.S., Mathew, J. and Philip, D. 2011. Phytosynthesis of Au, Ag and Au-Ag bimetallic nanoparticles using aqueous extract and dried leaf of *Anacardium*

occidentale. *Spectrochimica Acta Part A: Molecular and Biomolecular Spectroscopy*. **79**: 254-262.

Siddhuraju, P. and Becker, K. 2003. Antioxidant properties of various solvent extracts of total phenolic constituents from three different agroclimatic origins of drumstick tree (*Moringa oleifera* Lam.) leaves. *Journal of Agricultural Food Chemistry*. **51**(8): 2144-2155.

Singaravelu, G., Arockiyamari, J., Ganesh Kumar, V. and Govindaraju, K. 2007. A novel extracellular biosynthesis of monodisperse gold nanoparticles using marine algae, *Sargassum wightii* Greville. *Colloids and Surfaces B: Biointerfaces*. **57**: 97-101.

Singh, A., Jain, D., Upadhyay, M.K., Khandelwal, N. and Verma H.N. 2010. Green synthesis of silver nanoparticles using *argemone mexicana* leaf extract and evaluation of their antimicrobial activities. *Digest Journal of Nanomaterials and Biostructures*. **5**: 483-489.

Singh, S., Saikia, J.P. and Buragohain, A.K. 2013. A novel 'green' synthesis of colloidal silver nanoparticles (SNP) using *Dillenia indica* fruit extract. *Colloids and Surface B: Biointerfaces*. **102**: 83-85.

Sneha K., Sathishkumar M., Lee S.Y., Bae, M.A. Yun, Y.S. 2011. Counter ions and temperature incorporated tailoring of biogenic gold nanoparticles. *Journal of Nanoscience and Nanotechnology*. **11**: 1811-1814.

Sivaraman, S.K., Elango, I., Kumar, S. and Santhanam, V. 2009. A green protocol for room temperature synthesis of silver nanoparticles in seconds. *Current Science*. **97**: 1055-1065.

Smith L., Kuncic Z., Ostrikov K. and Kumar S. 2012. Nanoparticles in Cancer Imaging and Therapy. *Journal of Nanomaterials*. 891318: 1-7.

- Sonavane, G., Tomoda, K., Sano, A., Ohshima, H., Terada H. and Makino, K. 2008. *In vitro* permeation of gold nanoparticles through rat skin and rat intestine: Effect of particle size. *Colloids and Surfaces B: Biointerfaces*. **65**(1): 1–10.
- Song, J.Y., Kim, B.S. 2008. Biological synthesis of bimetallic Au/Ag nanoparticles using Persimmon (*Diopyros kaki*) leaf extract. *Korean Journal of Chemical Engineering*. **25**: 808-811.
- Song, J.Y. and Kim, B.S. 2009. Rapid biological synthesis of silver nanoparticles using plant extracts. *Bioprocess Biosystem Engineering*. **32**: 79-84.
- Songand, J.Y. and Kim, B.S. 2009. Biological synthesis of metal nanoparticles. *Biocatalysis and agricultural biotechnology*. pp. 399-407, CRC press.
- Stepp, J.R. and Moerman D.E. 2001. The importance of weeds in ethnopharmacology. *Journal of Ethnopharmacology*. **75**: 19-23.
- Sudhakar, A. 2009. History of cancer, ancient and modern treatment methods. *Journal of Cancer Science Therapy*. **1**: 1-4.
- Sudhasree, S., Shakila Banu, A., Brindha, P. and Kurian, G.A. 2014. Synthesis of nickel nanoparticles by chemical and green route and their comparison in respect to biological effect and toxicity. *Toxicological & Environmental Chemistry*. **96**(5):1-8.
- Sugunan, A., Melin, P., Schnürer, J. and Hilborn, J.G. 2007. Nutrition-driven assembly of colloidal nanoparticles: growing fungi assemble gold nanoparticles as microwires. *Journal of Advanced Materials*. **19**: 77-81.
- Sujitha, M.V. and Kannan, S. 2013. Green synthesis of gold nanoparticles using Citrus fruits (*Citrus limon*, *Citrus reticulata* and *Citrus sinensis*) aqueous extract and

its characterization. *Spectrochimica Acta Part A: Molecular and Biomolecular Spectroscopy*. **102**: 15-23.

Sun, R.W.-Y., Ma, D.-L., Wong, E.L.-M. and Che, C.-M. 2007. Some uses of transition metal complexes as anti-cancer and anti-HIV agents. *Dalton Trans.* **43**: 4884–4892.

Sun, S., Murray, C., Weller, D., Folks, L. and Moser, A. 2000. Monodisperse FePt nanoparticles and ferromagnetic FePt nanocrystal superlattices. *Science*. **287**: 1989-1992.

Suriyakalaa, U., Antony, J.J., Suganya, S., Siva, D., Sukirtha, R., Kamalakkannan, S., Pichiah, P.B.T. and Achiraman, S. 2013. Hepatocurative activity of biosynthesized silver nanoparticles fabricated using *Andrographis paniculata*. *Colloids and Surface B: Biointerfaces*. **102**: 189–194.

Swarnalatha, C., Rachela, S., Ranjan, P. and Baradwaj, P. 2012. Evaluation of Invitro Antidiabetic Activity of *Sphaeranthus Amaranthoides* Silver nanoparticles. *International Journal of Nanomaterials and Biostructures*. **2**: 25-29.

Tabrizi, A., Ayhan, F. and Ayhan, H. 2009. Gold nanoparticle synthesis and characterisation. *Journal of Biological Chemistry*. **37**(3): 217-226.

Tamokou, J.D., Mpetga, D.J.S., Lunga, P.K., Tene, M., Tane, P., Kuate, J.R., 2012. Antioxidant and antimicrobial activities of ethyl acetate extract, fractions and compounds from stem bark of *Albizia adianthifolia* (Mimosoideae). *BMC Complementary and Alternative Medicine*. **12**: 99.

Tao, F., Nguyen, L. and Zhang, S. 2014. Introduction: synthesis and catalysis on metal nanoparticles. RSC Catalysis Series, ISBN: 978-1-78262-033-4.

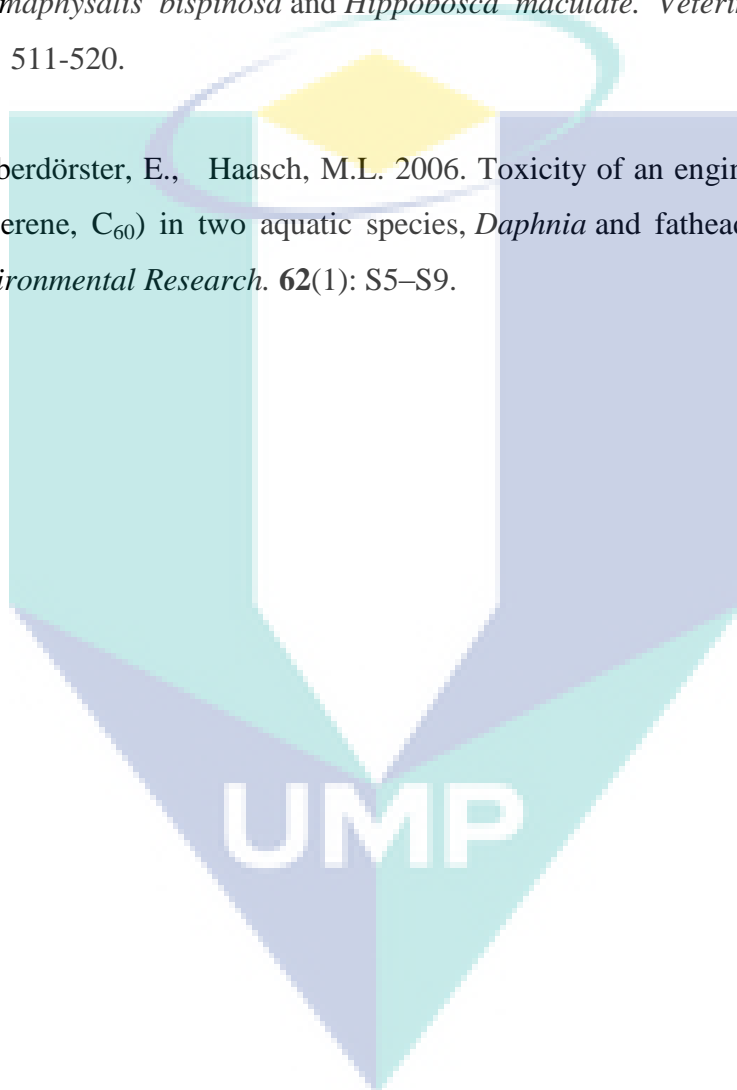
- Taylor, S., Wakem, M., Dijkman, G., Alsarraj, M. and Nguyen, M. 2010. A practical approach to RT-qPCR—publishing data that conform to the MIQE guidelines. *Methods*. **50**: S1–S5.
- Thirunavukkarasu, A., Prabhu, D., Geetha, R., Govindaraju, K., Manikandan, R., Arulvasu, C. and Singaravel, G. 2014. Apoptosis in liver cancer (HepG2) cells induced by functionalized gold nanoparticles. *Colloids and Surfaces B: Biointerfaces*. **123**(1): 549-556.
- Tomczak, M.M., Slocik, J.M., Stone, M.O. and Naik, R.R. 2007. Bio-based approaches to inorganic material synthesis. *Biochemical Society Transactions*. **35**: 512–515.
- Tong, R. 2010. Development of polymeric drug delivery vehicles for Targeted cancer therapy. Thesis. University of Illinois at Urbana-Champaign. 1-150.
- Trease, G.E. and W.C. Evans, 1989. Pharmacology 11th Edn., Bailliere Tindall Ltd., London, pp: 60-75.
- Ujowundu, C.O., Igwe, C.U., Enemor, V.H.A., Nwaogu, L.A. and Okafor, O.E. 2008. Nutritive and anti-nutritive properties of *Boerhavia diffusa* and *Commelina nudiflora* leaves. *Pakistan Journal of Nutrition*. **7**: 90-92.
- Vankar, P.S. and Bajpai, D. 2010. Preparation of gold nanoparticles from *Mirabilis jalapa* flowers. *Indian Journal of Biochemistry and Biophysics*. **47**: 157-160.
- Vasanth, K., Ilango, K., MohanKumar, R., Agrawal, A. and Dubey, G. P. 2014. Anticancer activity of *Moringa oleifera* mediated silver nanoparticles on human cervical carcinoma cells by apoptosis induction. *Colloids and Surfaces B: Biointerfaces*. **117**: 354–359.

- Vigneshwaran, N., Ashtaputre, N.M., Varadarajan, P.V., Nachane, R.P., Paralikar, K.M. and Balasubramanya, R.H. 2007. Biological synthesis of silver nanoparticles using the fungus *Aspergillus flavus*. *Materials Letters*. **61**: 1413–1418.
- Vijayakumar, R., Devi, V., Adavallan, K. and Saranya, D. 2011. Green synthesis and characterization of gold nanoparticles using extract of anti-tumor potent *Crocussativus*. *Physica E*. **44**: 665-671.
- Wahab, R., Dwivedi, S., Khan, F., Inho, Y.K.M., Hyung-Shik, H., Javed, S. et al. 2014. Statistical analysis of gold nanoparticle-induced oxidative stress and apoptosis in myoblast (C2C12) cells. *Colloids and Surfaces B: Biointerfaces*. (In press).
- Wani, I.A., and Ahmad, T. 2013. Size and shape dependant antifungal activity of gold nanoparticles: a case study of *Candida*. *Colloids and Surfaces B: Biointerfaces*. **101**: 162–170.
- Weiss, J., Takhistov, P. and Julianmcclements, D. 2006. Functional materials in food nanotechnology. *Journal of Food science*. **71**: 107-117.
- Yakimovich, N.O., Ezhevskii, A.A., Guseinov, D.V., Smirnova, L.A., Gracheva, T.A. and Klychkov, K.S. 2008. Gold nanoparticles studied by ESR spectroscopy. *Russian Chemical Bulletin*. **57**: 520-523.
- Yeo, S., Lee, H. and Jeong, S. 2003. Preparation of nanocomposite fibers for permanent antibacterial effect. *Journal of Materials Science*. **38**: 2143-2147.
- Yildirim, A., Mavi, A. and Kara, A.A. 2001. Determination of antioxidant and antimicrobial activities of *Rumex crispus* L. extracts. *Journal of Agricultural Food Chemistry*. **49**: 4083-4089.

Yoosaf, K., Ipe, B., Suresh, C.H., Thomas, K.G., 2007. In situ synthesis of metal nanoparticles and selective naked-eye detection of lead ions from aqueous media. *Journal of Physical Chemistry C*. **111**: 12839-12847.

Zahir, A.A. and Rahuman, A.A. 2012. Evaluation of different extracts and synthesized silver nanoparticles from leaves of *Euphorbia prostrata* against the plant *Haemaphysalis bispinosa* and *Hippobosca maculate*. *Veterinary Parasitology*. **187**: 511-520.

Zhu, S., Oberdörster, E., Haasch, M.L. 2006. Toxicity of an engineered nanoparticle (fullerene, C₆₀) in two aquatic species, *Daphnia* and fathead minnow. *Marine Environmental Research*. **62**(1): S5-S9.



APPENDICES

LIST OF PUBLICATIONS AND ACHIEVEMENTS

1. Journals

- **P. Kuppusamy**, M. M. Yusoff, G.P. Maniam, S.J.A. Ichwan, I. Soundharrajan, N. Govindan. 2014. Nutraceuticals as potential therapeutic agents for colon cancer: a review. *Acta Pharmaceutica Sinica B*. 4(3): 173–181. **(Elsevier Publications)**
- **P. Kuppusamy**, M.M. Yusoff, G. P. Maniam, N. Govindan. 2014. Biosynthesized gold nanoparticle developed as a tool for detection of HCG hormone in pregnant women urine sample. *Asian Pacific Journal of Tropical Disease*. 4(3): 237. **(Elsevier Publications)**
- **P. Kuppusamy**, N. Govindan, M. M. Yusoff, S. J.A. Ichwan. 2015. Proteins are potent biomarkers to detect colon cancer progression. *Saudi Journal of Biological Sciences*. **(Elsevier Publications)** (In Press).
- **P. Kuppusamy**, M.M. Yusoff, N. Govindan. 2015. Biosynthesis of metallic nanoparticles using plant derivatives and their new avenues in pharmacological applications - An updated report. *Saudi Pharmaceutical Journal*. **(Elsevier Publications)** (In Press).

- **P. Kuppusamy**, M. M. Yusoff, N. R. Parine, N. Govindan. 2015. Evaluation of *in-vitro* antioxidant and antibacterial properties of *Commelina nudiflora* L. extracts prepared by different polar solvents. *Saudi Journal of Biological Sciences* 22(3): 293-301. (**Elsevier Publications**)
- **P. Kuppusamy**, M. M. Yusoff, S.J.A. Ichwan, N. R. Parine, G. P. Maniam, N. Govindan. 2015. *Commelina nudiflora* L. edible weed as a novel source for gold nanoparticles synthesis and studies on different physical–chemical and biological properties. *Journal of Industrial and Engineering Chemistry* 27: 59-67. (**Elsevier Publications**)
- **P. Kuppusamy**, S. J. A. Ichwan, N. R. Parine, M. M. Yusoff, G. P. Maniam, N. Govindan. 2015. Intracellular biosynthesis of Au, Ag nanoparticles using ethanolic extract of *Brassica oleracea* L. and studies on their physicochemical, biological properties. *Journal of Environmental Sciences* 29: 151-157. (**Elsevier Publications**)
- **P. Kuppusamy**, M.M. Yusoff, S.J.A. Ichwan, N. R. Parine, N. Govindan. 2015. Biosynthesis and characterization of gold-silver alloy nanoparticles using *Commelina nudiflora* L. extract and efficacy of control plant pathogenic fungus activity. *3 Biotech* (**Springer Publications**) (Submitted).
- **P. Kuppusamy**, M.M. Yusoff, S.J.A. Ichwan, N. Govindan, N. R. Parine. 2015. Biosynthesis, characterization of AgNPs using edible weed *C. nudiflora* L. and efficacy of control oral pathogenic bacteria. *Journal of Biosciences*. (**Springer Publications**) (Submitted).
- **P. Kuppusamy**, M. M. Yusoff, N. Govindan. G.P. Maniam. 2015. Treatment of Palm oil mill effluent (POME) using plant mediated copper nanoparticles as a novel bio-control agent. *Industrial Crops and Products* (**Elsevier Publications**) (Submitted).

Conferences

- **P. Kuppusamy**, M. M. Yusoff, M. B. Suliman, N. Govindan. Isolation and Identification of bioactive compounds from weed plant *Commelina nudiflora*. L and its antioxidant, antibacterial activities. MUCET 2013 (Organised by UMP, UTem, UTHM, UniMAP), 3-4 December, 2013, M.S.Garden Hotel, Kuantan, Pahang, Malaysia.
- **P. Kuppusamy**, M. M Yusoff, G.P. Maniam, N. Govindan. Potential weed *Commelina nudiflora* L. plants extract using for biosynthesis of platinum nanoparticles and characterization their bioactivity against food pathogenic bacteria. Presented at 38th Annual Conference of the Malaysian Society for Biochemistry and Molecular Biology, 28-29 August, 2013, Kuala Lumpur, Malaysia.
- **P. Kuppusamy**, M. M.Yusoff, G. P. Maniam, N. Govindan. Green technology route for synthesis, aracterization of copper nanoparticles by using weed plant (*Commelina nudiflora*. L) and their *In-vitro* anti-inflammatory effect. Presented at International Conference on Nanomaterials (Nano Today, Elsevier), 24-26 June, 2013, Institute of Bioengineering and Nanotechnology, Biopolis, Singapore.

Exhibition

- N. Govindan, **P. Kuppusamy**, M. M.Yusoff, G. P. Maniam. A novel route for biosynthesis of silver nanoparticles using *C.nudiflora* for biomedical application in colon cancer therapeutics. Presented at (CITReX), 28-29 March, 2013, Universiti Malaysia Pahang (UMP), Gambang, Pahang, Malaysia. (**Silver Medal**)

- N. Govindan, **P. Kuppusamy**, S. J.A. Ichwan, M. M.Yusoff, G. P. Maniam. Enhancement of plant derived nano-mouthwash activity using silver nanoparticles as a novel ingredient – A first report. Presented at (CITReX), 3-4 March, 2014, Universiti Malaysia Pahang (UMP), Gambang, Pahang, Malaysia. **(Silver Medal)**

